Integration of Computational and Experimental Techniques for the Discovery of SARS-CoV-2 PL^{pro} Covalent Inhibitors.

Ho Ying Huang,[1] Sharon Pinus,[1] Xiaocong Zhang,[1] Guanyu Wang,[1] Andrés M. Rueda,[1] Yaouba Souaibou,[1] Solène Huck,[1] Mitchell Huot,[1] Danielle Vlaho,[1] Joshua Pottel,[2] Felipe A. Venegas,[1] Zhuoqun Lu,[1] Christopher Hennecker,[1] Julia Stille,[1] Jevgenijs Tjutrins,[1] Caitlin E. Miron,[1] Anne Labarre,[1] Jessica Plescia,[1] Mihai Burai-Patrascu,[1,2] Anthony K. Mittermaier[1,] and Nicolas Moitessier[1,2]**

[1] Department of Chemistry, McGill University, 801 Sherbrooke St W, Montreal, QC, Canada H3A 0B8 and [2] Molecular Forecaster 910-2075, Boul. Robert Bourassa, Montreal, QC, Canada H3A 2L1

*Corresponding authors: nicolas.moitessier@mcgill.ca; anthony.mittermaier@mcgill.ca

Abstract

Papain-like protease (PL^{pro}) and 3-chymotrypsin-like protease (3CL^{pro} or Mpro) are enzymes essential for the replication of SARS-CoV-2, the virus responsible for COVID-19. While 3CL^{pro} has been the main target of many potential antivirals including nirmatrelvir (active ingredient of Paxlovid), PL^{pro} has proven to be more difficult to target and only a handful of inhibitors have been disclosed. PL^{pro} inhibitors would be highly valuable tools in the fight against COVID19 resistant strains and in future coronavirus pandemics. Combining our experience with 3CL^{pro} covalent inhibitors with our expertise in structure-based covalent drug discovery, we rationally designed PL^{pro} inhibitors achieving a maximum potency of 13 µM through fusion of **GRL-0617** and **VIR-251.** In parallel, we launched an integrated large scale virtual screening/experimental approach, identifying four novel chemical series active at micromolar concentrations against PL^{pro}. We report herein our investigations including rational design, virtual screening, synthesis of selected structures and *in vitro* assays leading to novel PL^{pro} inhibitors.

Introduction

Coronaviruses. Coronaviruses belong to a highly diverse family of enveloped positive-sense single-stranded RNA (+ssRNA) viruses which are capable of infecting mammals, including humans, and birds.[1] They can cause respiratory tract infections ranging from mild symptoms such as nasal congestion to lethal symptoms such as pneumonia in humans.[2] Human coronaviruses, such as HCoV-229E, HCoV-OC43, HCoV-NL63, and HCoV-HKU1 only cause seasonal and usually mild respiratory tract infections generally known as the "common cold".[3] Since the discovery of the first human coronaviruses (HCoV-229E and HCoV-OC43) in the 1960s, the medicinal chemistry community has not paid much attention to these viruses as they were considered to be non-lethal. However, as the severe acute respiratory syndrome (SARS) in 2002, Middle East respiratory syndrome (MERS) in 2012, and coronavirus disease 2019 (COVID-19) appeared in humans and caused fatal respiratory illnesses, public health concerns for these

highly pathogenic and often fatal coronaviruses have emerged. The need for global collaboration to stop viral transmission, develop specific drugs for these viruses, and prevent future lethal coronaviruses from jumping to humans is clear.

COVID-19 and future pandemics. At the end of 2019, SARS-CoV-2, the viral species responsible for COVID-19, emerged in the city of Wuhan, China and the regional epidemic evolved into a global pandemic. As of July 2023, there have been at least 6.9 million confirmed deaths worldwide.[4] There was an urgent need for strategies that could stop the viral spread and reduce the severity of symptoms of infected people. While preventive measures and vaccination have quite effectively reduced the viral spread,[5] there is still a need for treatments against COVID-19 since the disease may be endemic, with no guarantee that future mutants would not escape any herd immunity.[6] Early efforts to repurpose multiple existing drugs (e.g., ivermectin, remdesivir, and hydroxychloroquine) for the treatment of COVID-19 did not lead to significant effectiveness against COVID-19. Even the highly anticipated (then approved[7]) Remdesivir showed mixed efficacy from different clinical trials.[8, 9] Fortunately, efforts to develop new drugs culminated with Molnupiravir (Merck) targeting the RNA-dependent RNA polymerase (RdRp)[10] first approved in the United Kingdom[11] then in various countries,[12] Paxlovid (nirmatrelvir and ritonavir, Pfizer)[13-15] and Xocova (Ensitrelvir, Shionogi)[16] both targeting $3CL^{pro}$ (also known as M^{pro}). However, resistance to Paxlovid emerged in both the omicron and WA1 strains meaning other drugs for COVID-19 may be needed in the near future.[17] In addition, considering the regular outcome from coronavirus (SARS in 2002, MERS in 2012, and COVID-19 in 2019), it is likely that other coronaviruses will appear in the future and a plethora of drugs in the tool box of physicians will better prepare us for future pandemics.

Coronavirus Lifecycle and Potential Drug Targets. Upon viral entry, the released and uncoated +ssRNA is translated into polyproteins pp1a and pp1ab. These polyproteins are post-translationally processed by both papain-like protease (PL^{pro}) and 3C-like protease ($3CL^{pro}$) into the individual non-structural proteins (nsp's) that form the viral replication and transcription complex.[18] Concordant with the expression of nsp's, the viral genome is replicated by the RdRp, which also directly mediates subgenomic mRNAs (sg mRNAs) comprising the characteristic nested set of coronavirus mRNAs.[2] Ultimately, virions are secreted from the infected cell by exocytosis. By closely inspecting the viral life cycle, several potential drug strategies were proposed, including the inhibition of viral proteases PL^{pro} and $3CL^{pro}$ to interrupt the production of nsp's.[19-23] While both $3CL^{pro}$ and PL^{pro} are essential coronavirus enzymes, required for processing viral polyproteins to generate a functional replicase complex and enable viral spread, PL^{pro} is also involved in cleaving proteinaceous post-translational modifications (namely, deubiquitination and deISGlation) on host proteins as an evasion mechanism against host antiviral immune responses.[23, 24]

PL^{pro} inhibitors. While several very potent $3CL^{pro}$ inhibitors rapidly emerged,[13-15, 25] and others were approved (Nirmatrelvir, Figure 1, and Ensitrelvir), the search for PL^{pro} inhibitors has been much less successful. In fact, designing inhibitors against PL^{pro} was found to be a lot more laborious due to its significant geometric constraints (long narrow tunnel-like shaped catalytic site) than with $3CL^{pro}$ (large, open catalytic site) which requires additional efforts to reach sub-micromolar potencies. As a result, most reported inhibitors do not bind to the catalytic site but rather bind to a distant site corresponding to the P4+ binding pockets. While this enzyme is more challenging, targeting an enzyme other than $3CL^{pro}$ will ultimately allow us to produce more diverse drugs.[26, 27] Drug repurposing has been the primary avenue by which PL^{pro} inhibitors have been proposed. Other than Ebselen, a reactive organoselenium drug with IC_{50} ~ 2 μM[28] that is often recognized as a pan-assay interference compound (PAINS), only seven drugs have shown modest potency (IC_{50} values ranging from 82 to 91 μM)[28-31] against PL^{pro}. Some PL^{pro} inhibitors of other coronaviruses of the same family (such as MERS-CoV and SARS-CoV) were also identified but, once more, with micromolar potency at best.[32] Among these was the previously reported SARS-CoV-1

PL^{pro} inhibitor **GRL0617**, which was also found to inhibit SARS-CoV-2 PL^{pro}.[29-35] A crystal structure (PDB code: 7CJM) revealed that this compound does not bind near the catalytic cysteine but rather at the entrance of the tunnel to the catalytic site (Figure 2). Similarly, another SARS-CoV-1 PL^{pro} (IC_{50} of 5 μM) and MERS PL^{pro} (IC_{50} of 4.4 μM) inhibitor, **6-thioguanine** (6-TG), was found to inhibit SARS-CoV-2 PL^{pro} in cell lines.[36]

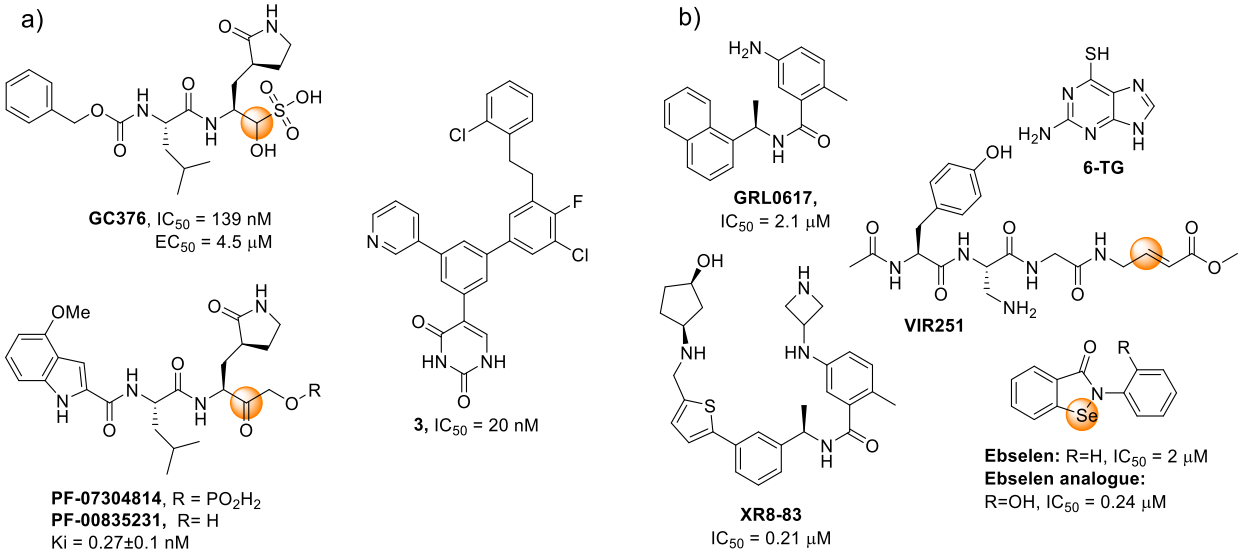

Figure 1. a) Selected 3CL^{pro} inhibitors (orange circles highlighting the covalent warheads) and b) Selected PL^{pro} inhibitors.

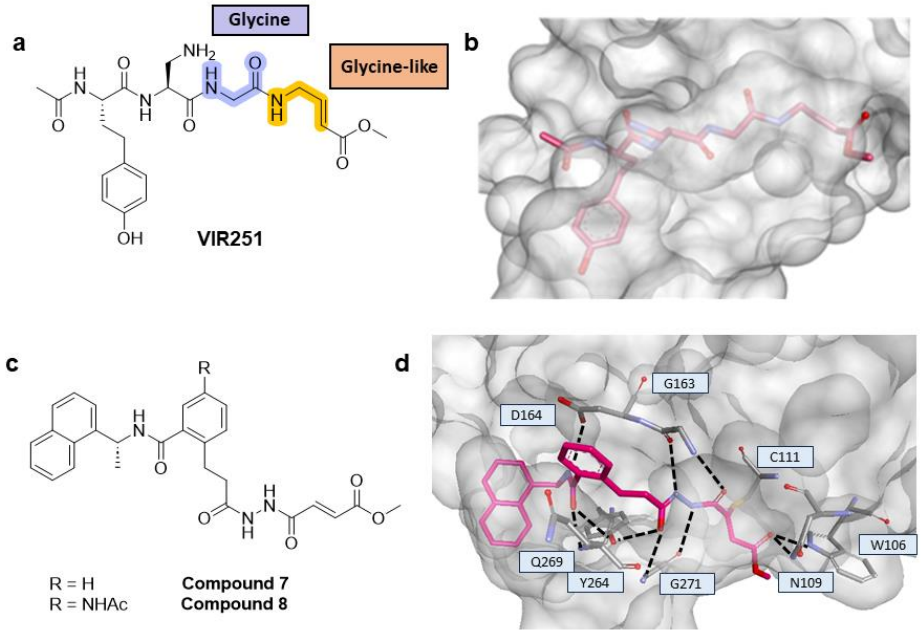

Figure 2. a) **S**tructure of **VIR251**; b) **VIR251** co-crystallized with PL^{pro} (PDB code: 6WX4); c) Covalent analogues of **GRL0617** synthesized by Sanders *et al.* d) Compound **7** (pink) co-crystallized with PL^{pro} (PDB code: 8EUA). Residues that form interactions with the compound are shown in sticks and labeled.

An alternative strategy is to modify the substrate peptide sequence into an inhibitor. The best tetrapeptide substrates were identified by Rut and co-workers[27] and these peptides were converted into

inhibitors like **VIR251,** which binds covalently to the catalytic cysteine (Figures 1 and 2) albeit with micromolar potency at best.

It was not until late 2021 that submicromolar PL^{pro} inhibitors were reported.[37] These non-covalent inhibitors, analogues of **GRL0617**, were crystallized (e.g., PDB ID: 7LLF). Recently, more analogues of **GRL0617** have been investigated.[38] Researchers replaced the methyl substituent of **GRL0617** with a peptidomimetic linker and an electrophile to react with Cys111 in the PL^{pro} active site (Figure 2). With the fumarate ester being an electrophile, this hybrid inhibitor's potency has reached 0.094 μM.

Structure-based discovery of PL^{pro} inhibitors. Shortly after the start of the COVID19 outbreak, high-quality crystal structures were published, creating an opportunity for structure-based drug design.[37, 39] Taking advantage of our expertise in covalent inhibition, computational drug discovery, and virtual screening of covalent inhibitors, we sought to design, synthesize and evaluate PL^{pro} inhibitors using rational design and large library virtual screening. We report herein our efforts over the past two years in the design and synthesis of PL^{pro} inhibitors and in the discovery through virtual screening of novel chemical series for this enzyme.

Results and Discussion

GRL0617-VIR251 hybrid. As a first strategy, we devised a molecular design based on available structural information. As discussed above, **VIR251** binds in the long narrow catalytic site making a covalent bond with the catalytic cysteine. In contrast, **GRL0617** blocks the entry of this tunnel sitting at more than 7 Å from the catalytic cysteine with some overlap with the far end of **VIR251**. We envisioned hybrid structures featuring both **GRL0617** and **VIR251**. Thus, from crystal structures of **VIR251** and **GRL0617** co-crystallized with PL^{pro} and their respective binding modes (Figure 3), we designed compound **SP-5**. This strategy is similar to that employed by Sanders *et al.*[38]

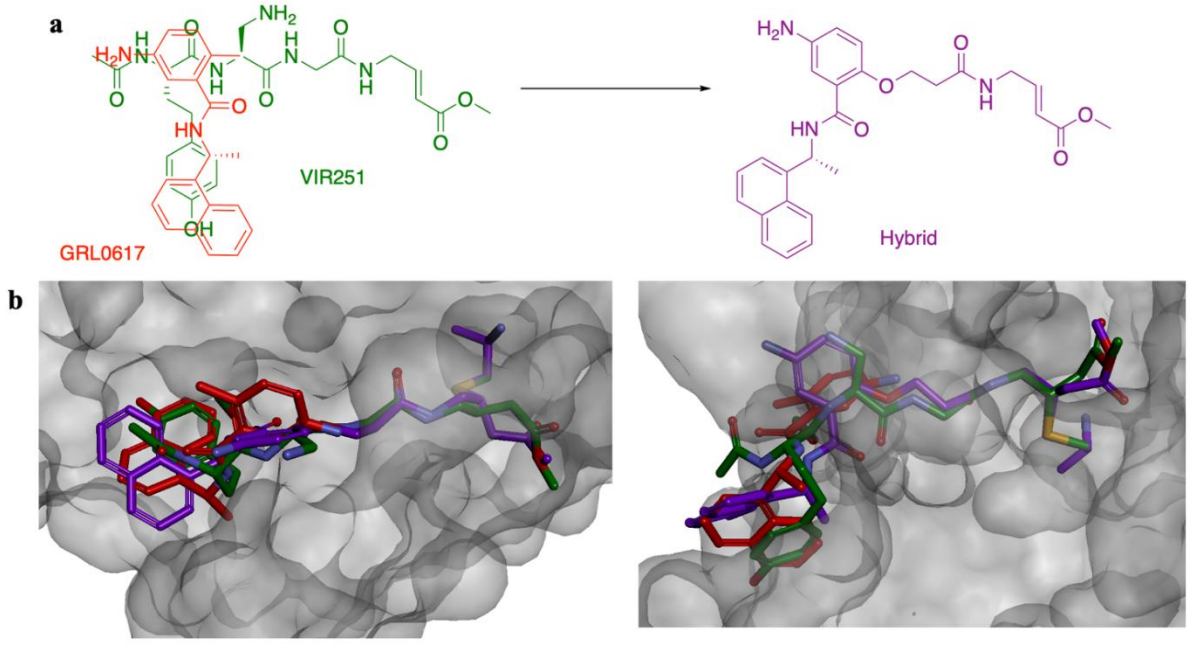

Figure 3. a) design of a hybrid structure; b) stacked view of GLR-0617 [red], VIR-251 [green] and proposed hybrid [purple] in PL^{pro} active site.

To evaluate not only the inhibitory potency of the designed hybrid, but also the impact of each group in this design, we first began with the synthesis of **GRL0617** analogues. This first set of compounds would inform us of the optimal linker between the two parts of the hybrid constructs and possible changes on the **GRL0617** portion. Compounds **SP-1a-l** were prepared from the coupling reaction of benzoic acids and (*R*)-1-(naphthalen-1-yl)ethan-1-amine (Scheme 1). All attempts of *O*-methylation of compound **SP-1d** were unsuccessful except the simple acetylation reaction to give **SP-2** (see Supporting Information). Compound **SP-1g/1k/1l** were then chosen as a building block for the synthesis of hybrid PL^{pro} inhibitors **SP-5a-c,** since the C-I bond is intrinsically weaker and is beneficial in cross-coupling reactions.[40]

The key intermediate **SP-3a-c** was synthesized through Ullmann amination, using CuI and β-alanine with Cs_2CO_3 as the base in DMF at 100 °C (Scheme 2). To install the glycine-like warhead, *N*-Boc-2-aminoacetaldehyde was reacted with triethylphosphonoacetate using the Horner-Woodward-Emmons reaction to form the Boc-protected product. This was followed by Boc deprotection using TFA to provide the unprotected amine salt (**SP-4**) in quantitative yield. **SP-3a-c** and **SP-4** were coupled to give the **GRL0617-VIR251** hybrid analogues (**SP-5a-c**).

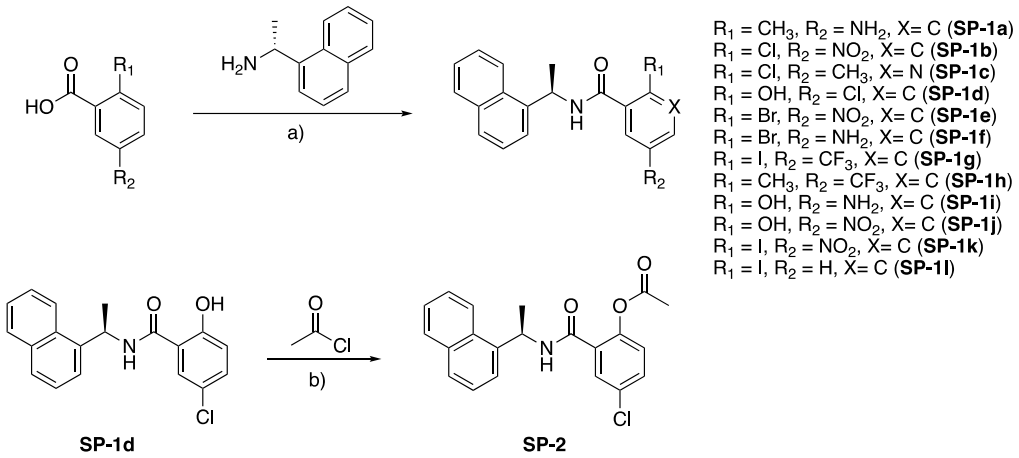

Scheme 1. Synthesis of **GRL-0617** and analogues. a) PyBOP, DIPEA, DCM, rt, 24h, 74% (**SP-1a)**, 91% (**SP-1f**), 51%, (**SP-1i**); HATU, DIPEA, acetonitrile, rt, 24h, 71% (**SP-1b)**, 71% (**SP-1c)**, 54% (**SP-1d**), 80% (**SP-1e**), 87% (**SP-1g**), 48% (**SP-1h**), 43% (**SP-1j**), 78% (**SP-1k**), 40% (**SP-1l**).

The original plan was to keep the amine in **GRL-0617** in all the analogues, however the amine group was not compatible with most of the reactions carried out in this study, added synthetic challenges, and got oxidized easily. Therefore, different groups have been used to replace the amine group including nitro, hydroxy, methyl, Cl and H. This was done to avoid the reactivity of the amine, and at the same time increase the reactivity for the R_1 group to perform coupling reactions.

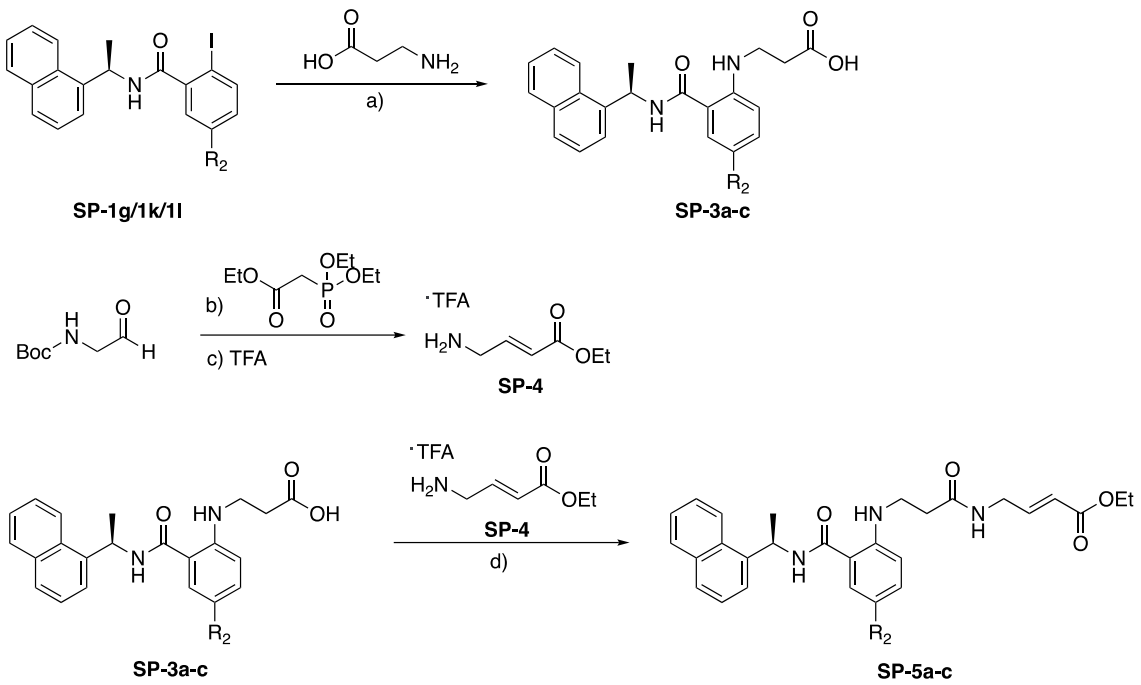

Scheme 2. Synthesis of hybrid PL^{pro} inhibitors. a) CuI, Cs_2CO_3, DMF, 100°C, 3 h, 50% (**SP-3a)**, 52% (**SP-3b**), 58% (**SP-3c)**; b) NaH, THF, 0°C to rt, 3.5 h, 60%, c) TFA, DCM, 0°C, 2 h, quantitative yield, d) DIPEA, PyBOP, DCM, 0°C to rt, 18 h, 37% (**SP-5a**), 58% (**SP-5b**), 11% (**SP-5c**).

Table 1. Biological evaluation of **GRL-0617** analogues and the hybrid analogue **SP-5a-c**

Compd	Peptide (50 μM, % inhibition)
SP-1b	12 ± 1
SP-1c	15 ± 3
SP-1e	< 5%
SP-1f	60 ± 3
SP-1g	< 5%
SP-1h	< 5%
SP-2	12 ± 0
SP-5a	80 ± 2
SP-5b	37 ± 1
SP-5c	27 ± 6

These compounds were tested against PL^{pro} at 50 μM using a peptide (Z-RLRGG-AMC) as a fluorescent substrate. Focusing on protease activity, all the compounds lost affinity when the amine group was absent (Table 1). **SP-1f**, although not as active as **GRL-0617 (SP-1a),** achieved 60% inhibition at 50 μM concentration with peptide as a substrate. The most potent compound, **SP-5a**, the designed hybrid analogue of **VIR-251** and **GRL-0617**, displayed 80% inhibition at 50 μM concentration with peptide as a substrate. From the dose-response curve, the IC_{50} of this compound is 13.3 ± 9 μM, reaching low micromolar potency, similar to **GRL0617** (Figure 4).

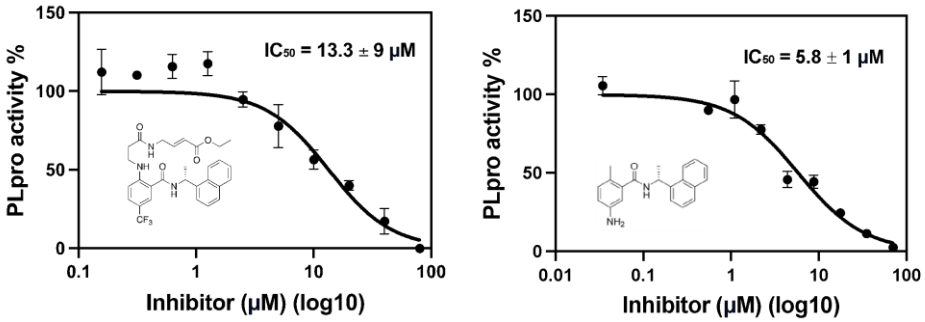

Figure 4. Dose-response curve for **SP-5** (left) and **GRL-0617** (right) against PL^{pro} with Z-RLRGG-AMC as substrate.

Virtual Screening. As the synthesis of the hybrid structures turned out to be a lot more difficult than anticipated (see Supporting Information), a virtual screening campaign was carried out concomitantly. High throughput docking and large computational resources may be envisioned (e.g., screening millions or even billions of compounds).[41, 42] This approach has been successful, illustrated by the screening of 40B molecules against $3CL^{pro}$ by Cherkasov and co-workers using a combined machine learning (ML)/docking approach.[43] Challenges with this approach include: analyzing the large resulting data (visual inspection is always recommended) can be time consuming,[44] many of these docked molecules may be intrinsically not good candidates (e.g., too large, featuring toxicophores, not drug-like) and some post-processing analysis removing undesired molecules is often required. In the case of covalent drugs, an additional step is to remove compounds not featuring a reactive warhead susceptible to make a covalent bond with the catalytic cysteine. In addition, it requires ultrafast docking programs, which are often less accurate as a trade-off.

Alternatively, we replaced this post-processing step with a pre-processing step with the goal of using our docking program FITTED which, sacrifices some runtime for higher accuracy.[45]. We started from libraries of sizes similar to those used in high throughput docking (several millions of molecules) and we removed compounds that are unlikely to bind and/or are not drug-like before docking. From the crystal structures of PL^{pro} co-crystallized with ligands, it was clear that hydrogen bond donors and acceptors were required. Finally, based on known inhibitors and on the structure of PLpro catalytic/binding site, we selected molecules with a net charge of 0 or +1 for docking to PL^{pro}. With all these filters, we generated a library of over 85,000 compounds featuring a covalent warhead from the ZINC database and of over 25,000 from the ChemSpace database.[46] These compounds were docked using FITTED which allows for automated covalent docking.[46] More specifically, FITTED automatically recognizes any potential warheads and docks the molecules considering both covalent and non-covalent binding modes in a single run.[47, 48]

Analysis. When the docking was complete, the 200 best scoring compounds were extracted, and their binding modes were investigated by our team of medicinal chemists, biochemists, and computational chemists. Through a voting system, 25 were selected for PL^{pro} and 21 of them purchased (Figure 5).

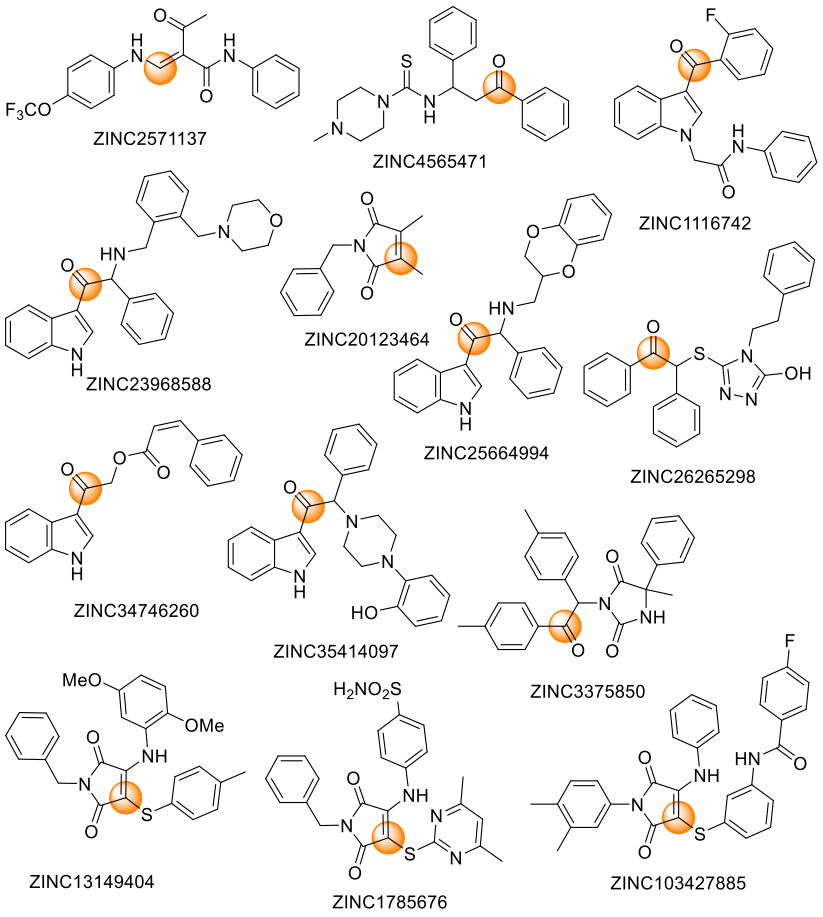

Figure 5. Example of purchased compounds from virtual screening on SARS-CoV-2 PL^{pro}. Any molecules containing chiral centers were purchased as racemic mixtures. Covalent warheads are highlighted in orange.

From virtual screening, a few molecules showed satisfactory interactions with PL^{pro} in their docking. For example, the catalytic Cys111 is predicted to react with the Michael acceptor warhead on **ZINC3276278** to form a covalent bond (Figure 6). The N-H on the backbone of Cys111 and Gly271 form H-bonds with the methoxy oxygen and the amide carbonyl, while the backbone of Gly163 acts both as a H-bond donor and acceptor. The side chain of Thr273 forms an H-bond with the carbonyl of the benzophenone moiety on the molecule. On the other hand, the catalytic Cys111 is predicted to react with the ketone group of **CSSS58908458**. The resulting hydroxyl is stabilized by the backbone of both Cys111 and Asn109. The carbonyl on the backbone of Gly163 forms H-bonds with both the amide N-H and the positively charged N-H on the molecule, while the amide carbonyl forms an H-bond with the backbone of Gly271. Overall, these two virtual hits demonstrate complementary interactions with PL^{pro} in docking.

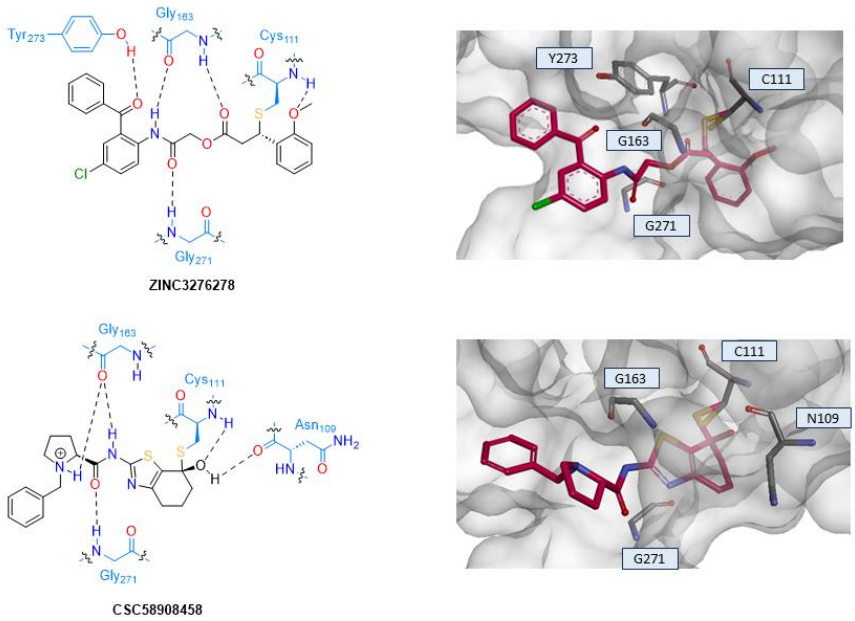

Figure 6 Predicted binding mode for two suggested (then confirmed, see blow) hits (**ZINC3276278** and **CSSS58908458**) against PL^{pro} (PDB code: 6WX4).

Inhibitory potency. Fluorescence assays were performed on the 21 purchased compounds. These compounds were tested against PL^{pro} at 25 µM using ubiquitin-AMC (Ub-AMC) and a peptide (Z-RLRGG-AMC) as fluorescent substrates. These two substrates allowed us to evaluate two activities of PL^{pro} as discussed above. **GRL0617** was used as a positive control. Four classes of inhibitors were identified with potencies in the mid-micromolar range which, for hit molecules, is close to **GRL0617**, one of the best inhibitors reported to date (IC_{50} = 5.8 ± 1 µM) (Figure 7).

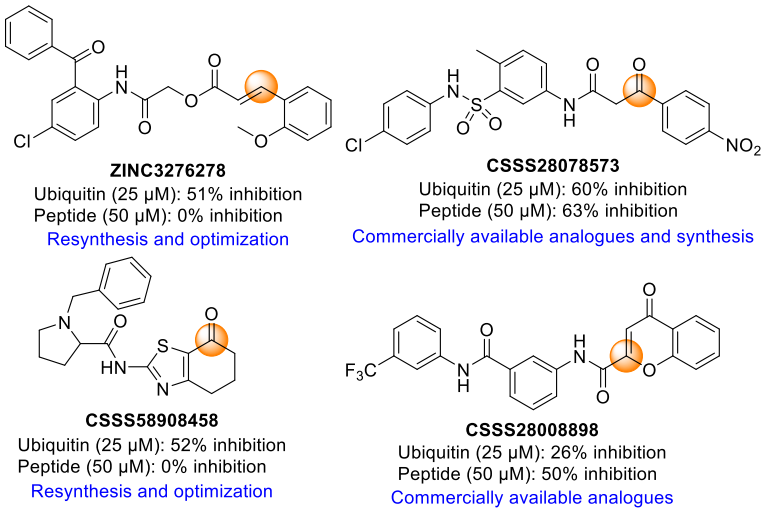

Figure 7. Hit molecules against PL^{pro} using ubiquitin and peptide as substrate and optimization strategies with hit molecules. Covalent warheads are highlighted in orange.

We decided to resynthesize and optimize two of the molecules (**ZINC3276278** and **CSSS58908458**) and carry out a preliminary structure-activity relationship of the other two hit molecules (**CSSS28078573** and **CSSS28008898**) using commercially available analogues to increase their potencies (Figure 8). Interestingly, a closer look at the docked binding modes of the first two hits identified by virtual screening

(see for example **ZINC3276278** in Figure 6) suggested that these compounds bind covalently and fill up the tunnel as does **VIR251** and feature aromatic functionalities in the allosteric site as does **GRL0617**. As a result, these are very similar to the hybrid molecule we designed and discussed above.

Resynthesis of ZINC3276278. The enzymatic assays showed that **ZINC3276278** displayed promising inhibitory potency against PL^{pro}. Prior to more complete structure-activity relationship investigations, we thought to resynthesize this compound to confirm its activity as weak potencies can be induced by impurities rather than the main molecule. We developed a concise 3-step synthesis of the target molecule from commercially available building blocks (Scheme 3). The synthesis began with a carbodiimide-catalyzed peptide coupling between acetoxyacetic acid and 2-amino-5-chlorobenzophenone to give intermediate **XZ-1**, which was then deacetylated by treatment with potassium carbonate in methanol into intermediate **XZ-2**. The last step involved a Steglich esterification between 2-methoxycinnamic acid and intermediate **XZ-2** to give **XZ-3a**, which is structurally identical to **ZINC3276278**.

Optimization through synthesis. This resynthesis was followed by preliminary structure-activity relationship investigations to further explore the potential of these structures as PL^{pro} inhibitors. We first thought to introduce diversity next to the covalent warhead (Scheme 3). Thus, the first set of analogues contained variation at the leftmost benzene ring of the original compound, where the methoxy group is at the *ortho* position. The first analogue (**XZ-3b**) contains a benzene ring where the *ortho* methoxy group was removed while the second analogue (**XZ-3c**) contains a trifluoromethyl moiety at the *para* position of the ring. These first two analogues will allow us to test the role of aromatic ring electronics in the activity. In particular, introducing an electron withdrawing trifluoromethyl group will lead to electronic effects on the Michael acceptor contrasting with those of the electron donating methoxy group. In the third analogue (**XZ-3d**) the benzene is removed further modulating the reactivity of the Michael acceptor but also significantly reducing the size of this part of the molecule. The fourth (**XZ-3e**) and fifth analogues (**XZ-3f**) with heterocycles, namely an imidazole ring and a furan ring, were designed to introduce hydrogen bond donors and acceptors at this position as water molecules have been observed in the cavity these are predicted to bind to.

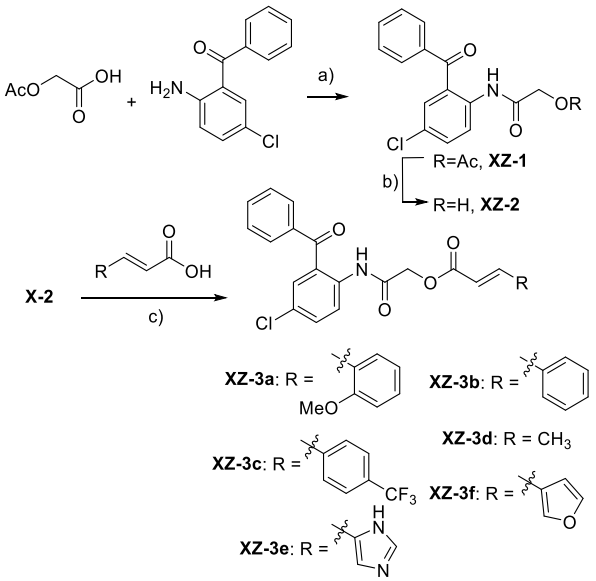

Scheme 3. a) DCC, DCM, rt, 4 h, 79%; b) K_2CO_3, MeOH, rt, 30 min, 74%; c) EDC·HCl, DMAP, DCM, rt, 24-48 h, 71% (**XZ-3a**), 74% (**XZ-3b**), 24 h, 80% (**XZ-3c**), 26 h, 35% (**XZ-3d**), 48 h, 36% (**XZ-3e**), 24 h, 54% (**XZ-3f**).

We next replaced the ester group as the second set of analogues, which may be labile, by an amide (Scheme 4) using glycine or β-alanine as building blocks. The synthesis began with an amide coupling between a Boc-protected glycine (n=1) or β-alanine (n=2) and 2-amino-5-chlorobenzophenone to afford intermediate **XZ-4a/b** (Scheme 4). Following the removal of the Boc protecting group was achieved quantitatively using HCl (4 M) in dioxane yielding compounds **XZ-5a/b**. The hydrochloride salts **XZ-5a/b** were then coupled with 2-methoxycinnamic acid to give the desired products **XZ-6a/b** (Scheme 4).

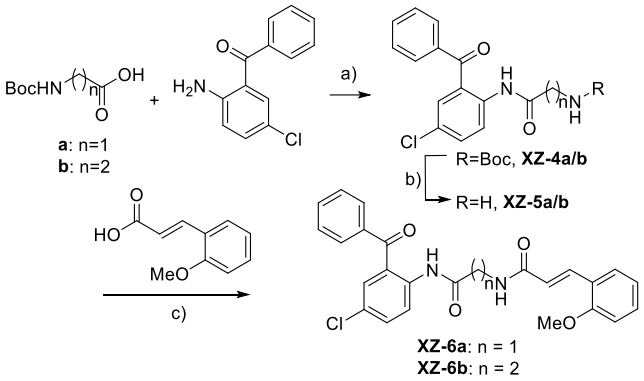

Scheme 4. MsCl, NMI, DCM, rt, 48 h, 21% (**XZ-4a**), 58% (**XZ-4b**); (b) HCl (4 M) in dioxane, rt, 2 h, quantitative (**XZ-5a**, **XZ-5b**); (c) EDC·HCl, DMAP, DCM, rt, 24 h, 36% (**XZ-6a**), 27% (**XZ-6b**).

The third set of analogues contains modifications of the ketone moiety in the original molecule to an amide. The synthesis began with a DCC-catalyzed coupling between methyl 2-amino-5-chlorobenzoate and acetoxyacetic acid to give intermediate **XZ-7** (Scheme 5). The acetyl group was then removed with potassium carbonate in methanol to provide alcohol **XZ-8**, which was then transformed into intermediate **XZ-9** via a Steglich esterification reaction. The last step involved a selective cleavage of the methyl ester using lithium iodide followed by an amide coupling to afford the desired product **XZ-10**.

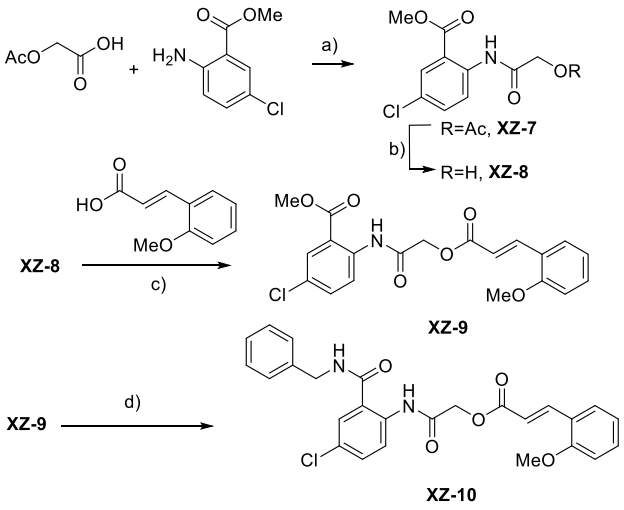

Scheme 5. a) DCC, DCM, rt, 4 h, 61%; b) K_2CO_3, MeOH, rt, 1 h, 64%; c) EDC·HCl, DMAP, DCM, rt, 20 h, 58%; d) LiI, pyridine, 160 °C, 15 min, microwave, then EDC·HCl, DMAP, benzylamine, rt, 20 h, 22%.

Biological evaluation revealed that the ester substitution for an amide is beneficial for the potency (**XZ-3a** vs. **XZ-6a** (Table 2). This change led to a structure closer to the Gly present in the natural substrate. As a result, the amide is forming an additional interaction with the binding site. Other changes did not

substantially improve the potency. Based on the docking study, we believe that changes on the right portion of the molecule combined with this amide change will lead to improved potencies.

Table 2. Biological evaluation of **ZINC3276278 (XZ-3a)** and analogues

Compd	Ubiquitin (25 μM, % inhibition)	Peptide (50 μM, % inhibition)
XZ-3a	19 ± 6	28 ± 22
XZ-3b	15 ± 2	23 ± 5
XZ-3c	25 ± 1	35 ± 8
XZ-3d	12 ± 4	33 ± 3
XZ-3e	10 ± 2	< 5%
XZ-3f	20 ± 1	28 ± 14
XZ-6a	86 ± 12	43 ± 15
XZ-6b	< 5%	41 ± 1
XZ-10	TBD	TBD
KH-6a	nd[a]	16 ± 10
KH-6b	nd[a]	18 ± 9
KH-11	nd[a]	12 ± 2

[a] not determined.

Optimization through docking. Hypothesizing that changing the right side of the molecule would impact its potency, we downloaded a library of commercially available amines from ChemSpace and did virtual synthesis using our VIRTUAL CHEMIST workflow on Forecaster.[49] This workflow enables us to prepare virtual combinatorial chemical libraries with the chemical schemes and the libraries of molecules provided to the program. A catalog of commercially available amines and **XZ-9** were input into the program and generated the coupled products by peptide coupling. The coupled products were then docked into the active site of PL^{pro} using FORECASTER. **KH-6a** and **KH-6b** were chosen to be synthesized based on visual inspection of the docking poses (Scheme 6).

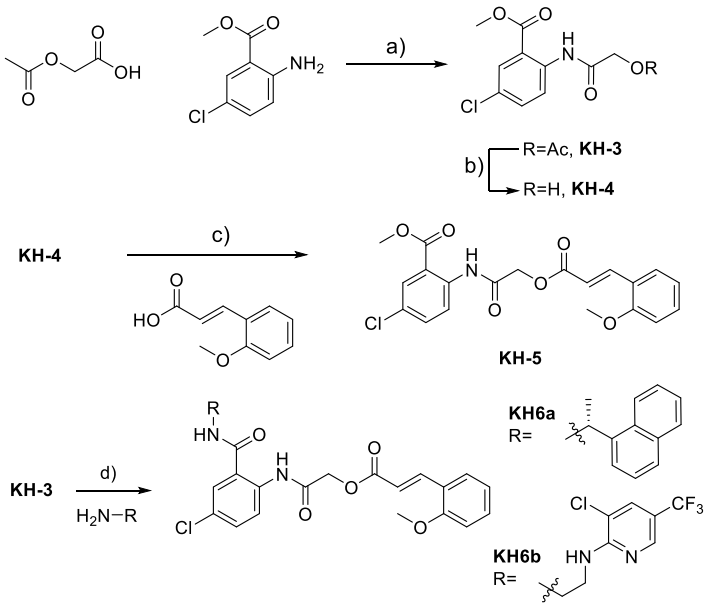

Scheme 6. a) DCC, DCM, rt, 16 h, 66%; b) K_2CO_3, MeOH, rt, 1 h, 91%; c) EDC·HCl, DMAP, DCM, rt, 20 h, 77%; d) LiI, pyridine, 160 °C, 30 min, microwave, then EDC·HCl, DMAP, rt, 24 h, KH-6a) 7%; KH-6b) 7%.

Combination of the best scaffolds. From the enzymatic assay results (Table 2), the groups with the best potency towards PL^{pro} (**XZ-3c** and **XZ-6a**) and the (*R*)-1-(naphthalen-1-yl)ethan-1-amine from **GRL-0617** are combined to form a new molecule, which should be able to achieve a higher potency than any of these molecules tested. Several synthetic pathways were tried, and only parallel synthesis afforded the final compound (Scheme 5). The target molecule was divided into two parts to do convergent synthesis. One of them coupled methyl glycinate with (*E*)-3-(4-(trifluoromethyl)phenyl)acrylic acid to give **KH-7**, and hydrolyze to give **KH-8**. The other synthesis was to hydrolyze methyl 2-amino-5-chlorobenzoate to form **KH-9** and coupled with (*R*)-1-(naphthalen-1-yl)ethan-1-amine to form **KH-10**. **KH-8** and **KH-10** were then coupled using an NMI/MsCl-mediated reaction to form the target product (Scheme 7).

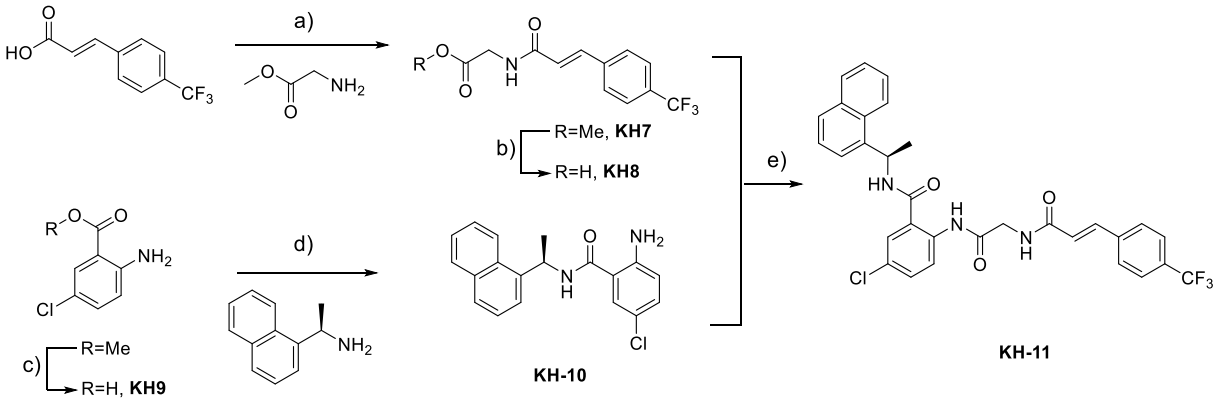

Scheme 7. a) EDC·HCl, DMAP, DCM, rt, 20 h, 56%; b) NaOH, H_2O rt, 16 h, 81%; c) NaOH, H_2O rt, 16 h, 57%; d) EDC·HCl, DMAP, DCM, rt, 20 h, 73%; e) MsCl, NMI, DCM, rt, 16 h, 2%.

Focusing on protease activity, the *in vitro* assay showed that changing the right side of the molecule to (*R*)-1-(naphthalen-1-yl)ethan-1-amine (**KH-6a**) or N^1-(3-chloro-5-(trifluoromethyl)pyridin-2-yl)ethane-1,2-diamine (**KH-6b**) did not improve the potency (Table 2). The combination of the best scaffolds from previous assays (**KH-11**) also did not improve the potency.

Resynthesis of CSSS58908458 and optimization through synthesis. Compounds **(*R*)-YSP9 and (*S*)-YSP8** were prepared by coupling tetrahydro-1,3-benzothiazol-2-amine and both enantiomers of *N*-benzyl proline to produce a compound identical to **CSSS58908458**. To confirm the role of the ketone as warhead for our other hit compound **CSSS58908458**, we synthesized the reduced analogues including **YSP-6**, **YSP-7**, **YSP-11**, **YSP-18**; these will also be used to assess the effect of the ring size and stereochemistry of the right side of the molecule (Scheme 8), as well as the heterocyclic analogues **YSP-13**, **YSP-14**, **YSP-19** and **YSP-20**. We also designed and synthesized the acyclic ketones analogues **YSP-22** and **YSP-29** and proposed to assess the substitution on the cyclohexanone ring **YSP-25** and **YSP-26**. All compounds were synthesized by EDC peptide coupling of the corresponding analogues.

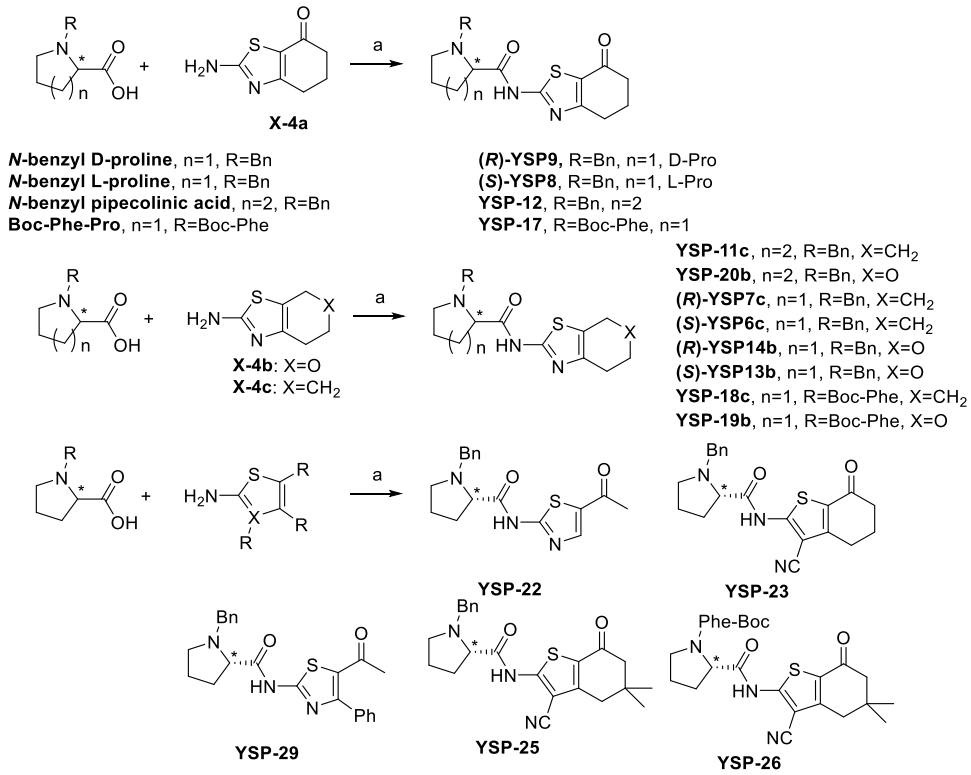

Scheme 8. a) EDC (1.2 eq), DIPEA, HOBt, acid, amine, DMF or DCM, r.t, 24h: *N*-benzyl D-proline, 2-amino-4,5,6,7-tetrahydro-1,3-benzothiazol-7-one 10% (**(*R*)-YSP9**); *N*-benzyl L-proline, 2-amino-4,5,6,7-tetrahydro-1,3-benzothiazol-7-one 15% (**(*S*)-YSP8**); *N*-benzyl L-proline, 4,5,6,7-tetrahydro-1,3-benzothiazol-2-amine 10% (**YSP-6**); *N*-benzyl D-proline, 4,5,6,7-tetrahydro-1,3-benzothiazol-2-amine 15% (**YSP-7**); 1-Benzylpiperidine-2-carboxylic acid, 2-amino-4,5,6,7-tetrahydro-1,3-benzothiazol-7-one 15% (**YSP-12**); 1-Benzylpiperidine-2-carboxylic acid, 4,5,6,7-tetrahydro-1,3-benzothiazol-2-amine 12% (**YSP-11**); Boc-Phe-Pro-OH, 2-amino-4,5,6,7-tetrahydro-1,3-benzothiazol-7-one 27% (**YSP-17**); 6,7-Dihydro-4h-pyrano[4,3-d]thiazol-2-ylamine, 1-Benzylpiperidine-2-carboxylic acid 32% (**YSP-20**); *N*-benzyl D-proline, 6,7-Dihydro-4h-pyrano[4,3-d]thiazol-2-ylamine 31% (**YSP-14**); *N*-benzyl D-proline, 6,7-Dihydro-4h-pyrano[4,3-d]thiazol-2-ylamine 20% (**YSP-13**); 4,5,6,7-tetrahydro-1,3-benzothiazol-2-amine, Boc-Phe-Pro-OH 24% (**YSP-18**); Boc-Phe-Pro-OH, 6,7-Dihydro-4h-pyrano[4,3-d]thiazol-2-ylamine 21% (**YSP-19**); *N*-benzyl L-proline, 2-Amino-4-methyl-5-acetylthiazole 23% (**YSP-22**); *N*-benzyl L-proline, 2-Amino-4,5,6,7-tetrahydro-7-oxobenzo[1]thiophene-3-carbonitrile 28% (**YSP-23**); N-benzyl L-proline, 2-Amino-5,5-dimethyl-5,6-dihydro-4h-benzothiazol-7-one 22% (**YSP-25**); 2-Amino-5,5-dimethyl-5,6-dihydro-4h-benzothiazol-7-one, Boc-Phe-Pro-OH 14% (**YSP-26**); *N*-benzyl L-proline, 1-(2-Amino-4-phenyl-thiazol-5-yl)-ethanone 15% (**YSP-29**).

Table 4. Biological evaluation of **CSSS58908458 (YSP8/9)** and analogues

Compd	Ubiquitin (25 μM, % inhibition)	Peptide (50 μM, % inhibition)
YSP6	20 ± 2	30 ± 1
YSP7	15 ± 5	29 ± 4
YSP8	39 ± 5	36 ± 7
YSP9	42 ± 3	40 ± 15
YSP11	20 ± 2	< 5%
YSP12	15 ± 5	< 5%
YSP13	39 ± 4	< 5%
YSP14	42 ± 5	30 ± 11
YSP17	< 5%	44 ± 9
YSP18	39 ± 3	24 ± 25
YSP19	< 5%	< 5%
YSP20	< 5%	27 ± 9
YSP22	< 5%	17 ± 5
YSP23	< 5%	43 ± 9
YSP25	< 5%	< 5%
YSP26	< 5%	< 5%
YSP29	< 5%	< 5%

Both compounds **YSP-17** and **YSP-23**, predicted to be covalent inhibitors, were active when the peptide was used as substrate, achieving a similar potency as the original hit molecule **YSP-9** (Table 3). The reduced analogues **YSP-6**, **YSP-7**, **YSP-11**, **YSP-18** are less active than the original hit molecule featuring a covalent warhead. The heterocyclic analogues **YSP-13**, **YSP-14**, **YSP-19** and **YSP-20**, and acyclic ketones analogues **YSP-22** and **YSP-29** all exhibited similar potencies which are less potent than the original hit molecule, suggesting the rigidity on the right-hand side of the molecules is necessary to maintain its potency while putting oxygen into the right hand side worsens the interaction with the enzyme. The substitution on the cyclohexanone ring **YSP-25** and **YSP-26** rendered the whole molecule inactive. It was realized that the ketone functional group, deemed to act as covalent warhead, was important for the observed activity. Overall **YSP-9**, the original hit molecule, remained the most active compound with both ubiquitin and peptide substrates.

Optimization through commercially available analogues and synthesis. Commercially available analogues of the two compounds shown in Figure 7 were also tested (Table 5). Unfortunately, the lack of diversity of **CSSS28078573** analogues did not allow an in-depth structure activity relationship. However, the drop in activity of compound **CSSS26687349** with both ubiquitin and peptide as substrate suggested that *ortho*-substitution was not tolerated on the terminal phenyl ring. More diversity was found for the **CSSS28008898** series but revealed that several modifications on the left-hand side of the molecule were tolerated, this group being predicted to be in the open P4+ pockets.

Table 5. Biological evaluation of **CSSS28078573** and analogues

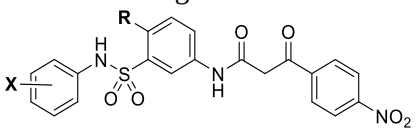

Compd	X	R	Ubiquitin (25 μM, % inhibition)	Peptide (50 μM, % inhibition)
CSSS28078573	4-Cl	Me	60 ± 9	63 ± 1
CSSS28077995	3-Cl	Me	46 ± 2	59 ± 14
CSSS28078486	4-Cl	Cl	< 5%	42 ± 12
CSSS28078547	4-Br	OMe	30 ± 2	59 ± 2
CSSS28078572	4-OMe	Cl	64 ± 5	74 ± 9
CSSS26687349	2-OMe	Me	12 ± 6	< 5%
KH-2			nd[a]	< 5%

[a] not determined.

Synthesis of analogue of CSSS28077995. From the commercially available analogues, modifications on the left-hand side of the molecules were investigated. The next step was to investigate the right-hand side of the molecule. We developed a simple 2-step strategy to synthesize **CSSS28077995** without a nitro group (**KH-2**) to see the effect of the nitro group in binding affinity to the enzyme (Scheme 9). The synthesis started with ethyl 3-(4-nitrophenyl)-3-oxopropanoate, hydrolysis of the ethyl ester gave intermediate **KH-1**, which was then coupled with 5-amino-*N*-(3-chlorophenyl)-2-methylbenzenesulfonamide in the presence of EDC.HCl and DMAP to give **KH-2** as the product. However, it was not active in 50 μM with peptide as a substrate, which suggests the nitro group is necessary for binding, likely to activate the ketone for covalent bond formation.

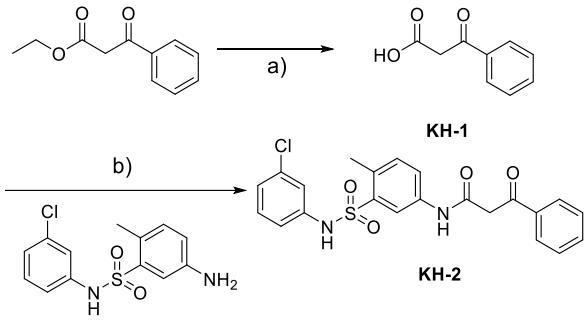

Scheme 9. a) NaOH, H_2O rt, 16 h, 63%; b) EDC·HCl, DMAP, DCM rt, 16 h, 53%

For *in vitro* assays of the commercially available analogues of **CSSS28008898**, the potency maintained the same (50 % inhibition at 50 μM with peptide as substrate) with the modifications on the left-hand side of the molecule (Table 6). Since there is not much improvement with the changes on the molecule, we suggested that this may be the best potency that this series is able to achieve.

Table 6. Biological evaluation of **CSSS28008898** and analogues

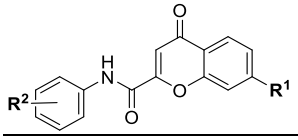

Compd	R^1 (structure and position)	R^2	Ubiquitin (25 μM, % inhibition)	Peptide (50 μM, % inhibition)
CSSS26427481	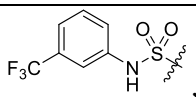 , para	H	< 5%	58 ± 3
CSSS26632702	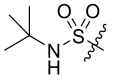 , meta	H	33 ± 5	46 ± 4
CSSS27787319	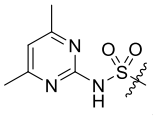 , para	Me	14 ± 13%	46 ± 2
CSSS28008898	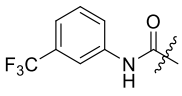 , meta	H	26 ± 4	50 ± 2
CSSS28020157	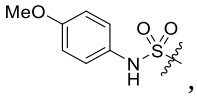 , para	H	< 5%	49 ± 10
CSSS28027203	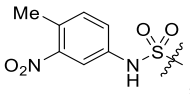 , para	H	55 ± 10	43 ± 25

Conclusion

Despite the absence of druggable binding pockets and the difficulty to engage strong interactions in the active site in PL^{pro}, our group rationally designed a first chemical series based on **VIR-251** and **GRL-0617** while four other novel chemical series of covalent inhibitors were discovered by virtual screening, all with micromolar range potencies *in vitro*. Preliminary SAR studies of the later four chemical series did not lead to inhibitors with potency low enough to warrant further investigation. In contrast, the design strategy of hybrid **VIR-251** and **GRL-0617** molecule was validated by biochemical assays which exhibited micromolar potency. Further optimization and testing of the hybrid molecule should be highly anticipated.

Experimental section

Virtual Screening

Structure-Based Drug Design and Virtual Screening. The FORECASTER (Suite2019-rev5679.1) developed by our group was used for the processing of chemical libraries and protein structures and for virtual screening.[49] BIOVIA Discovery Studio (version v20.1.0.1929) by Dassault Systèmes was used to visualize the docking-based virtual screening results.[50] PyMol (version 2.4.0a0) was used for additional structure visualization and generation of corresponding figures in this study.[51]

Library preparation. The ZINC molecular library with the following filters (1. Representation: 3D, 2. Reactivity: Hot, 3. Purchasability: Agent, 4. pH: Ref Mid, 5. Charge: 0, 5. Molecular Weight: 200 to 500, 6. LogP: -1 to 5.) was downloaded from the ZINC tranche browser

(http://zinc15.docking.org/tranches/home/).[46] This extracted library included more than 9 million compounds in 3D representation with hydrogen atoms added in sdf format. The acquired 3D Library was cleaned by the "Chemical library cleaning" module in FORECASTER. The full library was first processed by SMART (computing descriptors) and filtered by REDUCE to derive a focused library with desired physico-chemical properties and functional groups. In particular, only neutral molecules within molecular weights ranging from 150 to 550 g/mol and with at least one covalent warhead (aldehyde, boronic acid, ketone, Michael acceptor, nitrile, or epoxide) were included in this focused library. This finally led to the first library of 86,423 potential covalent inhibitors (library #1).

Alternatively, as it was reported that charged groups are tolerated by PL^{pro}, another library following the same criteria but with a net charge of 0 or +1 was also derived from a ChemSpace library of ca. 5M compounds. This library (library #2) included 25,640 compounds (15,142 with a charge of 0 and 10,498 with a charge of +1).

For virtual screening using our docking program FITTED, a structure of $3CL^{pro}$ co-crystallized to an α-ketoamide (PDB code: 6Y2G) and a structure of PL^{pro} in complex with a ubiquitin aldehyde covalently bound to the catalytic cysteine (PDB code: 4MM3) were selected and the libraries mentioned above were docked in covalent docking mode keeping the other parameters to their default values.

Analysis. The result files from virtual screening were post-processed using the "*Summarizing Results*" module in FORECASTER and the top 200 molecules with the highest FITTED_Score were selected. These docked molecules were visualized and inspected by a team of medicinal chemists, biochemists and computational chemists. Properties such as number of hydrogen bonds formed with the residues, conformational strains, whether the key interactions (hydrogen bond, hydrophobic) were present, predicted solubility were taken into consideration.

Synthesis and characterization

General Considerations. All commercially available reagents were used without further purification. All reactions, unless otherwise indicated, were carried out in flame-dried flasks under argon atmosphere with anhydrous solvents. FTIR spectra were recorded using a Perkin-Elmer Spectrum One FT-IR or Bruker ALPHA FTIR-ATR. ^{1}H and ^{13}C NMR spectra were recorded on Bruker 400 or 500 MHz or Varian 400 or 500 MHz spectrometers. Chemical shifts are reported in ppm using the residual of deuterated solvents as an internal standard. Thin layer chromatography visualization was performed by UV or by development using ninhydrin, para-anisaldehyde, vanillin, ceric ammonium molybdate, or KMnO4. Chromatography was performed on silica gel 60 (230−40 mesh) or using the Biotage One Isolera with ZIP cartridges. High resolution mass spectrometry was performed by ESI on a Bruker Maxis Impact API QqTOF or by ESI or APCI on a ThermoFisher Exactive Plus Orbitrap-API at McGill University. Prior to biological testing, reverse-phase HPLC was used to verify the purity of compounds on an Agilent 1100 series instrument, equipped with VWD-detector, using a C18 reverse column (Agilent, Eclipse -C18 150 mm Å~ 4.6 mm, 5 μm) with UV detection at 254 nm. All tested compounds were at least 95% pure. All compounds were stored at –20°C.

2-((2-benzoyl-4-chlorophenyl)amino)-2-oxoethyl acetate (XZ-1). DCC (0.372 g, 1.80 mmol) in DCM (2.5 mL) was added dropwise over 20 mins to a stirring solution of 2-amino-5-chlorobenzophenone (0.419 g, 1.81 mmol) and acetoxyacetic acid (0.197 g, 1.67 mmol) in DCM (2.5 mL) at 0 °C. The reaction mixture was then stirred for 4 h at room temperature. The mixture was filtered, and the filtrate concentrated. Recrystallization of the crude product in hexanes afforded the desired product (0.440 g, 79%). mp = 108 °C (hexanes). R_f = 0.41 (20% EtOAc/Hexanes). ^{1}H NMR ($CDCl_3$) δ 11.38 (s, 1 H), 8.68 (d, *J* = 9.6 Hz, 1 H), 7.72 3-7.68 m, 2 H), 7.64 (t, *J* = 7.5 Hz, 1 H), 7.57-7.50 (m, 4 H), 4.73 (s, 2 H), 2.35

(s, 3 H). ^{13}C NMR (126 MHz, $CDCl_3$) δ 198.34, 169.83, 166.56, 138.09, 137.98, 134.23, 133.13, 133.03, 130.01, 128.72, 128.11, 124.92, 123.03, 62.99, 20.88. HRMS (ESI/Q-TOF) m/z: calcd for $C_{17}H_{14}ClNNaO_4$ $[M + Na]^+$ 354.0504; found 354.0502. Percent purity: 97.4%.

***N*-(2-benzoyl-4-chlorophenyl)-2-hydroxyacetamide (XZ-2).** A solution of **XZ-1** (0.218 g, 0.657 mmol) and potassium carbonate (0.092 g, 0.666 mmol) in methanol (2.5 mL) was stirred at room temperature for 30 mins. The solution was quenched with saturated ammonium chloride, then extracted with DCM (3×10 mL). The organic layer was washed with brine, dried with sodium sulfate, and concentrated. Recrystallization in DCM/hexanes afforded the desired product (0.141 g, 74%). mp = 151 °C (DCM/hexanes). R_f = 0.53 (20% EtOAc/Hexanes). ^{1}H NMR ($CDCl_3$) δ 11.26 (s, 1 H), 8.67 (d, *J* = 8.8 Hz, 1 H), 7.73 (d, *J* = 8.2 Hz, 2 H), 7.65 (t, *J* = 7.5 Hz, 1 H), 7.58-7.500 (m, 4 H), 4.30 (s, 2 H), 2.61 (s, 1 H). ^{13}C NMR (126 MHz, $CDCl_3$) δ 197.99, 170.68, 137.80, 137.70, 133.87, 133.15, 132.58, 130.02, 128.60, 127.88, 125.34, 123.10, 62.88. HRMS (ESI/Q-TOF) m/z: calcd for $C_{15}H_{12}ClNNaO_3$ $[M + Na]^+$ 312.0398; found 312.0397. Percent purity: 99.6%.

2-((2-benzoyl-4-chlorophenyl)amino)-2-oxoethyl (*E*)-3-(2-methoxyphenyl)acrylate (XZ-3a). A solution of **XZ-2** (0.120 g, 0.414 mmol), 2-Methoxycinnamic acid (0.089 g, 0.499 mmol), and 4-Dimethylaminopyridine (0.011 g, 0.0900 mmol) in DCM (2.5 mL) was stirred at room temperature for 10 mins. EDC·HCl (0.096 g, 0.501 mmol) was then added, and the solution was stirred at room temperature for 24 h. The reaction mixture was quenched with saturated sodium bicarbonate stirring for 10 mins, then extracted with DCM (3×5 mL). The organic layer was washed with brine, dried with sodium sulfate, and concentrated. Column chromatography (15% to 80% EtOAc/hexanes) followed by recrystallization in DCM/hexanes afforded the desired product (0.132 g, 71% yield). mp = 131 °C (DCM/hexanes). R_f = 0.39 (20% EtOAc/Hexanes). ^{1}H NMR (500 MHz, $CDCl_3$) δ 11.46 (s, 1 H), 8.73 (dd, *J* = 8.5, 0.8 Hz, 1 H), 8.24 (d, *J* = 16.2 Hz, 1 H), 7.74-7.71 (m, 2 H), 7.67-7.56 (m, 4 H), 7.52 (t, *J* = 8.0 Hz, 2H), 7.41 (ddd, *J* = 8.4, 7.4, 1.7 Hz, 1 H), 7.00 (td, *J* = 7.5, 1.1 Hz, 1 H), 6.96 (dd, *J* = 8.4, 1.0 Hz, 1 H), 6.87 (d, *J* = 16.2 Hz, 1 H), 4.87 (s, 2 H), 3.88 (s, 3 H). ^{13}C NMR (126 MHz, $CDCl_3$) δ 197.88, 166.70, 165.99, 158.82, 142.71, 137.94, 137.83, 133.96, 132.95, 132.70, 131.85, 130.13, 129.95, 128.51, 127.96, 125.07, 123.28, 123.10, 120.66, 117.42, 111.17, 63.06, 55.42. HRMS (ESI/Q-TOF) m/z: calcd for $C_{25}H_{20}ClNNaO_5$ $[M + Na]^+$ 472.0922; found 472.0914. Percent purity: 98.9%。

2-((2-benzoyl-4-chlorophenyl)amino)-2-oxoethyl cinnamate (XZ-3b). A solution of **XZ-2** (30.1 mg, 0.104 mmol), *trans*-cinnamic acid (18.2 mg, 0.123 mmol), and 4-Dimethylaminopyridine (2.45 mg, 0.0201 mmol) in DCM (1 mL) was stirred at room temperature for 10 mins. EDC·HCl (23.6 mg, 0.123 mmol) was then added, and the solution was stirred at room temperature for 24 h. The reaction mixture was quenched with saturated sodium bicarbonate stirring for 10 mins, then extracted with DCM (3×5 mL). The organic layer was washed with brine, dried with sodium sulfate, and concentrated. Column chromatography (15% to 80% EtOAc/hexanes) followed by recrystallization in DCM/hexanes afforded the desired product (32.1 mg, 74% yield). mp = 148 °C (DCM/hexanes). R_f = 0.43 (20% EtOAc/Hexanes). ^{1}H NMR (500 MHz, $CDCl_3$) δ 11.49 (s, 1 H), 8.74 (dd, *J* = 8.0, 1.4 Hz, 1 H), 8.11 (d, *J* = 16.2 Hz, 1 H), 7.76-7.72 (m, 2 H), 7.69-7.62 (m, 3 H), 7.61 – 7.57 (m, 2 H), 7.54, (t, *J* = 8.1 Hz, 2 H), 7.48-7.41 (m, 3 H), 6.68 (d, *J* = 16.1 Hz, 1 H), 4.88 (s, 2 H). ^{13}C NMR (126 MHz, $CDCl_3$) δ 198.07, 166.46, 165.26, 146.90, 137.91, 137.78, 134.32, 134.04, 133.09, 132.75, 130.69, 130.01, 128.91, 128.57, 128.46, 128.03, 125.04, 123.08, 116.57, 63.20. HRMS (ESI/Q-TOF) m/z: calcd for $C_{24}H_{18}ClNNaO_4$ $[M + Na]^+$ 442.0817; found 442.0800. Percent purity: 99.2%.

2-((2-benzoyl-4-chlorophenyl)amino)-2-oxoethyl (*E*)-3-(4-(trifluoromethyl)phenyl)acrylate (XZ-3c). A solution of **XZ-2** (30.0 mg, 0.104 mmol), 4-(trifluoromethyl)cinnamic acid (26.8 mg, 0.124 mmol), and 4-dimethylaminopyridine (2.51 mg, 0.0205 mmol) in DCM (1 mL) was stirred at room temperature

for 10 mins. EDC·HCl (23.9 mg, 0.125 mmol) was then added, and the solution was stirred at room temperature for 24 h. The reaction mixture was quenched with saturated sodium bicarbonate stirring for 10 mins, then extracted with DCM (3×5 mL). The organic layer was washed with brine, dried with sodium sulfate, and concentrated. Column chromatography (15% to 80% EtOAc/hexanes) followed by recrystallization in DCM/hexanes afforded the desired product (40.5 mg, 80% yield). mp = 163 °C (DCM/hexanes). R_f = 0.39 (20% EtOAc/Hexanes). ^{1}H NMR (500 MHz, $CDCl_3$) δ 11.52 (s, 1 H), 8.75 (d, *J* = 8.7 Hz, 1 H), 8.14 (d, *J* = 16.2 Hz, 1 H), 7.77-7.65 (m, 7 H), 7.62 – 7.58 (m, 2 H), 7.55 (t, *J* = 7.8 Hz, 2 H), 6.74 (d, *J* = 16.2 Hz, 1 H), 4.89 (s, 2 H). ^{13}C NMR (200 MHz, $CDCl_3$) δ 198.32, 166.19, 164.67, 144.94, 137.92, 137.83, 137.66, 134.17, 133.17, 132.88, 132.11 (q, *J* = 32.7 Hz), 129.91, 128.62, 128.54, 128.11, 125.87 (q, *J* = 3.7 Hz), 124.92, 123.82 (q, *J* = 272.5 Hz), 123.03, 119.16, 63.33. ^{19}F NMR (470 MHz, $CDCl_3$) δ -62.87. HRMS (ESI/Q-TOF) m/z: calcd for $C_{25}H_{17}ClF_3NNaO_4$ $[M + Na]^+$ 510.0690; found 510.0705. Percent purity: 97.9%.

2-((2-benzoyl-4-chlorophenyl)amino)-2-oxoethyl (*E*)-but-2-enoate (XZ-3d). A solution of **XZ-2** (20.1 mg, 0.0694 mmol), crotonic acid (7.18 mg, 0.0834 mmol), and 4-Dimethylaminopyridine (1.77 mg, 0.0145 mmol) in DCM (1 mL) was stirred at room temperature for 10 mins. EDC·HCl (15.9 mg, 0.0829 mmol) was then added, and the solution was stirred at room temperature for 24 h. Additional amounts of crotonic acid (5.94 mg, 0.0690 mmol), EDC·HCl (13.2 mg, 0.0689 mmol), and DMAP (1.40 mg, 0.0165 mmol) were added, and the solution was stirred for another 2 h. The reaction mixture was quenched with saturated sodium bicarbonate stirring for 10 mins, then extracted with DCM (3×5 mL). The organic layer was washed with brine, dried with sodium sulfate, and concentrated. Column chromatography (15% to 80% EtOAc/hexanes) followed by recrystallization in DCM/hexanes afforded the desired product (8.68 mg, 35% yield). mp = 108 °C (DCM/hexanes). R_f = 0.35 (20% EtOAc/Hexanes). ^{1}H NMR (500 MHz, CD_3OD) δ 8.26 (d, *J* = 8.8 Hz, 1 H), 7.77-7.73 (m, 2 H), 7.69 (tt, *J* = 7.5, 1.3 Hz, 1 H), 7.65 (dd, *J* = 8.9, 2.5 Hz, 1 H), 7.59-7.53 (m, 3 H), 7.21 (dq, *J* = 15.6, 6.9 Hz, 1 H), 6.04 (dq, *J* = 15.6, 1.7 Hz, 1 H), 4.63 (s, 2 H), 1.95 (dd, *J* = 6.9, 1.7 Hz, 3 H). ^{13}C NMR (126 MHz, $CDCl_3$) δ 196.71, 167.24, 165.11, 146.99, 137.39, 136.10, 132.90, 132.67, 131.31, 129.51, 128.84, 128.49, 128.25, 124.04, 120.97, 62.21, 16.85. HRMS (ESI/Q-TOF) m/z: calcd for $C_{19}H_{16}ClNNaO_4$ $[M + Na]^+$ 380.0660; found 380.0656. Percent purity: 99.0%.

2-((2-benzoyl-4-chlorophenyl)amino)-2-oxoethyl (*E*)-3-(1H-imidazol-5-yl)acrylate (XZ-3e). a solution of **XZ-2** (20.0 mg, 0.0690 mmol), 4-Imidazoleacrylic acid (11.4 mg, 0.0825 mmol), and 4-Dimethylaminopyridine (3.21 mg, 0.0263 mmol) in DMSO (1 mL) was stirred at room temperature for 10 mins. EDC·HCl (31.5 mg, 0.164 mmol) was then added, and the solution was stirred at room temperature for 24 h. Additional amounts of EDC·HCl (16.0 mg, 0.0835 mmol), and DMAP (1.72 mg, 0.0141 mmol) were added, and the solution was stirred for another 24 h. The reaction mixture was quenched with saturated sodium bicarbonate stirring for 10 mins, then extracted with DCM (3×5 mL). The organic layer was washed with brine, dried with sodium sulfate, and concentrated. Column chromatography (40% to 100% EtOAc/hexanes) followed by recrystallization in DCM/hexanes afforded the desired product (10.3 mg, 36% yield). mp = 173 – 175 °C (DCM/hexanes). R_f = 0.10 (80% EtOAc/Hexanes). ^{1}H NMR (500 MHz, CD_3OD) δ 8.28 (d, *J* = 8.8 Hz, 1 H), 7.87 – 7.81 (m, 2 H), 7.76 – 7.72 (m, 2 H), 7.69-7.64 (m, 2 H), 7.56-7.51 (m, 3 H), 7.44 (s, 1 H), 6.55 (d, *J* = 15.8 Hz, 1 H), 4.69 (s, 2 H). ^{13}C NMR (100 MHz, CD_3OD) δ 196.59, 167.24, 166.04, 137.79, 137.40, 136.13, 132.93, 132.68, 131.27, 129.59, 128.83, 128.77, 128.28, 124.23, 113.33, 62.46. HRMS (ESI/Q-TOF) m/z: calculated for $C_{21}H_{16}ClN_3NaO_4$ $[M + Na]^+$ 432.0722; found 432.0722. Percent purity: 98.5%.

2-((2-benzoyl-4-chlorophenyl)amino)-2-oxoethyl (*E*)-3-(furan-3-yl)acrylate (XZ-3f). A solution of **XZ-2** (20.1 mg, 0.0694 mmol), 3-(3-Furyl)acrylic acid (11.5 mg, 0.0833 mmol), and 4-

dimethylaminopyridine (1.77 mg, 0.0145 mmol) in DCM (1 mL) was stirred at room temperature for 10 mins. EDC·HCl (15.9 mg, 0.0829 mmol) was then added, and the solution was stirred at room temperature for 24 h. The reaction mixture was quenched with saturated sodium bicarbonate stirring for 10 mins, then extracted with DCM (3×5 mL). The organic layer was washed with brine, dried with sodium sulfate, and concentrated. Column chromatography (15% to 80% EtOAc/hexanes) followed by recrystallization in DCM/hexanes afforded the desired product (15.39 mg, 54% yield). mp = 160 °C (DCM/hexanes). R_f = 0.35 (20% EtOAc/Hexanes). ^{1}H NMR (500 MHz, $CDCl_3$) δ 11.44 (s, 1 H), 8.73 (d, *J* = 9.0 Hz, 1 H), 8.00 (d, *J* = 15.9 Hz, 1 H), 7.75 – 7.70 (m, 3 H), 7.67 (tt, 7.4, 1.3 Hz, 1 H), 7.61-7.52 (m, 4 H), 7.50 – 7.48 (m, 1 H), 6.69 (d, *J* = 1.8 Hz, 1 H), 6.38 (d, *J* = 15.9 Hz, 1 H), 4.85 (s, 2 H). ^{13}C NMR (126 MHz, $CDCl_3$) δ 198.09, 166.49, 165.22, 145.17, 144.56, 137.88, 137.84, 136.97, 134.04, 133.10, 132.75, 129.91, 128.61, 128.03, 125.06, 123.09, 122.71, 116.26, 107.50, 63.11. HRMS (ESI/Q-TOF) m/z: calcd for $C_{22}H_{16}ClNNaO_5$ $[M + Na]^+$ 432.0609; found 432.0615. Percent purity: 99.7%.

***tert*-Butyl (2-((2-benzoyl-4-chlorophenyl)amino)-2-oxoethyl)carbamate (XZ-4a).** to a solution of Boc-Gly-OH (35.48 mg, 0.203 mmol) in DCM (2 mL), N-methylimidazole (31.9 μL, 0.400 mmol) and methanesulfonyl chloride (31.0 μL, 0.401 mmol) were added at 0 °C. The solution was stirred for 20 mins at room temperature, then 2-amino-5-chlorobenzophenone (51.11 mg, 0.221 mmol) was added at 0 °C. The solution was stirred for 48 h at room temperature. The reaction mixture was then diluted with water and the aqueous layer was extracted with DCM (3×5 mL). The organic layer was washed with brine, dried with sodium sulfate, and concentrated. Column chromatography (20% to 80% EtOAc/hexanes) followed by recrystallization in DCM/hexanes afforded the desired product (16.48 mg, 21% yield). R_f = 0.60 (40% EtOAc/Hexanes). ^{1}H NMR ($CDCl_3$) δ 11.14 (s, 1H), 8.65 (d, *J* = 8.8 Hz, 1H), 7.72 – 7.69 (m, 2H), 7.66 – 7.62 (m, 1H), 7.56 – 7.50 (m, 4H), 5.17 (s, 1H), 3.99 (d, *J* = 5.0 Hz, 2H), 1.46 (s, 9H). ^{13}C NMR (126 MHz, $CDCl_3$) δ 197.94, 168.76, 138.30, 137.77, 133.90, 132.97, 132.61, 129.94, 128.53, 127.65, 124.89, 122.98, 80.63, 45.37, 28.28. HRMS (ESI/Q-TOF) m/z: $[M + Na]^+$ calculated for $C_{20}H_{21}ClN_2NaO_4$ 411.1082; found 411.1078.

***tert*-Butyl (3-((2-benzoyl-4-chlorophenyl)amino)-3-oxopropyl)carbamate (XZ-4b).** to a solution of Boc-β-Ala-OH (37.82 mg, 0.200 mmol) in DCM, N-methylimidazole (31.9 μL, 0.400 mmol) and methanesulfonyl chloride (31.0 μL, 0.401 mmol) were added at 0 °C. The solution was stirred for 20 mins at room temperature, then 2-amino-5-chlorobenzophenone (50.27 mg, 0.217 mmol) was added at 0 °C. The solution was stirred for 48 h at room temperature. The reaction mixture was then diluted with water and the aqueous layer was extracted with DCM (3×5 mL). The organic layer was washed with brine, dried with sodium sulfate, and concentrated. Column chromatography (20% to 80% EtOAc/hexanes) followed by recrystallization in DCM/hexanes afforded the desired product (46.37 mg, 58% yield). R_f = 0.51 (40% EtOAc/Hexanes). ^{1}H NMR ($CDCl_3$) δ 10.65 (s, 1H), 8.60 (d, *J* = 9.6 Hz, 1H), 7.73 – 7.70 (m, 2H), 7.65 (tt, *J* = 7.4, 1.2 Hz, 1H), 7.56 – 7.51 (m, 4H), 5.15 (s, 1H), 3.50 (q, *J* = 5.9 Hz, 2H), 2.66 (t, *J* = 6.0 Hz, 2H), 1.42 (s, 9H). ^{13}C NMR (126 MHz, $CDCl_3$) δ 198.28, 170.76, 155.86, 138.58, 137.77, 133.90, 133.06, 132.68, 129.94, 128.60, 127.50, 124.75, 123.13, 79.34, 37.80, 36.32, 28.38. HRMS (ESI/Q-TOF) m/z: $[M + Na]^+$ calculated for $C_{21}H_{23}ClN_2NaO_4$ 425.1239; found 425.1236.

2-((2-benzoyl-4-chlorophenyl)amino)-2-oxoethan-1-aminium chloride (XZ-5a). compound **XZ-4a** (33.38 mg, 0.0858 mmol) was dissolved in a solution of 4 M HCl in dioxane (2 mL). The reaction mixture was stirred at room temperature for 2 h, and the solvent was removed in vacuo. Diethyl ether (1 mL) was then added to obtain the hydrochloric salt in quantitative yield. ^{1}H NMR (DMSO-d_6) δ 10.67 (s, 1H), 8.07 (s, 3H), 7.76 – 7.73 (m, 2H), 7.71 – 7.66 (m, 2H), 7.58 – 7.53 (m, 3H), 7.39 (d, *J* = 2.6 Hz, 1H), 3.55 (s, 2H). ^{13}C NMR (126 MHz, DMSO-d_6) δ 193.23, 165.06, 136.20, 133.67, 133.30, 131.43, 129.93, 128.91,

128.89, 128.49, 125.78, 40.55. HRMS (ESI/Q-TOF) m/z: $[M + Na]^+$ calculated for $C_{15}H_{13}ClN_2NaO_2$ 311.0558; found 311.0553.

3-((2-benzoyl-4-chlorophenyl)amino)-3-oxopropan-1-aminium chloride (XZ-5b). compound **XZ-4b** (35.28 mg, 0.0876 mmol) was dissolved in a solution of 4 M HCl in dioxane (2 mL). The reaction mixture was stirred at room temperature for 2 h, and the solvent was removed in vacuo. Diethyl ether (1 mL) was then added to obtain the hydrochloric salt in quantitative yield. ^{1}H NMR (DMSO-d_6) δ 10.31 (s, 1H), 7.72 – 7.64 (m, 7H), 7.54 – 7.50 (m, 3H), 7.42 (d, *J* = 2.6 Hz, 1H), 2.79 (s, 2H), 2.37 (t, *J* = 7.2 Hz, 2H). ^{13}C NMR (126 MHz, DMSO-d_6) δ 193.30, 168.27, 136.43, 134.34, 133.15, 133.09, 131.41, 129.56, 129.06, 128.74, 128.38, 125.98, 34.71, 32.64. HRMS (ESI/Q-TOF) m/z: $[M + Na]^+$ calculated for $C_{16}H_{15}ClN_2NaO_2$ 325.0714; found 325.0716.

(*E*)-*N*-(2-((2-benzoyl-4-chlorophenyl)amino)-2-oxoethyl)-3-(2-methoxyphenyl)acrylamide (XZ-6a). a solution of 2-Methoxycinnamic acid (19.44 mg), EDC·HCl (20.48 mg, 0.107 mmol), and 4-Dimethylaminopyridine (2.83 mg, 0.0232 mmol) in DCM (1 mL) was stirred at room temperature for 10 mins. **XZ-5a** (34.80 mg, 0.107 mmol) was then added, and the solution was stirred at room temperature for 24 h. Additional amounts of EDC·HCl (20.47 mg, 0.107 mmol), and DMAP (2.89 mg, 0.0237 mmol) were added, and the solution was stirred for another 21 h. The reaction mixture was quenched with saturated sodium bicarbonate stirring for 10 mins, then extracted with DCM (3×5 mL). The organic layer was washed with brine, dried with sodium sulfate, and concentrated. Column chromatography (50% to 100% EtOAc/hexanes) followed by recrystallization in DCM/hexanes afforded the desired product (17.28 mg, 36% yield). R_f = 0.39 (60% EtOAc/Hexanes). ^{1}H NMR ($CDCl_3$) δ 11.02 (s, 1H), 8.62 (d, *J* = 8.5 Hz, 1H), 7.96 (d, *J* = 15.9 Hz, 1H), 7.73 – 7.70 (m, 2H), 7.65 (tt, *J* = 7.5, 1.2 Hz, 1H), 7.59 – 7.50 (m, 5H), 7.36 (ddd, *J* = 8.4, 7.5, 1.8 Hz, 1H), 7.00 (dd, *J* = 7.6, 1.1 Hz, 1H), 6.95 (d, *J* = 8.4 Hz, 1H), 6.71 (d, *J* = 15.9 Hz, 1H), 6.32 (t, *J* = 5.0 Hz, 1H), 4.30 (d, *J* = 5.3 Hz, 2H), 3.91 (s, 3H). ^{13}C NMR (126 MHz, $CDCl_3$) δ 198.01, 168.06, 166.97, 158.40, 138.13, 137.67, 133.90, 133.00, 132.65, 131.00, 129.96, 129.33, 128.55, 127.89, 125.07, 123.64, 123.18, 120.66, 120.61, 111.12, 55.43, 44.33. HRMS (ESI/Q-TOF) m/z: $[M + Na]^+$ calculated for $C_{25}H_{21}ClN_2NaO_4$ 471.1082; found 471.1084.

(*E*)-*N*-(3-((2-benzoyl-4-chlorophenyl)amino)-3-oxopropyl)-3-(2-methoxyphenyl)acrylamide (XZ-6b). a solution of 2-Methoxycinnamic acid (22.75 mg, 0.128 mmol), EDC·HCl (48.31 mg, 0.252 mmol), and 4-Dimethylaminopyridine (6.43 mg, 0.0526 mmol) in DCM (1 mL) was stirred at room temperature for 10 mins. **XZ-5b** (42.92 mg, 0.127 mmol) was then added, and the solution was stirred at room temperature for 22 h. The reaction mixture was quenched with saturated sodium bicarbonate stirring for 10 mins, then extracted with DCM (3×5 mL). The organic layer was washed with brine, dried with sodium sulfate, and concentrated. Column chromatography (50% to 100% EtOAc/hexanes) followed by recrystallization in DCM/hexanes afforded the desired product (16.05 mg, 27% yield). R_f = 0.33 (60% EtOAc/Hexanes). ^{1}H NMR ($CDCl_3$) δ 10.65 (s, 1H), 8.59 (d, J = 8.7 Hz, 1H), 7.87 (d, J = 15.9 Hz, 1H), 7.74 – 7.71 (m, 2H), 7.64 (tt, J = 7.5, 1.2 Hz, 1H), 7.58 – 7.50 (m, 4H), 7.45 (dd, J = 7.7, 1.8 Hz, 2H), 7.32 (ddd, J = 8.2, 7.3, 1.7 Hz, 1H), 6.95 (t, J = 7.6 Hz, 1H), 6.92 (d, J = 8.2 Hz, 1H), 6.53 (d, J = 15.7 Hz, 1H), 6.41 (t, J = 5.8 Hz, 1H), 3.89 (s, 3H), 3.78 (q, J = 6.2 Hz, 2H), 2.77 (t, J = 5.8 Hz, 2H). ^{13}C NMR (126 MHz, $CDCl_3$) δ 198.16, 171.05, 166.49, 158.27, 138.38, 137.66, 136.66, 133.83, 133.08, 132.67, 130.70, 129.96, 129.22, 128.58, 127.67, 125.01, 123.81, 123.17, 121.62, 120.62, 111.05, 55.40, 37.18, 35.18. HRMS (ESI/Q-TOF) m/z: $[M + Cl]^-$ calculated for $C_{26}H_{23}Cl_2N_2O_4$ 497.1040; found 497.1052.

Methyl 2-(2-acetoxyacetamido)-5-methylbenzoate (XZ-7). DCC (0.371 g, 1.80 mmol) in DCM (2.5 mL) was added dropwise to a stirring solution of methyl 2-amino-5-chlorobenzoate (0.300 g, 1.62 mmol) and acetoxyacetic acid (0.197 g, 1.67 mmol) in DCM (2.5 mL) at 0 °C. The reaction mixture was then stirred for 20 h at room temperature. The mixture was filtered, and the filtrate concentrated.

Recrystallization of the crude product in DCM/hexanes afforded the desired product (0.285 g, 61% yield). R_f = 0.32 (20% EtOAc/Hexanes). ^{1}H NMR ($CDCl_3$) δ 11.67 (s, 1H), 8.76 (d, J = 9.2 Hz, 1H), 8.04 (d, J = 2.6 Hz, 1H), 7.53 (dd, J = 9.2, 2.6 Hz, 1H), 4.76 (s, 2H), 3.97 (s, 3H), 2.34 (s, 3H). ^{13}C NMR (126 MHz, $CDCl_3$) δ 169.72, 167.49, 166.33, 139.05, 134.57, 130.53, 128.29, 121.81, 116.70, 62.92, 52.66, 20.65. HRMS (ESI/Q-TOF) m/z: $[M + Na]^+$ calculated for $C_{12}H_{12}ClNNaO_5$ 308.0296; found 308.0286.

Methyl 5-chloro-2-(2-hydroxyacetamido)benzoate (XZ-8). a solution of **XZ-7** (0.285 g, 0.998 mmol) and potassium carbonate (0.138 g, 0.998 mmol) in methanol (3 mL) was stirred at room temperature for 1 h. The solution was diluted with water, and the product was collected by vacuum filtration (0.156 g, 64%). ^{1}H NMR ($CDCl_3$) δ 11.66 (s, 1H), 8.75 (d, *J* = 9.3 Hz, 1H), 8.03 (d, *J* = 1.8 Hz, 1H), 7.52 (dd, *J* = 8.8, 2.4 Hz, 1H), 4.31 (d, *J* = 5.2 Hz, 2H), 3.95 (s, 3H), 2.48 (t, *J* = 5.4 Hz, 1H). ^{13}C NMR (126 MHz, $CDCl_3$) δ 171.32, 165.94, 138.50, 133.35, 133.31, 129.73, 126.66, 120.99, 116.33, 61.87, 51.93. HRMS (ESI/Q-TOF) m/z: $[M + Na]^+$ calculated for $C_{10}H_{10}ClNNaO_4$ 266.0191; found 266.0188.

Methyl (*E*)-5-chloro-2-(2-((3-(2-methoxyphenyl)acryloyl)oxy)acetamido)benzoate (XZ-9). a solution of 2-Methoxycinnamic acid (87.4 mg, 0.491 mmol), EDC·HCl (94.6 mg, 0.493 mmol), and 4-Dimethylaminopyridine (10.1 mg, 0.0824 mmol) in DMF (3 mL) was stirred at room temperature for 10 mins. **XZ-8** (100.0 mg, 0.410 mmol) was then added, and the solution was stirred at room temperature for 20 h. The precipitate that was formed was filtered and washed with DMF, dried and collected. (96.8 mg, 58% yield). ^{1}H NMR ($CDCl_3$) δ 11.76 (s, 1H), 8.78 (d, *J* = 9.0 Hz, 1H), 8.22 (d, *J* = 16.2 Hz, 1H), 8.03 (d, *J* = 2.6 Hz, 1H), 7.62 (dd, *J* = 7.7, 1.8 Hz, 1H), 7.53 (dd, *J* = 9.0, 2.7 Hz, 1H), 7.44 – 7.37 (m, 1H), 7.00 (t, *J* = 7.5 Hz, 1H), 6.96 (d, *J* = 8.3 Hz, 1H), 6.82 (d, *J* = 16.2 Hz, 1H), 4.87 (s, 2H), 3.92 (s, 3H), 3.91 (s, 3H). ^{13}C NMR (126 MHz, $CDCl_3$) δ 167.32, 166.64, 166.03, 158.72, 142.41, 139.09, 134.50, 131.91, 130.50, 129.59, 128.24, 123.31, 121.96, 120.70, 117.37, 116.85, 111.25, 63.09, 55.49, 52.57. HRMS (ESI/Q-TOF) m/z: $[M + Na]^+$ calculated for $C_{20}H_{18}ClNNaO_6$ 426.0715; found 426.0710

2-((2-(benzylcarbamoyl)-4-chlorophenyl)amino)-2-oxoethyl (E)-3-(2-methoxyphenyl)acrylate (XZ-10). Lithium iodide (7.1 mg, 0.0533 mmol) was added to a solution of **XZ-9** (20.1 mg, 0.0498 mmol) in anhydrous pyridine (2 mL) and the solution was heated to 160 °C for 15 mins in a microwave reactor. The solvent was then removed in vacuo. The crude product was redissolved in DCM (1 mL) followed by addition of EDC·HCl (12.0 mg, 0.0627 mmol), DMAP (1.4 mg, 0.0115 mmol), and benzylamine (5.4 µL, 0.0495 mmol), and the solution was stirred at room temperature for 20 h. The reaction mixture was diluted with water and extracted with DCM (3×5 mL). The organic layer was washed with brine, dried with sodium sulfate, and concentrated. Column chromatography (20% to 80% EtOAc/hexanes) followed by recrystallization in DCM/hexanes afforded the desired product (5.27 mg, 22% yield). R_f = 0.16 (20% EtOAc/Hexanes). ^{1}H NMR (500 MHz, $CDCl_3$) δ 11.71 (s, 1H), 8.66 (d, *J* = 9.3 Hz, 1H), 8.22 (d, *J* = 16.3 Hz, 1H), 7.58 (dd, *J* = 7.9, 1.7 Hz, 1H), 7.46 – 7.42 (m, 2H), 7.36 – 7.27 (m, 6H), 6.92 – 6.88 (m, 2H), 6.82 (d, *J* = 16.3 Hz, 1H), 6.40 (s, 1H), 4.84 (s, 2H), 4.54 (d, *J* = 5.6 Hz, 2H), 3.86 (s, 3H). ^{13}C NMR (126 MHz, $CDCl_3$) δ 167.28, 166.53, 166.17, 158.71, 142.39, 137.27, 137.17, 132.53, 131.77, 129.81, 128.94, 128.40, 127.96, 127.88, 126.26, 123.33, 123.06, 122.21, 120.67, 117.57, 111.15, 63.02, 55.44, 44.11. HRMS (ESI/Q-TOF) m/z: $[M + Na]^+$ calculated for $C_{26}H_{23}ClN_2NaO_5$ 501.1188; found 501.1167.

(*S*)-1-Benzyl-*N*-(4,5,6,7-tetrahydrobenzo[1]thiazol-2-yl)pyrrolidine-2-carboxamide (YSP-6). 1-Ethyl-3-(3-dimethylaminopropyl)carbodiimide hydrochloride (EDC.HCl, 1.2 eq, 0.72 mmol, 138 mg) and *N*,*N*-diisopropylethylamine (2 eq, 1.3 mmol, 168 mg) were added to a solution of 4,5,6,7-tetrahydro-1,3-benzothiazol-2-amine (1 eq, 0.65 mmol, 100 mg) and (*R*)-1-benzyl-pyrrolidine-2-carboxylic acid (1.5 eq, 0.975 mmol, 199.9 mg) in dichloromethane (10 mL). The mixture was stirred for 24 h at room temperature. After the reaction is complete, the solvent was evaporated, and the residue dissolved in EtOAc, water was

added and the mixture was extracted with ethyl acetate. The organic layers were combined, washed with water, brine, dried over sodium sulfate and evaporated under vacuum. The residue was purified by flash chromatography using 20-100% EtOAc in hexane to afford **YSP-6** (22 mg, 10%). White solid, mp = 86 °C, EtOAc), R*f* = 0.76 (Hex/EtOAc, 1:9). HPLC (t_R=16.2 min; purity: 95.9 %, H_2O/MeCN). ^{1}H NMR (CD_3OD) δ 7.37 (d, *J* = 7.2 Hz, 2H), 7.26 (dd, *J* = 8.4, 6.8 Hz, 2H), 7.18 (t, *J* = 7.4 Hz, 1H), 3.79 (d, *J* = 12.6 Hz, 1H), 3.72 (d, *J* = 12.6 Hz, 1H), 3.38 (dd, *J* = 10.2, 4.6 Hz, 1H), 3.15 (ddd, *J* = 8.7, 6.3, 2.2 Hz, 1H), 2.70 – 2.58 (m, 4H), 2.53 (td, *J* = 9.8, 6.5 Hz, 1H), 2.28 (dtd, *J* = 12.9, 9.9, 7.9 Hz, 1H), 1.94 – 1.72 (m, 7H). ^{13}C NMR (CD_3OD) δ 174.67, 156.31, 145.14, 139.27, 130.31, 129.50, 128.44, 124.13, 67.62, 60.84, 55.30, 31.71, 27.14, 25.07, 24.38, 24.04, 23.66. HRMS (ESI+) for $C_{19}H_{24}N_3OS$ [M + H], calcd: 342.1635, found: 342.1631

(*R*)-1-Benzyl-N-(4,5,6,7-tetrahydrobenzo[1]thiazol-2-yl)pyrrolidine-2-carboxamide (YSP-7). Following the protocol used with **YSP-6**, the coupling of (*S*)-1-benzyl-pyrrolidine-2-carboxylic acid (1.5 eq, 0.975 mmol, 199.9 mg) and 4,5,6,7-tetrahydro-1,3-benzothiazol-2-amine (1eq, 0.65 mmol, 100 mg) led to **YSP-6** (33 mg 15%). White solid, mp = 91 °C, EtOAc), R*f* = 0.72 (Hex/EtOAc, 1:9). HPLC (t_R= 16.2 min; purity: 97.3%, 5-95% MeCN in H_2O). ^{1}H NMR (500 MHz, DMSO-d6) δ 11.29 (s, 1H), 7.36 – 7.31 (m, 2H), 7.31 – 7.26 (m, 2H), 7.26 – 7.19 (m, 1H), 3.81 (d, *J* = 13.2 Hz, 1H), 3.56 (d, *J* = 13.2 Hz, 1H), 3.41 (dd, *J* = 9.3, 4.7 Hz, 2H), 3.31 (s, 4H), 2.99 – 2.92 (m, 1H), 2.63 (tt, *J* = 4.5, 1.6 Hz, 2H), 2.55 (td, *J* = 5.4, 2.9 Hz, 2H), 2.42 – 2.34 (m, 1H), 2.19 – 2.08 (m, 1H), 1.85 – 1.71 (m, 7H). ^{13}C NMR (126 MHz, DMSO-d6) δ 171.95, 154.09, 143.98, 138.67, 128.57, 128.21, 126.97, 121.45, 65.76, 57.99, 52.84, 29.69, 25.99, 23.35, 22.94, 22.63, 22.27. HRMS (ESI+) for $C_{19}H_{24}N_3OS$ [M + H], calcd: 342.1635, found: 342.1655.

(*S*)-1-Benzyl-*N*-(7-oxo-4,5,6,7-tetrahydrobenzo[1]thiazol-2-yl)pyrrolidine-2-carboxamide (YSP-8). Following the protocol used with **YSP-6**, 2-amino-4,5,6,7-tetrahydro-1,3-benzothiazol-7-one (1 eq, 0.60 mmol, 100 mg) and (*R*)-1-benzyl-pyrrolidine-2-carboxylic acid (1.2 eq, 0.72 mmol, 147.6 mg) led to **YSP-8** (27 mg 9%). Yellowish solid, mp = 93 °C, EtOAc), R*f* = 0.57 (Hex/EtOAc, 1:9). HPLC (t_R= 14.5 min; purity: 94.9 %, 5-95% MeCN in H_2O). ^{1}H NMR (500 MHz, DMSO-d6) δ 12.08 (s, 1H), 7.35 – 7.24 (m, 4H), 7.24 – 7.16 (m, 1H), 3.81 (d, *J* = 13.1 Hz, 1H), 3.60 (d, *J* = 13.1 Hz, 1H), 3.48 (dd, *J* = 9.2, 4.7 Hz, 1H), 3.02 – 2.94 (m, 1H), 2.91 – 2.81 (m, 2H), 2.48 (s, 3H), 2.45 – 2.36 (m, 1H), 2.23 – 2.11 (m, 1H), 2.08 (p, *J* = 6.2 Hz, 2H), 1.88 – 1.80 (m, 2H), 1.80 – 1.70 (m, 1H). ^{13}C NMR (126 MHz, DMSO-d6) δ 192.07, 173.44, 164.11, 162.33, 138.55, 128.64, 128.13, 126.94, 123.47, 65.77, 57.89, 52.94, 37.24, 29.69, 26.36, 23.28, 22.66. HRMS (ESI+) for $C_{19}H_{21}N_3O_2NaS$ [M + Na], calcd: 378.1247, found: 378.1254.

(*R*)-1-Benzyl-*N*-(7-oxo-4,5,6,7-tetrahydrobenzo[1]thiazol-2-yl)pyrrolidine-2-carboxamide (YSP-9). Following the protocol used with **YSP-6**, 2-amino-4,5,6,7-tetrahydro-1,3-benzothiazol-7-one (1 eq, 0.60 mmol, 100 mg) and (*S*)-1-benzyl-pyrrolidine-2-carboxylic acid (1.2 eq, 0.72 mmol, 147.6 mg) led to **YSP-9** (39 mg 13%). White solid, mp = 107°C (EtOAc), R*f* = 0.52 (Hex/EtOAc, 1:9). HPLC (t_R = 14.5 min; purity: 98.7 %, 5-95% MeCN in H_2O). ^{1}H NMR (500 MHz, DMSO-d6) δ 12.08 (s, 1H), 7.35 – 7.23 (m, 4H), 7.23 – 7.16 (m, 1H), 3.81 (d, *J* = 13.1 Hz, 1H), 3.60 (d, *J* = 13.1 Hz, 1H), 3.48 (dd, *J* = 9.3, 4.8 Hz, 1H), 2.98 (dtd, *J* = 9.1, 4.6, 3.1 Hz, 1H), 2.91 – 2.82 (m, 2H), 2.48 (s, 1H), 2.46 – 2.36 (m, 1H), 2.21 – 2.11 (m, 1H), 2.11 – 2.04 (m, 2H), 1.88 – 1.82 (m, 1H), 1.82 – 1.78 (m, 1H), 1.75 (ddt, *J* = 11.0, 7.2, 4.1 Hz, 1H). ^{13}C NMR (126 MHz, DMSO-d6) δ 192.07, 173.45, 164.11, 162.34, 138.55, 128.64, 128.13, 126.94, 123.46, 65.77, 57.88, 52.94, 37.24, 29.69, 26.36, 23.28, 22.66. HRMS (ESI+) for $C_{19}H_{21}N_3O_2NaS$ [M + Na], calcd: 378.1245, found: 378.1242.

1-Benzyl-*N*-(7-oxo-4,5,6,7-tetrahydrobenzo[1]thiazol-2-yl)piperidine-2-carboxamide (YSP-12). 1-Ethyl-3-(3-dimethylaminopropyl)carbodiimide hydrochloride (EDC.HCl, 1.2eq, 0.72 mmol, 138 mg) and N,N-diisopropylethylamine (2eq, 1.2 mmol, 155.1 mg) was added to a solution of 2-amino-4,5,6,7-

tetrahydro-1,3-benzothiazol-7-one (1eq, 0.60 mmol, 100 mg), 1-Benzyl piperidine-2-carboxylic acid (1.2eq, 0.72 mmol, 157.9 mg) and 1-hydroxybenzotriazole hydrate (1.2eq, 0.72 mmol, 97.2 mg) in dimethylformamide (10 ml). The mixture was stirred for 24h at room temperature. After the reaction is complete, the solvent was evaporated, and the residue dissolved in EtOAc (15 mL), water was added and the mixture was extracted with ethyl acetate (3x30 mL). The organic layers were combined, washed with water, brine, dried over sodium sulfate and evaporated under vacuum using a rotatory evaporator. The residue was purified by flash chromatography using 20-100% EtOAc in hexane to afford **YSP-12** (33 mg 15%). White solid, mp = 156 °C (EtOAc), R*f* = 0.61 (Hex/EtOAc, 1:9). HPLC (t_R = 14.36 min; purity: 95.9 %, 5-95% MeCN in H_2O). ^{1}H NMR (500 MHz, DMSO) δ 12.52 (s, 1H), 7.33 – 7.28 (m, 4H), 7.23 (td, *J* = 5.7, 5.3, 2.8 Hz, 1H), 3.65 (d, *J* = 13.5 Hz, 1H), 3.28 (d, *J* = 4.0 Hz, 2H), 2.92 – 2.83 (m, 3H), 2.48 (s, 1H), 2.08 (qd, *J* = 6.6, 2.9 Hz, 3H), 1.75 (ddd, *J* = 31.5, 12.9, 9.3 Hz, 3H), 1.62 (dd, *J* = 10.8, 6.1 Hz, 1H), 1.52 – 1.42 (m, 2H), 1.38 – 1.27 (m, 1H). ^{13}C NMR (126 MHz, DMSO) δ 192.04, 164.17, 162.58, 138.23, 129.91, 128.65, 128.14, 126.95, 123.43, 64.88, 59.42, 49.97, 37.26, 28.96, 26.38, 24.46, 22.66, 22.26. HRMS (ESI+) for $C_{20}H_{24}N_3O_2S$ (M + H), calcd: 370.15837, found: 370.15850.

***tert*-Butyl ((*S*)-1-oxo-1-((*S*)-2-((7-oxo-4,5,6,7-tetrahydrobenzo[1]thiazol-2-yl)carbamoyl)pyrrolidin-1-yl)-3-phenylpropan-2-yl)carbamate (YSP-17).** Following the protocol used with **YSP-12**, 2-amino-4,5,6,7-tetrahydro-1,3-benzothiazol-7-one (1eq, 0.60 mmol, 100 mg) and Boc-Phe-Pro-OH (1.2eq, 0.72 mmol, 261 mg) led to **YSP-17** (83 mg 27%). White solid, mp = 151 °C (EtOAc), R*f* = 0.87 (Hex/EtOAc, 1:9). HPLC (t_R = 14.08 min; purity: 99.82 %, 5-95% MeCN in H_2O). ^{1}H NMR (500 MHz, DMSO) δ 12.70 (s, 1H), 7.32 – 7.24 (m, 4H), 7.22 – 7.19 (m, 1H), 7.06 (d, *J* = 8.3 Hz, 1H), 4.58 (dd, *J* = 8.5, 5.1 Hz, 1H), 4.41 – 4.33 (m, 1H), 4.03 (q, *J* = 7.1 Hz, 1H), 3.72 (dt, *J* = 9.7, 6.7 Hz, 1H), 3.64 (dt, *J* = 9.9, 6.8 Hz, 1H), 2.96 (dd, *J* = 14.0, 4.0 Hz, 1H), 2.87 (t, *J* = 6.2 Hz, 2H), 2.74 (dd, *J* = 14.0, 10.0 Hz, 1H), 2.20 (dq, *J* = 12.6, 7.3 Hz, 1H), 2.13 – 2.04 (m, 2H), 2.04 – 1.83 (m, 4H), 1.29 (s, 7H), 1.22 (s, 1H), 1.17 (t, *J* = 7.1 Hz, 1H), 1.10 (s, 1H). ^{13}C NMR (126 MHz, DMSO) δ 192.06, 171.40, 170.51, 164.24, 162.69, 155.32, 137.90, 129.33, 128.07, 126.27, 123.51, 78.03, 53.82, 46.78, 37.25, 36.14, 28.97, 28.14, 26.39, 24.88, 22.67, 20.76. HRMS (ESI+) for $C_{26}H_{32}N_4O_5NaS$ (M + Na), calcd: 535.1986, found: 535.1974.

1-Benzyl-*N*-(4,5,6,7-tetrahydrobenzo[1]thiazol-2-yl)piperidine-2-carboxamide (YSP-11). Following the protocol used with **YSP-12** of 4,5,6,7-tetrahydro-1,3-benzothiazol-2-amine (1eq, 0.65 mmol, 100 mg) and 1-Benzyl piperidine-2-carboxylic acid (1.2eq, 0.78 mmol, 171.1 mg) led to **YSP-11** (27 mg 12%). White solid, mp = 117°C (EtOAc), R*f* = 0.69 (Hex/EtOAc, 1:9). HPLC (t_R = 16.69 min; purity: 98.2 %, 5-95% MeCN in H_2O). ^{1}H NMR (500 MHz, DMSO) δ 11.74 (s, 1H), 7.35 – 7.27 (m, 4H), 7.23 (m, 1H), 3.64 (d, *J* = 13.4 Hz, 1H), 3.25 (d, *J* = 13.4 Hz, 1H), 3.18 (dd, *J* = 8.6, 3.9 Hz, 1H), 2.85 (dt, *J* = 11.5, 4.4 Hz, 1H), 2.62 (m, *J* = 2.1 Hz, 2H), 2.55 (td, *J* = 5.8, 5.0, 2.9 Hz, 2H), 2.10 – 1.97 (m, 2H), 1.76 (m, 5H), 1.74 – 1.69 (m, 1H), 1.69 – 1.60 (m, 1H), 1.53 – 1.40 (m, 2H), 1.29 (s, 1H). ^{13}C NMR (126 MHz, DMSO) δ 171.70, 154.34, 143.99, 138.36, 128.64, 128.12, 126.90, 121.37, 65.06, 59.34, 50.10, 29.05, 25.99, 24.49, 22.94, 22.63, 22.47, 22.23. HRMS (ESI+) for $C_{20}H_{26}N_3OS$ (M + H), calcd: 356.17911, found: 356.17927.

1-Benzyl-*N*-(6,7-dihydro-4*H*-pyrano[4,3-d]thiazol-2-yl)piperidine-2-carboxamide (YSP-20). Following the protocol used with **YSP-12**, 6,7-dihydro-4H-pyrano[4,3-d]thiazol-2-ylamine (1eq, 0.64 mmol, 100 mg) and 1-benzyl piperidine-2-carboxylic acid (1.2eq, 0.77 mmol, 168.9 mg) led to **YSP-20** (72 mg 32%). White solid, mp = 112 °C (EtOAc), R*f* = 0.55 (Hex/EtOAc, 1:9). HPLC (t_R = 15.03 min; purity: 95.3 %, 5-95% MeCN in H_2O). ^{1}H NMR (500 MHz, DMSO) δ 7.35 – 7.28 (m, 4H), 7.23 (ddd, *J* = 8.6, 5.4, 2.5 Hz, 1H), 4.67 (t, *J* = 2.0 Hz, 2H), 3.90 (t, *J* = 5.6 Hz, 2H), 3.64 (d, *J* = 13.3 Hz, 1H), 3.26 (d, *J* = 13.4 Hz, 1H), 3.21 (dd, *J* = 8.7, 3.9 Hz, 1H), 2.86 (dt, *J* = 11.5, 4.4 Hz, 1H), 2.66 (td, *J* = 5.5, 2.8

Hz, 2H), 2.10 – 2.00 (m, 2H), 1.83 – 1.60 (m, 3H), 1.47 (dtq, *J* = 18.6, 9.4, 4.3 Hz, 2H), 1.31 (ddt, *J* = 13.9, 9.5, 4.8 Hz, 1H). ^{13}C NMR (126 MHz, DMSO) δ 171.93, 155.60, 141.85, 138.34, 128.65, 128.13, 126.91, 119.38, 64.98, 64.58, 63.22, 59.37, 50.09, 29.07, 26.84, 24.50, 22.44. HRMS (ESI+) for $C_{19}H_{24}N_3O_2S$ (M + H), calcd: 358.1584, found: 358.1576.

(*S*)-1-benzyl-*N*-(6,7-dihydro-4*H*-pyrano[4,3-d]thiazol-2-yl)pyrrolidine-2-carboxamide (YSP-13). Following the protocol used with **YSP-12**, 6,7-dihydro-4H-pyrano[4,3-d]thiazol-2-ylamine (1eq, 0.64 mmol, 100 mg) and (*S*)-1-*N*-benzyl-proline (1.2eq, 0.72 mmol, 157.9 mg) led to **YSP-13** (43 mg 20%). White solid, mp = 132 °C (EtOAc), R*f* = 0.50 (Hex/EtOAc, 1:9). HPLC (t_R = 14.55 min; purity: 99.3 %, 5-95% MeCN in H_2O). ^{1}H NMR (500 MHz, DMSO) δ 11.52 (s, 1H), 7.42 – 7.32 (m, 4H), 7.32 – 7.25 (m, 1H), 4.73 (d, *J* = 1.9 Hz, 2H), 3.97 (t, *J* = 5.6 Hz, 2H), 3.88 (d, *J* = 13.2 Hz, 1H), 3.64 (d, *J* = 13.1 Hz, 1H), 3.53 – 3.42 (m, 2H), 3.06 – 2.99 (m, 1H), 2.71 (dd, *J* = 11.7, 9.8 Hz, 2H), 2.56 (p, *J* = 1.8 Hz, 4H), 2.45 (q, *J* = 8.0 Hz, 1H), 2.26 – 2.15 (m, 1H), 1.84 (ddddd, *J* = 19.9, 15.7, 12.2, 7.9, 4.4 Hz, 3H). ^{13}C NMR (126 MHz, DMSO) δ 172.67, 155.85, 142.29, 139.13, 129.05, 128.66, 127.43, 119.89, 66.19, 65.06, 63.70, 58.46, 53.34, 30.17, 27.32, 23.82. HRMS (ESI+) for $C_{18}H_{22}N_3O_2S$ (M + H), calcd: 344.14272, found: 344.14282.

(*R*)-1-Benzyl-*N*-(6,7-dihydro-4*H*-pyrano[4,3-d]thiazol-2-yl)pyrrolidine-2-carboxamide (YSP-14). Following the protocol used with **YSP-12**, 6,7-dihydro-4H-pyrano[4,3-d]thiazol-2-ylamine (1eq, 0.64 mmol, 100 mg) and (*R*)-1-benzyl-pyrrolidine-2-carboxylic acid (1.2eq, 0.77 mmol, 157.9 mg) led to **YSP-14** (67 mg 31%). White solid, melting point (119°C, EtOAc), R*f* = 0.61 (Hex/EtOAc, 1:9). HPLC (t_R =14.26 min; purity: 99.8 %, 5-95% MeCN in H_2O). ^{1}H NMR (500 MHz, DMSO) δ 11.45 (m, 4H), 7.36 – 7.26 (m, 4H), 7.25 – 7.18 (m, 1H), 4.67 (t, *J* = 1.9 Hz, 2H), 3.90 (t, *J* = 5.6 Hz, 2H), 3.82 (d, *J* = 13.1 Hz, 1H), 3.58 (d, *J* = 13.1 Hz, 1H), 3.43 (dd, *J* = 9.2, 4.7 Hz, 1H), 3.00 – 2.93 (m, 1H), 2.66 (tq, *J* = 5.8, 2.0 Hz, 2H), 2.43 – 2.35 (m, 1H), 2.20 – 2.08 (m, 1H), 1.78 (dtt, *J* = 20.1, 8.0, 4.1 Hz, 3H). ^{13}C NMR (126 MHz, DMSO) δ 172.19, 155.37, 141.81, 138.65, 128.58, 128.18, 126.96, 119.41, 65.71, 64.58, 63.23, 57.98, 52.87, 29.70, 26.84, 23.34. HRMS (ESI+) for $C_{18}H_{22}N_3O_2S$ (M + H), calcd: 344.14272, found: 344.14284.

***tert*-Butyl ((*S*)-1-oxo-3-phenyl-1-((*S*)-2-((4,5,6,7-tetrahydrobenzo[1]thiazol-2-yl)carbamoyl)pyrrolidin-1-yl)propan-2-yl)carbamate (YSP-18).** Following the protocol used with **YSP-12**, 4,5,6,7-tetrahydro-1,3-benzothiazol-2-amine (1eq, 0.65 mmol, 100 mg) and Boc-Phe-Pro-OH (1.2eq, , 0.78 mmol, 282.7 mg) led to **YSP-18** (77 mg 24%). White solid, mp = 196 °C (EtOAc), R*f* = 0.54 (Hex/EtOAc, 1:9). HPLC (t_R =15.46 min; purity: 99.3 %, 5-95% MeCN in H_2O). ^{1}H NMR (500 MHz, DMSO) δ 11.91 (s, 1H), 7.34 – 7.29 (m, 2H), 7.27 (t, *J* = 7.6 Hz, 2H), 7.24 – 7.17 (m, 1H), 7.05 (d, *J* = 8.4 Hz, 1H), 4.55 (dd, *J* = 8.4, 4.9 Hz, 1H), 4.37 (td, *J* = 9.1, 8.3, 3.9 Hz, 1H), 3.71 (dt, *J* = 9.7, 6.9 Hz, 1H), 3.67 – 3.59 (m, 1H), 2.96 (dd, *J* = 14.0, 3.9 Hz, 1H), 2.75 (dd, *J* = 14.0, 10.1 Hz, 1H), 2.64 (dq, *J* = 6.1, 3.0 Hz, 2H), 2.57 (s, 2H), 2.17 (dq, *J* = 12.4, 7.6 Hz, 1H), 2.05 – 1.80 (m, 4H), 1.80 – 1.74 (m, 4H), 1.30 (s, 6H), 1.23 (s, 1H), 1.17 (s, 1H). ^{13}C NMR (126 MHz, DMSO) δ 170.43, 170.06, 155.31, 154.62, 144.00, 141.68, 137.99, 129.33, 128.07, 126.24, 121.28, 78.00, 59.49, 53.85, 36.18, 29.11, 28.14, 26.01, 24.78, 22.96, 22.64, 22.24. HRMS (ESI+) for $C_{26}H_{34}N_4O_4NaS$ (M + Na), calcd: 521.21930, found: 521.21814.

***tert*-Butyl ((*S*)-1-((*S*)-2-((6,7-dihydro-4*H*-pyrano[4,3-d]thiazol-2-yl)carbamoyl)pyrrolidin-1-yl)-1-oxo-3-phenylpropan-2-yl)carbamate (YSP-19).** Following the protocol used with **YSP-12**, 6,7-dihydro-4H-pyrano[4,3-d]thiazol-2-ylamine (1eq, 0.64 mmol, 100 mg) and Boc-Phe-Pro-OH (1.2eq, 0.77 mmol, 279 mg) led to **YSP-19** (67 mg 21%). White solid, mp = 139°C (EtOAc), R*f* = 0.47 (Hex/EtOAc, 1:9). HPLC (t_R=14.31 min; purity: 98.3 %, 5-95% MeCN in H_2O). ^{1}H NMR (500 MHz, DMSO) δ 12.06 (s, 1H), 7.33 – 7.16 (m, 5H), 7.04 (d, *J* = 8.3 Hz, 1H), 4.73 – 4.62 (m, 2H), 4.56 (dd, *J* = 8.5, 5.0 Hz, 1H),

4.37 (td, *J* = 9.0, 8.3, 3.9 Hz, 1H), 3.91 (td, *J* = 5.7, 2.4 Hz, 2H), 3.71 (dt, *J* = 9.8, 6.9 Hz, 1H), 3.62 (dt, *J* = 17.8, 7.4 Hz, 1H), 2.95 (dd, *J* = 13.9, 4.0 Hz, 1H), 2.78 – 2.70 (m, 1H), 2.68 (d, *J* = 5.9 Hz, 2H), 2.18 (dq, *J* = 12.4, 7.6 Hz, 1H), 2.05 – 1.81 (m, 4H), 1.29 (s, 7H), 1.24 – 1.14 (m, 3H). ^{13}C NMR (126 MHz, DMSO) δ 170.92, 170.76, 156.34, 155.79, 142.34, 138.43, 129.81, 128.54, 126.72, 119.78, 78.48, 65.08, 63.70, 59.96, 54.32, 47.26, 36.66, 29.57, 28.62, 27.34, 25.29. HRMS (ESI+) for $C_{25}H_{32}N_4O_5NaS$ (M + Na), calcd: 523.1986, found: 523.1989.

1-Benzyl-*N*-(6,7-dihydro-4H-pyrano[4,3-d]thiazol-2-yl)piperidine-2-carboxamide (YSP-20). Following the protocol used with **YSP-12** of 6,7-dihydro-4H-pyrano[4,3-d]thiazol-2-ylamine (1eq, 0.64 mmol, 100 mg) and 1-Benzyl piperidine-2-carboxylic acid (1.2eq, 0.77 mmol, 168.9 mg) lead to **YSP-20** (72 mg 32%). White solid, melting point (112°C, EtOAc), R*f* = 0.55 (Hex/EtOAc, 1:9). HPLC (t_R=15.03 min; purity: 95.33 %, 5-95% MeCN in H_2O). ^{1}H NMR (500 MHz, DMSO) δ 7.35 – 7.28 (m, 4H), 7.23 (ddd, *J* = 8.6, 5.4, 2.5 Hz, 1H), 4.67 (t, *J* = 2.0 Hz, 2H), 3.90 (t, *J* = 5.6 Hz, 2H), 3.64 (d, *J* = 13.3 Hz, 1H), 3.26 (d, *J* = 13.4 Hz, 1H), 3.21 (dd, *J* = 8.7, 3.9 Hz, 1H), 2.86 (dt, *J* = 11.5, 4.4 Hz, 1H), 2.66 (td, *J* = 5.5, 2.8 Hz, 2H), 2.10 – 2.00 (m, 2H), 1.83 – 1.60 (m, 3H), 1.47 (dtq, *J* = 18.6, 9.4, 4.3 Hz, 2H), 1.31 (ddt, *J* = 13.9, 9.5, 4.8 Hz, 1H). ^{13}C NMR (126 MHz, DMSO) δ 171.93, 155.60, 141.85, 138.34, 128.65, 128.13, 126.91, 119.38, 64.98, 64.58, 63.22, 59.37, 50.09, 29.07, 26.84, 24.50, 22.44. HRMS (ESI+) for $C_{19}H_{24}N_3O_2S$ (M + H), calcd: 358.1584, found: 358.1576.

***N*-(5-Acetyl-4-methylthiazol-2-yl)-1-benzylpyrrolidine-2-carboxamide (YSP-22).** Following the protocol used with **YSP-12** of 2-Amino-4-methyl-5-acetylthiazole (1eq, 0.64 mmol, 100 mg) and (S)-1-(N)-Benzyl proline (1.2eq, 0.77 mmol, 157.9 mg) lead to **YSP-22** (51 mg, 23 %). White solid, melting point (102°C, EtOAc), R*f* = 0.74 (Hex/EtOAc, 1:9). HPLC (t_R=14.67 min; purity: 95.7 %, 5-95% MeCN in H_2O). ^{1}H NMR (500 MHz, DMSO) δ 7.32 (d, *J* = 7.5 Hz, 2H), 7.27 (t, *J* = 7.4 Hz, 2H), 7.23 – 7.17 (m, 1H), 3.80 (d, *J* = 13.1 Hz, 1H), 3.60 (d, *J* = 13.1 Hz, 1H), 3.47 (dd, *J* = 9.3, 4.3 Hz, 1H), 3.01 – 2.94 (m, 1H), 2.56 (s, 3H), 2.47 (s, 3H), 2.41 (q, *J* = 7.9 Hz, 1H), 2.15 (qt, *J* = 9.9, 4.9 Hz, 1H), 1.86 – 1.71 (m, 3H). ^{13}C NMR (126 MHz, DMSO) δ 190.67, 173.35, 158.98, 154.26, 138.61, 128.64, 128.13, 126.95, 125.35, 65.66, 57.86, 52.91, 30.11, 29.71, 23.27, 18.02. HRMS (ESI+) for $C_{18}H_{22}N_3O_2S$ (M + H), calcd: 344.1427, found: 344.1422.

(*S*)-1-Benzyl-N-(3-cyano-7-oxo-4,5,6,7-tetrahydrobenzo[1]thiophen-2-yl)pyrrolidine-2-carboxamide (YSP-23). Following the protocol used with **YSP-12** of 2-Amino-4,5,6,7-tetrahydro-7-oxobenzo[1]thiophene-3-carbonitrile (1eq, 0.52 mmol, 100 mg) and (S)-1-(N)-Benzyl proline (1.2eq, 0.62 mmol, 127.2 mg) lead to **YSP-23** (56 mg 28 %). White solid, melting point (138°C, EtOAc), R*f* = 0.64 (Hex/EtOAc, 1:9). HPLC (t_R=14.29 min; purity: 91.9 %, 5-95% MeCN in H_2O). ^{1}H NMR (500 MHz, DMSO) δ 7.56 – 7.51 (m, 2H), 7.40 – 7.30 (m, 3H), 4.35 (d, *J* = 12.7 Hz, 1H), 4.07 – 4.00 (m, 1H), 4.00 – 3.94 (m, 1H), 3.23 (d, *J* = 9.3 Hz, 2H), 2.94 (q, *J* = 8.8 Hz, 1H), 2.77 (t, *J* = 6.1 Hz, 2H), 2.47 – 2.29 (m, 4H), 2.06 (dq, *J* = 12.1, 6.2 Hz, 2H), 2.02 – 1.87 (m, 3H), 1.84 – 1.74 (m, 1H). ^{13}C NMR (126 MHz, DMSO) δ 190.18, 172.03, 151.19, 133.94, 130.00, 128.55, 128.49, 123.81, 115.23, 94.18, 67.98, 58.06, 53.61, 37.25, 29.22, 24.13, 23.39, 22.62. HRMS (ESI+) for $C_{21}H_{22}N_3O_2S$ (M + H), calcd: 380.1427, found: 380.1429.

(*S*)-1-Benzyl-*N*-(5,5-dimethyl-7-oxo-4,5,6,7-tetrahydrobenzo[1]thiazol-2-yl)pyrrolidine-2-carboxamide (YSP-25). Following the protocol used with **YSP-12** of 2-Amino-5,5-dimethyl-5,6-dihydro-4h-benzothiazol-7-one (1eq, 0.509 mmol, 100 mg) and (S)-1-(N)-Benzyl proline (1.2eq, 0.611 mmol, 125.3 mg) lead to **YSP-25** (44 mg, 22 %). White solid, melting point (111°C, EtOAc), R*f* = 0.76 (Hex/EtOAc, 1:9). HPLC (t_R=14.67 min; purity: 95.7 %, 5-95% MeCN in H_2O). ^{1}H NMR (500 MHz, DMSO) δ 7.36 – 7.30 (m, 2H), 7.27 (dd, *J* = 8.3, 6.8 Hz, 2H), 7.22 – 7.15 (m, 1H), 3.80 (d, *J* = 13.2 Hz, 1H), 3.61 (d, *J* = 13.1 Hz, 1H), 3.48 (dd, *J* = 9.4, 4.8 Hz, 1H), 3.02 – 2.95 (m, 1H), 2.78 (d, *J* = 1.5 Hz,

2H), 2.40 (d, *J* = 3.8 Hz, 3H), 2.21 – 2.10 (m, 1H), 1.88 – 1.70 (m, 3H), 1.06 (s, 5H). ^{13}C NMR (126 MHz, DMSO) δ 191.58, 173.38, 162.60, 162.53, 138.53, 128.64, 128.10, 126.90, 122.15, 65.80, 57.89, 52.95, 51.06, 34.73, 29.70, 27.82, 27.78, 23.26. HRMS (ESI+) for $C_{21}H_{25}N_3NaO_2S$ (M + H), calcd: 406.1560, found: 406.1554.

***tert*-Butyl ((*S*)-1-((*S*)-2-((5,5-dimethyl-7-oxo-4,5,6,7-tetrahydrobenzo[1]thiazol-2-yl)carbamoyl)pyrrolidin-1-yl)-1-oxo-3-phenylpropan-2-yl)carbamate (YSP-26).** Following the protocol used with **YSP-12** of 2-Amino-4-methyl-5-acetylthiazole (1eq, 0.64 mmol, 100 mg) and (S)-1-(N)-Benzyl proline (1.2eq, 0.77 mmol, 157.9 mg) lead to **YSP-26** (37 mg, 14%). White solid, melting point (116°C, EtOAc), R*f* = 0.58 (Hex/EtOAc, 1:9). HPLC (t_R=15.08 min; purity: 93.8 %, 5-95% MeCN in H_2O). ^{1}H NMR (500 MHz, DMSO) δ 12.71 (s, 1H), 7.33 – 7.16 (m, 4H), 7.06 (d, *J* = 8.3 Hz, 1H), 4.57 (dd, *J* = 8.5, 5.1 Hz, 1H), 4.38 (td, *J* = 9.2, 3.9 Hz, 1H), 3.76 – 3.57 (m, 2H), 2.96 (dd, *J* = 13.9, 4.0 Hz, 1H), 2.79 (s, 1H), 2.74 (dd, *J* = 14.2, 10.0 Hz, 1H), 2.58 (s, 1H), 2.47 – 2.35 (m, 2H), 2.04 – 1.84 (m, 3H), 1.29 (s, 5H), 1.23 (d, *J* = 8.7 Hz, 2H), 1.10 – 1.00 (m, 7H), 0.84 (dt, *J* = 14.3, 6.7 Hz, 1H). ^{13}C NMR (126 MHz, DMSO) δ 191.59, 171.34, 170.49, 162.68, 155.30, 143.92, 137.89, 129.33, 128.06, 126.26, 122.21, 78.02, 59.67, 53.79, 51.07, 50.71, 46.78, 40.53, 40.02, 39.95, 39.85, 39.78, 39.69, 39.52, 39.44, 39.35, 39.19, 39.02, 36.14, 34.75, 34.32, 28.95, 28.13, 27.87, 27.73, 24.87. HRMS (ESI+) for $C_{28}H_{36}NaN_4O_2S$ (M + H), calcd: 563.2299, found: 563.2286.

***N*-(5-acetyl-4-phenylthiazol-2-yl)-1-benzylpyrrolidine-2-carboxamide (YSP-29).** Following the protocol used with **YSP-12** of 1-(2-Amino-4-phenyl-thiazol-5-yl)-ethanone (1eq, 0.459 mmol, 100 mg) and (S)-1-(N)-Benzyl proline (1.2eq, 0.55 mmol, 112.8 mg) lead to **YSP-29** (28 mg, 15%). White solid, melting point (107°C, EtOAc), R*f* = 0.82 (Hex/EtOAc, 1:9). HPLC (t_R=16.22 min; purity: 97.6 %, 5-95% MeCN in H_2O). ^{1}H NMR (500 MHz, DMSO) δ 7.76 – 7.70 (m, 2H), 7.68 – 7.61 (m, 1H), 7.55 (t, *J* = 7.7 Hz, 2H), 7.35 – 7.30 (m, 2H), 7.28 (t, *J* = 7.6 Hz, 2H), 7.24 – 7.16 (m, 1H), 3.80 (d, *J* = 13.1 Hz, 1H), 3.59 (d, *J* = 13.2 Hz, 1H), 3.48 (dd, *J* = 9.2, 4.6 Hz, 1H), 3.01 – 2.93 (m, 1H), 2.44 (s, 4H), 2.15 (tt, *J* = 8.6, 4.3 Hz, 1H), 1.81 (dq, *J* = 13.2, 6.6 Hz, 2H), 1.77 – 1.69 (m, 1H). ^{13}C NMR (126 MHz, DMSO) δ 188.30, 173.44, 159.86, 156.05, 139.93, 138.60, 132.19, 128.61, 128.59, 128.14, 128.11, 126.91, 122.98, 65.68, 57.81, 52.85, 29.68, 23.24, 18.16. HRMS (ESI+) for $C_{23}H_{24}N_3O_2S$ (M + H), calcd: 406.1584, found: 406.1576.

(*R*)-5-Amino-2-methyl-*N*-(1-(naphthalen-1-yl)ethyl)benzamide (**SP-1a**). To a solution of 5-amino-2-methylbenzoic acid (200 mg, 1.32 mmol) in DCM (5.5 mL, 0.25M) under Argon at 0°C was added DIPEA (0.58 mL, 3.31 mmol, 2.5 equiv.), (R)-(+)-1-(1-naphthyl)ethylamine (0.23 mL, 1.45 mmol, 1.1 equiv.), and PyBOP (0.772 g, 1.45 mmol, 1.1 equiv.). Reaction was allowed back to room temperature and stirred at room temperature for 24 h. Water and an aq. Saturated solution of NH_4Cl were added to the reaction mixture. Phases were separated and the organic phase was washed with aq. saturated NH_4Cl (x2), aq. saturated $NaHCO_3$ (x2), and brine (x1). Combined organic layers were dried (Na_2SO_4), filtered, and concentrated to give an orange oil. Crude was purified by column chromatography on silica gel using 0-40% (10% MeOH/1% NH_4OH in DCM) in DCM as an eluent. Product was triturated with heptane and evaporated to afford a beige powder, 300 mg, 74% yield. ^{1}H NMR (500 MHz, $CDCl_3$) δ 8.23 (d, J = 8.5 Hz, 1H), 7.88 (dd, J = 8.1, 1.5 Hz, 1H), 7.81 (d, J = 8.2 Hz, 1H), 7.61 – 7.43 (m, 4H), 6.94 (d, J = 8.0 Hz, 1H), 6.62 – 6.54 (m, 2H), 6.11 (p, J = 7.0 Hz, 1H), 5.97 (d, J = 8.4 Hz, 1H), 3.53 (s, 2H), 2.29 (s, 3H), 1.77 (d, J = 6.7 Hz, 3H). ^{13}C NMR (126 MHz, $CDCl_3$) δ 169.18, 144.23, 138.22, 137.13, 134.09, 131.94, 131.34, 128.92, 128.60, 126.73, 126.08, 125.48, 125.32, 123.72, 122.69, 116.78, 113.50, 44.93, 20.78, 18.86. HRMS (ESI+) for $C_{20}H_{20}N_2NaO$ (M+Na) calcd 327.1468 found 327.1465.

(*R*)-2-chloro-*N*-(1-(naphthalen-1-yl)ethyl)-5-nitrobenzamide (**SP-1b**). To a solution of 5-chloronitrobenzoic acid (100 mg, 0.496 mmol, 1.2 equiv.) in acetonitrile(5 mL, 0.1M) under Argon at 0°C

was added DIPEA (0.08 mL, 0.455 mmol, 1.1 equiv.), and HATU (187 mg, 0.496 mmol, 1.2 equiv.). Mixture stirred at 0°C for 25 minutes. (R)-(+)-1-(1-naphthyl)ethylamine (0.07 mL, 0.413 mmol, 1 equiv.) was added, a precipitate formed soon after the addition. Reaction was allowed back to room temperature and stirred at room temperature for 24 hours. Solvent was removed under reduced pressure, ethyl acetate was added, and precipitate was filtered and washed with ethyl acetate (precipitate is clean product, white solid). Filtrate was then washed with aq. saturated NH_4Cl (x3), aq. saturated $NaHCO_3$ (x2), and brine (x2), dried (Na_2SO_4), filtered, and concentrated to give an orange solid. Washed crude was recrystallized from ethyl acetate to afford a white fluffy solid, combined product,104 mg, 71% yield. ^{1}H NMR (500 MHz, DMSO) δ 9.32 (d, J = 7.8 Hz, 1H), 8.31 – 8.17 (m, 3H), 7.97 (dd, J = 8.1, 1.4 Hz, 1H), 7.87 (d, J = 8.1 Hz, 1H), 7.82 (d, J = 8.8 Hz, 1H), 7.67 – 7.50 (m, 4H), 5.91 (p, J = 7.0 Hz, 1H), 1.62 (d, J = 6.9 Hz, 3H). ^{13}C NMR (126 MHz, DMSO) δ 163.40, 145.96, 139.21, 137.75, 137.15, 133.39, 131.27, 130.35, 128.70, 127.53, 126.29, 125.71, 125.48, 125.38, 123.54, 123.15, 122.69, 44.88, 21.27. HRMS (ESI+) for $C_{19}H_{15}ClN_2NaO_3$ calcd 377.0663 found 377.0657.

(*R*)-2-chloro-5-methyl-*N*-(1-(naphthalen-1-yl)ethyl)nicotinamide (**SP-1c**). To a solution of 5-chloro-5-methylnicotinic acid (150 mg, 0.874 mmol, 1.2 equiv.) in acetonitrile(8.5 mL, 0.1M) under Argon at 0°C was added DIPEA (0.15 mL, 0.874 mmol, 1.2 equiv.), and HATU (335 mg, 0.881 mmol, 1.2 equiv.). Mixture stirred at 0°C for 25 minutes. (R)-(+)-1-(1-naphthyl)ethylamine (0.12 mL, 0.728 mmol, 1 equiv.) was added. Reaction was allowed back to room temperature and stirred at room temperature for 24 hours. Solvent was removed under reduced pressure, ethyl acetate was added and crude was washed with aq. saturated NH_4Cl (x2), aq. saturated $NaHCO_3$ (x2), and brine (x1), dried (Na_2SO_4), filtered, and concentrated to give a dark orange solid. Crude was recrystallized from methanol to afford a beige solid, 145 mg, 61% yield ^{1}H NMR (500 MHz, $CDCl_3$) δ 8.23 (d, J = 2.4 Hz, 1H), 8.21 – 8.17 (m, 1H), 7.91 – 7.86 (m, 2H), 7.82 (d, J = 8.1 Hz, 1H), 7.62 – 7.55 (m, 2H), 7.55 – 7.44 (m, 2H), 6.71 (d, J = 8.0 Hz, 1H), 6.13 (p, J = 7.0 Hz, 1H), 2.32 (s, 3H), 1.81 (d, J = 6.8 Hz, 3H). ^{13}C NMR (126 MHz, $CDCl_3$) δ 163.91, 151.31, 144.34, 140.35, 137.68, 134.12, 133.03, 131.15, 130.50, 129.02, 128.79, 126.80, 126.12, 125.40, 123.48, 122.90, 45.98, 20.82, 17.65. HRMS (ESI+) for $C_{19}H_{17}ClN_2NaO$ calcd 347.0927 found 347.0925.

(*R*)-5-chloro-2-hydroxy-*N*-(1-(naphthalen-1-yl)ethyl)benzamide (**SP-1d**). To a solution of 5-chlorosalycilic acid (200 mg, 1.16 mmol, 1.2 equiv.) in DCM (10 mL, 0.1M) under Argon at 0°C was added DIPEA (0.17 mL, 0.96 mmol, 1 equiv.), and HATU (440.67 mg, 1.16 mmol, 1.2 equiv.). DMF (0.5 mL) was added to help dissolve the starting material. Mixture stirred at 0°C for 20 minutes. (R)-(+)-1-(1-naphthyl)ethylamine (0.15 mL, 0.96 mmol, 1 equiv.), and DIPEA (0.17 mL, 0.96 mmol, 1 equiv.) were added. Reaction was allowed back to room temperature and stirred at room temperature for 24 hours. DCM and water were added. Phases were separated and the aqueous phase was extracted with DCM (x3). Combined organic phases were washed with aq. saturated NH_4Cl (x1), aq. saturated $NaHCO_3$ (x1), and brine (x1), dried (Na_2SO_4), filtered, and concentrated to give an orange oil. Crude was purified by column chromatography on silica gel using 2-20% ethyl acetate in hexanes as an eluent to afford an off-white powder, 169 mg, 54% yield. ^{1}H NMR (500 MHz, $CDCl_3$) δ 12.29 (s, 1H), 8.11 – 8.06 (m, 1H), 7.93 – 7.83 (m, 2H), 7.64 – 7.47 (m, 4H), 7.31 (dd, J = 8.9, 2.5 Hz, 1H), 7.22 (d, J = 2.5 Hz, 1H), 6.93 (d, J = 8.8 Hz, 1H), 6.42 (d, J = 7.8 Hz, 1H), 6.10 (p, J = 7.0 Hz, 1H), 1.79 (d, J = 6.8 Hz, 3H). ^{13}C NMR (126 MHz, $CDCl_3$) δ 168.01, 160.41, 137.27, 134.29, 134.17, 131.12, 129.15, 129.06, 127.07, 126.23, 125.41, 125.08, 123.40, 123.04, 122.93, 120.33, 115.14, 45.37, 20.70. HRMS (ESI+) for $C_{19}H_{15}O_2NCl$ calcd 324.07968 found 324.07927.

(*R*)-2-bromo-*N*-(1-(naphthalen-1-yl)ethyl)-5-nitrobenzamide (**SP-1e**). To a solution of 2-bromo-5-nitrobenzoic acid (400 mg, 1.63 mmol, 1.2 equiv.) in acetonitrile (10 mL, 0.1M) under Argon at 0°C was

added DIPEA (0.28 mL, 1.63 mmol, 1.2 equiv.), and HATU (620 mg, 1.63 mmol, 1.2 equiv.). Mixture stirred at 0°C for 25 minutes. (R)-(+)-1-(1-naphthyl)ethylamine (0.22 mL, 1.36 mmol, 1 equiv.) was added. Reaction was allowed back to room temperature and stirred at room temperature for 19 hours. Solvent was removed under reduced pressure, solid was washed with ethanol and recrystallized from ethyl acetate to afford beige needle like crystals, 435 mg, 80% yield ^{1}H NMR (500 MHz, DMSO) δ 9.30 (d, J = 7.9 Hz, 1H), 8.22 (d, J = 8.5 Hz, 1H), 8.17 (dd, J = 8.7, 2.8 Hz, 1H), 8.13 (d, J = 2.7 Hz, 1H), 8.01 – 7.94 (m, 2H), 7.87 (d, J = 8.1 Hz, 1H), 7.68 – 7.60 (m, 2H), 7.59 – 7.51 (m, 2H), 5.90 (p, J = 7.0 Hz, 1H), 1.63 (d, J = 6.9 Hz, 3H). ^{13}C NMR (126 MHz, DMSO) δ 164.39, 146.46, 139.98, 139.13, 134.47, 133.39, 130.36, 128.69, 127.54, 126.83, 126.33, 125.71, 125.48, 125.22, 123.22, 123.18, 122.77, 44.84, 21.24. HRMS (ESI+) for $C_{19}H_{15}O_3N_2BrNa$ calcd 421.01583 found 421.-1570.

(*R*)-5-amino-2-bromo-*N*-(1-(naphthalen-1-yl)ethyl)benzamide (SP-1f). To a suspension of 5-amino-2-bromobenzoic acid (500 mg, 2.31 mmol, 1.2 equiv.) in acetonitrile (9 mL, 0.2 M) under Argon at 0°C were added DIPEA (0.4 mL, 2.31 mmol, 1.2 equiv.), PyBOP (1.24 gr, 2.38 mmol, 1.2 equiv.), and (R)-(+)-1-(1-naphthyl)ethylamine (0.31 mL, 1.93 mmol, 1 equiv.). Reaction was allowed back to room temperature and stirred at room temperature for 20 hours. Solvent was removed under reduced pressure, and ethyl acetate was added. Organic phase was washed with aq. saturated NH_4Cl (x3), then with aq. saturated $NaHCO_3$ (x2), aq. saturated NaCl (x2), and water (x1). Organic phase was then dried (Na_2SO_4), filtered and concentrated to give an orange solid. Crude was purified by flash column chromatography with 60 – 100% ethyl acetate in hexanes as eluent to give a pale orange solid, 496 mg, 70% yield. ^{1}H NMR (500 MHz, $CDCl_3$) δ 8.21 (dd, J = 8.6, 3.7 Hz, 1H), 7.90 – 7.77 (m, 2H), 7.57 (ddd, J = 8.6, 6.8, 1.4 Hz, 2H), 7.53 – 7.41 (m, 2H), 7.22 (d, J = 8.5 Hz, 1H), 6.76 (d, J = 2.9 Hz, 1H), 6.50 (dd, J = 8.6, 2.9 Hz, 1H), 6.28 (d, J = 8.3 Hz, 1H), 6.14 – 6.06 (m, 1H), 3.51 (s, 3H), 1.79 (d, J = 6.8 Hz, 3H). ^{13}C NMR (126 MHz, $CDCl_3$) δ 166.87, 146.05, 137.99, 137.88, 134.02, 131.24, 128.91, 128.64, 126.73, 126.06, 125.34, 123.74, 122.89, 118.03, 115.93, 106.55, 45.65, 20.72. HRMS (ESI+) for $C_{19}H_{18}ON_2Br$ calcd 369.05970 found 369.05927.

(*R*)-2-iodo-N-(1-(naphthalen-1-yl)ethyl)-5-(trifluoromethyl)benzamide (SP-1g). To a solution of 2-iodo-5-(trifluoromethyl)benzoic acid (400 mg, 1.266 mmol, 1.2 equiv.) in DCM (8 mL, 0.16M) under Argon at 0°C was added DIPEA (0.22 mL, 1.266 mmol, 1.2 equiv.), and HATU (480 mg, 1.266 mmol, 1.2 equiv.). Mixture stirred at 0°C for 25 minutes. (R)-(+)-1-(1-naphthyl)ethylamine (0.17 mL, 1.055 mmol, 1 equiv.) was added. Reaction was allowed back to room temperature and stirred at room temperature for 18 hours. Solvent was removed under reduced pressure, ethyl acetate was added, and precipitate was filtered and washed with ethyl acetate (precipitate is clean product, white solid). Filtrate was then washed with aq. saturated NH_4Cl (x2), aq. saturated $NaHCO_3$ (x2), and brine (x1), dried (Na_2SO_4), filtered, and concentrated to give an orange solid. Washed crude was recrystallized from isopropanol to afford a pale orange solid, combined product, 431 mg, 87% yield. ^{1}H NMR (500 MHz, $CDCl_3$) δ 8.25 (d, J = 9.0 Hz, 1H), 7.96 (d, J = 8.3 Hz, 1H), 7.89 (dd, J = 8.2, 1.4 Hz, 1H), 7.83 (d, J = 8.2 Hz, 1H), 7.64 – 7.57 (m, 2H), 7.57 – 7.51 (m, 2H), 7.48 (dd, J = 8.2, 7.2 Hz, 1H), 7.29 (dd, J = 8.3, 2.2 Hz, 1H), 6.20 – 6.10 (m, 1H), 6.03 (d, J = 8.3 Hz, 1H), 1.86 (d, J = 6.7 Hz, 3H). ^{13}C NMR (126 MHz, $CDCl_3$) δ 167.14, 142.99, 140.75, 137.24, 134.12, 131.26, 131.11, 130.84, 129.01, 128.95, 127.58, 127.55, 126.97, 126.24, 125.32, 125.03, 125.00, 123.70, 123.11, 122.46, 97.02, 45.76, 20.45. HRMS (ESI+) for $C_{20}H_{15}F_3INNaO$ calcd 492.0043 found 492.0055.

(*R*)-2-methyl-*N*-(1-(naphthalen-1-yl)ethyl)-5-(trifluoromethyl)benzamide (SP-1h). To a solution of 2-methyl-5-(trifluoromethyl)benzoic acid (200 mg, 0.980 mmol, 1.2 equiv.) in acetonitrile (6.5 mL, 0.15M) under Argon at 0°C was added DIPEA (0.17 mL, 0.980 mmol, 1.2 equiv.), and HATU (373 mg, 0.980 mmol, 1.2 equiv.). Mixture stirred at 0°C for 30 minutes. (R)-(+)-1-(1-naphthyl)ethylamine (0.13

mL, 0.817 mmol, 1 equiv.) was added. Reaction was allowed back to room temperature and stirred at room temperature for 24 hours. Solvent was removed under reduced pressure, ethyl acetate was added, and precipitate was filtered and washed with ethyl acetate (precipitate is clean product, beige solid). Filtrate was then washed with aq. saturated NH_4Cl (x2), aq. saturated $NaHCO_3$ (x2), and brine (x1), dried (Na_2SO_4), filtered, and concentrated to give an orange solid. Washed crude was recrystallized from isopropanol to afford a pale yellow solid, combined product, 141 mg, 48% yield. ^{1}H NMR (500 MHz, $CDCl_3$) δ 8.22 (d, J = 8.5 Hz, 1H), 7.89 (dd, J = 8.1, 1.4 Hz, 1H), 7.83 (d, J = 8.1 Hz, 1H), 7.63 – 7.44 (m, 6H), 7.30 (d, J = 7.8 Hz, 1H), 6.15 (p, J = 6.9 Hz, 1H), 6.00 (d, J = 8.4 Hz, 1H), 2.47 (s, 3H), 1.82 (d, J = 6.7 Hz, 3H). ^{13}C NMR (126 MHz, $CDCl_3$) δ 167.72, 140.45, 137.68, 137.14, 134.15, 131.55, 131.28, 129.06, 128.86, 128.53, 128.26, 126.84, 126.60, 126.57, 126.54, 126.51, 126.21, 125.34, 125.01, 123.63, 123.60, 123.57, 123.54, 123.48, 122.85, 45.25, 20.68, 19.91. HRMS (ESI+) for $C_{21}H_{18}F_3NNaO$ calcd 380.1233 found 380.1232.

(*R*)-5-Amino-2-hydroxy-N-(1-(naphthalen-1-yl)ethyl)benzamide (**SP-1i**). To a solution of 5-aminosalycilic acid (300 mg, 1.96 mmol) in DCM (10 mL, 0.2M) under Argon at 0°C was added DIPEA (0.68 mL, 3.92 mmol, 2 equiv.), (R)-(+)-1-(1-naphthyl)ethylamine (0.35 mL, 2.15 mmol, 1.1 equiv.), and PyBOP (1.143 g, 2.15 mmol, 1.1 equiv.). Reaction was allowed back to room temperature and stirred at room temperature for 24 hours. DCM and an aq. Saturated solution of NH_4Cl were added to the reaction mixture. Phases were separated and the organic phase was washed with aq. saturated NH_4Cl (x2), aq. saturated $NaHCO_3$ (x2), and brine (x1). Combined organic layers were dried (Na_2SO_4), filtered, and concentrated to give an orange oil. Crude was purified by column chromatography on silica gel using 0-20% (10% MeOH/1% NH_4OH in DCM) in DCM as an eluent. Product was triturated with hexanes and evaporated to afford an off-white powder, 306 mg, 51% yield. ^{1}H NMR (800 MHz, $CDCl_3$) δ 11.64 (s, 1H), 8.11 – 8.08 (m, 1H), 7.91 – 7.87 (m, 1H), 7.84 (d, J = 8.2 Hz, 1H), 7.59 (dt, J = 7.2, 1.0 Hz, 1H), 7.57 – 7.45 (m, 3H), 6.81 (d, J = 8.7 Hz, 1H), 6.74 (dd, J = 8.7, 2.7 Hz, 1H), 6.55 (d, J = 2.7 Hz, 1H), 6.44 (d, J = 7.7 Hz, 1H), 6.07 (p, J = 7.0 Hz, 1H), 3.29 (s, 2H), 1.77 (d, J = 6.8 Hz, 3H). ^{13}C NMR (201 MHz, $CDCl_3$) δ 168.94, 154.77, 137.99, 137.72, 134.13, 131.20, 129.04, 128.87, 127.02, 126.18, 125.37, 123.27, 123.01, 122.87, 119.37, 114.23, 111.09, 45.17, 20.68. HRMS (ESI+) for C19H18N2NaO2 (M+Na) calcd 329.1258 found 329.1261.

(*R*)-2-Hydroxy-N-(1-(naphthalen-1-yl)ethyl)-5-nitrobenzamide (**SP-1j**). To a suspension of 5-nitrosalycilic acid (200 mg, 1.09 mmol) in DCM (10 mL, 0.1M) under Argon at 0°C was added EDCl (251.24 mg, 1.31 mmol, 1.2 equiv.). Reaction stirred for 30 minutes at 0°C (turned clear). HOBt·H_2O (54 mg, 0.328 mmol, 0.3 equiv.), .), (R)-(+)-1-(1-naphthyl)ethylamine (0.21 mL, 1.31 mmol, 1.2 equiv.), and DIPEA (0.19 mL, 1.09 mmol, 1 equiv.) were added. Reaction was allowed back to room temperature and stirred at room temperature for 24 hours. DCM and an aq. Saturated solution of NH_4Cl were added. Phases were separated and the organic phase was washed with aq. saturated NH_4Cl (x2), aq. saturated $NaHCO_3$ (x2), and brine (x1). Combined organic layers were dried (Na_2SO_4), filtered, and concentrated to give a yellow oil. Crude was purified by column chromatography on silica gel using 0-20% ethyl acetate in hexanes as an eluent. Product was triturated with heptane and evaporated to afford a yellow powder, 157 mg, 43% yield. ^{1}H NMR (500 MHz, $CDCl_3$) δ 8.29 (d, J = 2.6 Hz, 1H), 8.23 (dd, J = 9.2, 2.6 Hz, 1H), 8.07 (d, J = 8.4 Hz, 1H), 7.92 – 7.82 (m, 2H), 7.62 (d, J = 7.1 Hz, 1H), 7.60 – 7.45 (m, 3H), 7.05 (d, J = 9.2 Hz, 1H), 6.77 (d, J = 7.7 Hz, 1H), 6.12 (p, J = 7.0 Hz, 1H), 1.82 (d, J = 6.8 Hz, 3H). ^{13}C NMR (126 MHz, $CDCl_3$) δ 167.61, 167.42, 139.26, 136.86, 134.16, 131.05, 129.46, 129.23, 129.18, 127.08, 126.24, 125.46, 123.07, 122.83, 122.43, 119.58, 113.57, 45.60, 20.67. HRMS (ESI+) for C19H16N2NaO4 (M+Na) calcd 359.1002 found 359.1005.

(*R*)-2-iodo-*N*-(1-(naphthalen-1-yl)ethyl)-5-nitrobenzamide (**SP-1k**). To a suspension of 2-iodo-5-nitrobenzoic acid (200 mg, 0.68 mmol) in ACN (8 mL, 0.1M) under Argon at 0°C was added DIPEA (0.12 mL, 0.68 mmol, 1.2 equiv.), and HATU (259.5 mg, 0.68 mmol, 1.2 equiv.). Mixture stirred at 0°C for 30 minutes. (R)-(+)-1-(1-naphthyl)ethylamine (0.09 mL, 0.57 mmol, 1 equiv.) was added. Reaction was allowed back to room temperature and stirred at room temperature for 24 hours. Solvent was removed under reduced pressure, ethyl acetate was added, and precipitate was filtered and washed with ethyl acetate (precipitate is clean product, beige solid). Filtrate was then washed with aq. saturated NH_4Cl (x2), aq. saturated $NaHCO_3$ (x2), and brine (x1), dried (Na_2SO_4), filtered, and concentrated to give an orange solid. Washed crude was recrystallized from isopropanol to afford a white solid, combined product, 199 mg, 78% yield. ^{1}H NMR (500 MHz, DMSO) δ 9.25 (d, *J* = 7.8 Hz, 1H), 8.22 (dd, *J* = 20.1, 8.5 Hz, 2H), 8.02 – 7.93 (m, 3H), 7.87 (d, *J* = 8.1 Hz, 1H), 7.70 – 7.60 (m, 2H), 7.59 – 7.49 (m, 2H), 5.90 (p, *J* = 7.1 Hz, 1H), 1.64 (d, *J* = 6.9 Hz, 3H).

(R)-2-iodo-*N*-(1-(naphthalen-1-yl)ethyl)benzamide (SP-1l). To a suspension of 2-iodobenzoic acid (200 mg, 0.81 mmol) in ACN (8 mL, 0.1M) under Argon at 0°C was added DIPEA (0.14 mL, 0.81 mmol, 1.2 equiv.), and HATU (306.5 mg, 0.81 mmol, 1.2 equiv.). Mixture stirred at 0°C for 30 minutes. (R)-(+)-1-(1-naphthyl)ethylamine (0.11 mL, 0.67 mmol, 1 equiv.) was added. Reaction was allowed back to room temperature and stirred at room temperature for 24 hours. Solvent was removed under reduced pressure, ethyl acetate was added, and precipitate was filtered and washed with ethyl acetate (precipitate is clean product, beige solid). Filtrate was then washed with aq. saturated NH_4Cl (x2), aq. saturated $NaHCO_3$ (x2), and brine (x1), dried (Na_2SO_4), filtered, and concentrated to give an orange solid. Washed crude was recrystallized from isopropanol to afford a white solid, combined product, 107 mg, 40% yield. ^{1}H NMR (500 MHz, $CDCl_3$) δ 8.27 (d, *J* = 8.5 Hz, 1H), 7.91 – 7.85 (m, 1H), 7.82 (dd, *J* = 8.2, 1.7 Hz, 2H), 7.63 – 7.56 (m, 2H), 7.52 (ddd, *J* = 8.1, 6.9, 1.2 Hz, 1H), 7.47 (dd, *J* = 8.2, 7.2 Hz, 1H), 7.35 – 7.27 (m, 2H), 7.05 (ddd, *J* = 7.9, 6.5, 2.6 Hz, 1H), 6.19 – 6.10 (m, 1H), 5.98 (d, *J* = 8.4 Hz, 1H), 1.84 (d, *J* = 6.7 Hz, 3H).

(*R*)-4-chloro-2-((1-(naphthalen-1-yl)ethyl)carbamoyl)phenyl acetate (SP-2). To a solution of (*R*)-5-chloro-2-hydroxy-N-(1-(naphthalen-1-yl)ethyl)benzamide (1e) (73.7 mg, 0.23 mmol, 1 equiv.) in DCM (2 mL, 0.1 M) under Argon at 0°C was added triethyl amine (67 µL, 0.48 mmol, 2.1 equiv.) and acetyl chloride (18 µL, 0,25 mmol, 1.1 equiv.). Reaction was allowed back to room temperature and stirred at room temperature for 24 hours. Water and DCM were added. Phases were separated and the aqueous phase was extracted with DCM (x3). Combined organic layers were washed with aq. Saturated NH_4Cl (x1), aq. saturated $NaHCO_3$ (x1), and brine (x1), dried (Na_2SO_4), filtered, and concentrated to give a white solid, 52 mg, 61% yield ^{1}H NMR (500 MHz, $CDCl_3$) δ 8.16 – 8.10 (m, 1H), 7.91 – 7.80 (m, 3H), 7.60 – 7.45 (m, 4H), 7.38 (ddd, J = 8.7, 2.7, 1.5 Hz, 1H), 6.95 (dd, J = 8.7, 0.9 Hz, 1H), 6.59 – 6.50 (m, 1H), 6.10 (p, J = 7.0 Hz, 1H), 1.77 (d, J = 6.7 Hz, 3H), 1.54 (s, 4H). ^{13}C NMR (126 MHz, $CDCl_3$) δ 168.66, 163.04, 146.24, 137.59, 134.12, 132.15, 131.81, 131.32, 130.38, 129.66, 128.95, 128.88, 127.13, 126.32, 125.38, 124.74, 123.54, 122.93, 45.13, 20.25, 20.00. HRMS (ESI+) for $C_{21}H_{18}O_3NClNa$ calcd 390.08674 found 390.08617.

(*R*)-3-((2-((1-(naphthalen-1-yl)ethyl)carbamoyl)-4-(trifluoromethyl)phenyl)amino)propanoic acid (SP-3a). (R)-2-iodo-N-(1-(naphthalen-1-yl)ethyl)-5-(trifluoromethyl)benzamide (**SP-1g**, 75 mg, 0.160 mmol, 1 equiv.), β-alanine (16 mg, 0.176 mmol, 1.1 equiv.), Cs_2CO_3 (stored in the oven, 130 mg, 0.4 mmol, 2.5 equiv.), CuI (15 mg, 0.08 mmol, 0.5 equiv.) were added to a flask. The flask was capped and purged with vacuum and argon (x3). DMF was added (1 mL, 0.16M) and solution was degassed by bubbling argon into it while stirring. Flask was kept under argon atmosphere and heated to 105ºC.

Reaction was monitored by TLC and was completed after 3 hours. Reaction mixture was then cooled to room temperature and filtered through celite using ethyl acetate, filtrate is a pale green solution. Water was added to the filtrate and pH was adjusted to 3 using 1M HCl. Phases were separated and aqueous phase was extracted with ethyl acetate (x5). Combined organic layers were washed with acidic water (pH 3) (x3), brine (x2), dried (Na_2SO_4), filtered and concentrated to give an orange oil. Crude was co-evaporated with heptane to remove as much DMF as possible. Crude was purified by flash column chromatography on silica gel using 0-5% methanol in DCM as eluent. Solvent was removed from combined fractions to give a pale orange solid, 69 mg, 50% yield. ^{1}H NMR (500 MHz, $CDCl_3$) δ 8.11 (d, J = 8.4 Hz, 1H), 7.87 (dd, J = 8.0, 1.5 Hz, 1H), 7.81 (d, J = 8.2 Hz, 1H), 7.59 – 7.45 (m, 6H), 6.71 (d, J = 9.3 Hz, 1H), 6.36 (d, J = 7.6 Hz, 1H), 6.04 (p, J = 6.9 Hz, 1H), 3.51 (t, J = 6.9 Hz, 2H), 2.68 (t, J = 6.9 Hz, 2H), 1.74 (d, J = 6.8 Hz, 3H). ^{13}C NMR (126 MHz, $CDCl_3$) δ 176.23, 167.91, 151.36, 138.02, 134.14, 131.14, q: (129.81, 129.78, 129.75, 129.72, $^3J_{C-F}$=3.51 Hz), 129.07, 128.71, q: (127.84, 125.69, 123.54, 121.39, $^1J_{C-F}$=270 Hz), 126.81, 126.07, 125.44, q: (124.96, 124.93, 124.90, 124.87, $^3J_{C-F}$=3.84 Hz), 123.23, 122.75, q: (117.16, 116.90, 116.63, 116.37, $^2J_{C-F}$=33.07 Hz), 114.79, 111.22, 53.57, 45.39, 38.39, 21.02. . HRMS (ESI+) for $C_{23}H_{21}F_3N_2NaO_3$ calcd 453.1396 found 453.1396.

(*R*)-3-((2-((1-(naphthalen-1-yl)ethyl)carbamoyl)-4-nitrophenyl)amino)propanoic acid (SP-3b). (*R*)-2-iodo-*N*-(1-(naphthalen-1-yl)ethyl)-5-nitrobenzamide (**SP-1k**, 190 mg, 0.42 mmol, 1 equiv.), β-alanine (41.7 mg, 0.47 mmol, 1.1 equiv.), Cs_2CO_3 (stored in the oven, 346.8 mg, 1.06 mmol, 2.5 equiv.), CuI (40.5 mg, 0.21 mmol, 0.5 equiv.) were added to a flask. The flask was capped and purged with vacuum and argon (x3). DMF was added (2.5 mL, 0.16M) and solution was degassed by bubbling argon into it while stirring. Flask was kept under argon atmosphere and heated to 105ºC. Reaction was monitored by TLC and was completed after 3 hours. Reaction mixture was then cooled to room temperature and filtered through celite using ethyl acetate, filtrate is a pale green solution. Water was added to the filtrate and pH was adjusted to 3 using 1M HCl. Phases were separated and aqueous phase was extracted with ethyl acetate (x5). Combined organic layers were washed with acidic water (pH 3) (x3), brine (x2), dried (Na_2SO_4), filtered and concentrated to give an orange oil. Crude was co-evaporated with heptane to remove as much DMF as possible. Crude was purified by flash column chromatography on silica gel using 0-5% methanol in DCM as eluent. Solvent was removed from combined fractions to give a pale orange solid, 170 mg, 52% yield. ^{1}H NMR (500 MHz, DMSO) δ 9.25 (d, *J* = 7.8 Hz, 1H), 8.22 (dd, *J* = 20.1, 8.5 Hz, 2H), 8.02 – 7.93 (m, 3H), 7.87 (d, *J* = 8.1 Hz, 1H), 7.70 – 7.60 (m, 2H), 7.59 – 7.49 (m, 2H), 5.90 (p, *J* = 7.1 Hz, 1H), 1.64 (d, *J* = 6.9 Hz, 3H).

(*R*)-3-((2-((1-(naphthalen-1-yl)ethyl)carbamoyl)-4-nitrophenyl)amino)propanoic acid (SP-3c). (R)-2-iodo-*N*-(1-(naphthalen-1-yl)ethyl)benzamide (**SP-1l**, 100 mg, 0.25 mmol, 1 equiv.), β-alanine (24.4 mg, 0.27 mmol, 1.1 equiv.), Cs_2CO_3 (stored in the oven, 203 mg, 0.62 mmol, 2.5 equiv.), CuI (23.7 mg, 0.12 mmol, 0.5 equiv.) were added to a flask. The flask was capped and purged with vacuum and argon (x3). DMF was added (2.5 mL, 0.16M) and solution was degassed by bubbling argon into it while stirring. Flask was kept under argon atmosphere and heated to 105ºC. Reaction was monitored by TLC and was completed after 3 hours. Reaction mixture was then cooled to room temperature and filtered through celite using ethyl acetate, filtrate is a pale green solution. Water was added to the filtrate and pH was adjusted to 3 using 1M HCl. Phases were separated and aqueous phase was extracted with ethyl acetate (x5). Combined organic layers were washed with acidic water (pH 3) (x3), brine (x2), dried (Na_2SO_4), filtered and concentrated to give an orange oil. Crude was co-evaporated with heptane to remove as much DMF as possible. Crude was purified by flash column chromatography on silica gel using 0-5% methanol in DCM as eluent. Solvent was removed from combined fractions to give a translucent oil, 52 mg, 58% yield. ^{1}H NMR (500 MHz, $CDCl_3$) δ 8.13 (d, *J* = 8.4 Hz, 1H), 7.86 (dd, *J* = 7.7, 1.4 Hz, 1H), 7.80 (d, *J* = 8.1 Hz, 1H), 7.59 – 7.42 (m, 4H), 7.29 – 7.27 (m, 1H), 7.24 (d, *J* = 1.6 Hz, 1H), 6.70 (dd, *J* = 8.5, 1.1 Hz, 1H),

6.54 (ddd, *J* = 8.1, 7.2, 1.1 Hz, 1H), 6.34 (d, *J* = 7.8 Hz, 1H), 6.06 – 5.91 (m, 1H), 3.49 (t, *J* = 6.9 Hz, 2H), 2.67 (t, *J* = 6.9 Hz, 2H), 1.74 (d, *J* = 6.8 Hz, 3H).

Ethyl (*E*)-4-aminobut-2-enoate trifluoroacetic acid salt (SP-4). A solution of Ethyl (E)-4-((tert-butoxycarbonyl)amino)but-2-enoate (50 mg, 0.22 mmol, 1 equiv.) in DCM (0.5 mL, 0.4 M) was cooled to 0°C, and TFA (0.07 mL, 0.92 mmol, 4 equiv.) was added dropwise. The reaction stirred at 0°C for 10 minutes, and then allowed back to room temperature for 2 hours. Solvent was removed to give an orange oil. Product was used for the next reaction without further purification.

Ethyl (*R*,*E*)-4-(3-((2-((1-(naphthalen-1-yl)ethyl)carbamoyl)-4-(trifluoromethyl)phenyl)amino)-propanamido)but-2-enoate (SP- 5a). To a solution of (R)-3-((2-((1-(naphthalen-1-yl)ethyl)carbamoyl)-4-(trifluoromethyl)phenyl)amino)propanoic acid (**SP-3a**, 88 mg, 0.204 mmol, 1.2 equiv.) in DCM (0.6 mL) under Argon at 0°C were added DIPEA (0.04 mL, 0.229 mmol, 1.3 equiv.) and PyBOP (106 mg, 0.204 mmol, 1.2 equiv.). In a separate flask, ethyl (E)-4-aminobut-2-enoate trifluoroacetic acid salt (**SP-4**, 43 mg, 0.177 mmol, 1 equiv.) was dissolved in DCM (0.6 mL) and DIPEA (0.04 mL, 0.229 mmol, 1.3 equiv.) was added to neutralize the salt. Neutralized amine mixture was added to reaction mixture (DCM final amount 1.2 mL, 0.17M, DIPEA 0.08 mL, 0.458 mmol, 2.6 equiv.). Reaction was allowed back to room temperature and stirred at room temperature for 18 hours. Solvent was removed under reduced pressure and ethyl acetate and an aq. Saturated solution of NH_4Cl were added. Phases were separated and the organic phase was washed with aq. saturated NH_4Cl (x2), aq. saturated $NaHCO_3$ (x1), and brine (x1). Combined organic layers were dried (Na_2SO_4), filtered, and concentrated to give an orange solid. Crude was purified by flash column chromatography on silica gel using 5-60% ethyl acetate in DCM as an eluent. The product was co-evaporated with chloroform to afford a white solid, 36 mg, 37% yield. ^{1}H NMR (500 MHz, $CDCl_3$) δ 8.18 (d, J = 8.4 Hz, 1H), 7.91 – 7.83 (m, 2H), 7.80 (d, J = 8.2 Hz, 1H), 7.59 – 7.41 (m, 6H), 6.73 (d, J = 8.7 Hz, 2H), 6.62 (dt, J = 15.7, 5.1 Hz, 1H), 6.06 (p, J = 7.0 Hz, 1H), 5.70 (t, J = 5.9 Hz, 1H), 5.64 (dt, J = 15.7, 1.9 Hz, 1H), 4.11 (q, J = 7.1 Hz, 2H), 3.93 (dddd, J = 17.5, 6.2, 5.1, 1.9 Hz, 1H), 3.81 (dtd, J = 17.5, 5.5, 1.9 Hz, 1H), 3.53 (ddt, J = 16.1, 13.3, 6.7 Hz, 2H), 2.51 – 2.36 (m, 2H), 1.74 (d, J = 6.8 Hz, 3H), 1.23 (t, J = 7.1 Hz, 3H). ^{13}C NMR (126 MHz, $CDCl_3$) δ 170.77, 167.98, 166.08, 151.21, 143.61, 138.39, 134.12, 131.17, q: (129.63, 129.60, 129.58, 129.55, $^3J_{C-F}$=3.66 Hz), 129.11, 128.53, q: (127.85, 125.70, 123.55, 121.40, $^1J_{C-F}$=270 Hz), 126.64, 126.00, 125.51, q: (125.15, 125.13, 125.09, 125.06, $^3J_{C-F}$=3.66 Hz), 123.36, 122.79, 121.65, q: (117.16, 116.90, 116.63, 116.37, $^2J_{C-F}$=32.92 Hz), 115.18, 111.40, 60.66, 45.14, 40.13, 39.15, 36.53, 21.05, 14.27. HRMS (ESI+) for $C_{29}H_{30}O_4N_3F_3Na$ calcd 564.20806 found 564.20820.

Ethyl (*R*,*E*)-4-(3-((2-((1-(naphthalen-1-yl)ethyl)carbamoyl)-4-nitrophenyl)amino)propanamido)but-2-enoate (SP- 5b). (*R*)-3-((2-((1-(naphthalen-1-yl)ethyl)carbamoyl)-4-nitrophenyl)amino)propanoic (**SP-3b**, 140 mg, 0.34 mmol, 1.2 equiv.) in DCM (0.6 mL) under Argon at 0°C were added DIPEA (0.04 mL, 0.229 mmol, 1.2 equiv.) and PyBOP (177 mg, 0.34 mmol, 1.2 equiv.). In a separate flask, ethyl (E)-4-aminobut-2-enoate trifluoroacetic acid salt (**SP-4**, 43 mg, 0.177 mmol, 1 equiv.) was dissolved in DCM (0.6 mL) and DIPEA (0.06 mL, 0.34 mmol, 1 equiv.) was added to neutralize the salt. Neutralized amine mixture was added to reaction mixture (DCM final amount 3.5 mL, 0.17M, DIPEA 0.11 mL, 0.62 mmol, 2.2 equiv.). Reaction was allowed back to room temperature and stirred at room temperature for 18 hours. Solvent was removed under reduced pressure and ethyl acetate and an aq. Saturated solution of NH_4Cl were added. Phases were separated and the organic phase was washed with aq. saturated NH_4Cl (x2), aq. saturated $NaHCO_3$ (x1), and brine (x1). Combined organic layers were dried (Na_2SO_4), filtered, and concentrated to give an orange solid. Crude was purified by flash column chromatography on silica gel using 5-60% ethyl acetate in DCM as an eluent.

The product was co-evaporated with chloroform to afford a white solid, 148. mg, 58% yield. ^{1}H NMR (500 MHz, DMSO) δ 9.31 (d, *J* = 7.6 Hz, 1H), 8.97 (t, *J* = 5.7 Hz, 1H), 8.66 (d, *J* = 2.7 Hz, 1H), 8.26 (t, *J* = 5.7 Hz, 1H), 8.18 (d, *J* = 8.4 Hz, 1H), 8.13 (dd, *J* = 9.4, 2.6 Hz, 1H), 7.95 (dd, *J* = 8.0, 1.6 Hz, 1H), 7.84 (d, *J* = 8.1 Hz, 1H), 7.64 (dd, *J* = 7.2, 1.2 Hz, 1H), 7.60 – 7.49 (m, 3H), 6.87 (d, *J* = 9.5 Hz, 1H), 6.80 (dt, *J* = 15.7, 4.7 Hz, 1H), 5.93 (p, *J* = 7.0 Hz, 1H), 5.85 (dt, *J* = 15.7, 1.9 Hz, 1H), 4.07 (q, *J* = 7.1 Hz, 2H), 3.85 (dq, *J* = 5.6, 1.9 Hz, 2H), 3.56 – 3.43 (m, 2H), 2.47 (t, *J* = 6.7 Hz, 2H), 1.62 (d, *J* = 7.0 Hz, 3H), 1.16 (t, *J* = 7.1 Hz, 3H). ^{13}C NMR (126 MHz, DMSO) δ 170.15, 166.60, 165.43, 153.80, 145.74, 140.04, 134.60, 133.36, 130.39, 128.69, 128.15, 127.33, 126.22, 125.56 (d, *J* = 11.0 Hz), 123.01, 122.57, 120.31, 113.28, 110.85, 59.83, 44.66, 34.37, 21.20, 14.08. HRMS (ESI+) for $C_{28}H_{30}O_6N_4$ calcd 541.20576 found 541.20448.

Ethyl (*R*,*E*)-4-(3-((2-((1-(naphthalen-1-yl)ethyl)carbamoyl)phenyl)amino)propanamido)but-2-enoate (SP- 5c). (*R*)-3-((2-((1-(naphthalen-1-yl)ethyl)carbamoyl)-4-nitrophenyl)amino)propanoic acid (**SP-3c**, 200 mg, 0.55 mmol, 1.2 equiv.) in DCM (3.5 mL) under Argon at 0°C were added DIPEA (0.09 mL, 0.55 mmol, 1.2 equiv.) and PyBOP (286 mg, 0.55 mmol, 1.2 equiv.). In a separate flask, ethyl (E)-4-aminobut-2-enoate trifluoroacetic acid salt (**SP-4**, 104.9 mg, 0.46 mmol, 1 equiv.) was dissolved in DCM (0.6 mL) and DIPEA (0.08 mL, 0.46 mmol, 1 equiv.) was added to neutralize the salt. Neutralized amine mixture was added to reaction mixture (DCM final amount 6 mL, 0.17M, DIPEA 0.17 mL, 1.01 mmol, 2.2 equiv.). Reaction was allowed back to room temperature and stirred at room temperature for 18 hours. Solvent was removed under reduced pressure and ethyl acetate and an aq. Saturated solution of NH_4Cl were added. Phases were separated and the organic phase was washed with aq. saturated NH_4Cl (x2), aq. saturated $NaHCO_3$ (x1), and brine (x1). Combined organic layers were dried (Na_2SO_4), filtered, and concentrated to give an orange solid. Crude was purified by flash column chromatography on silica gel using 5-60% ethyl acetate in DCM as an eluent. The product was co-evaporated with chloroform to afford a white solid, 213. mg, 52% yield. ^{1}H NMR (500 MHz, $CDCl_3$) δ 8.17 (d, *J* = 8.4 Hz, 1H), 7.91 – 7.85 (m, 1H), 7.81 (d, *J* = 8.2 Hz, 1H), 7.59 – 7.42 (m, 4H), 6.77 – 6.72 (m, 1H), 6.71 (t, *J* = 5.2 Hz, 0H), 6.56 (td, *J* = 7.5, 1.1 Hz, 1H), 6.48 (d, *J* = 7.8 Hz, 1H), 6.04 (p, *J* = 7.0 Hz, 1H), 5.92 (s, 1H), 5.75 (dt, *J* = 15.8, 1.9 Hz, 1H), 4.12 (q, *J* = 3.6 Hz, 2H), 4.02 – 3.84 (m, 2H), 3.53 (td, *J* = 6.6, 3.0 Hz, 2H), 2.50 (td, *J* = 6.6, 4.3 Hz, 2H), 2.04 (s, 0H), 1.74 (d, *J* = 6.8 Hz, 3H), 1.24 (t, *J* = 7.1 Hz, 4H). ^{13}C NMR (126 MHz, $CDCl_3$) δ 171.26, 168.76, 166.01, 148.96, 143.70, 138.43, 134.00, 132.91, 131.10, 128.90, 128.39, 127.54, 126.58, 125.90, 125.32, 123.35, 122.56, 121.67, 116.02, 115.54, 111.99, 60.46, 44.94, 40.10, 39.49, 36.67, 20.91, 14.21. HRMS (ESI+) for $C_{28}H_{31}O_4N_3$ calcd 496.2207 found 496.2204.

3-oxo-3-phenylpropanoic acid (KH-1). Ethyl-3-oxo-3-phenyl propanoate (0.9 mL, 5.20 mmol) was dissolved in 1M NaOH (5.2 mL) at room temperature for 16 h. The reaction mixture was washed with DCM (4 x 10 mL). The aqueous layer was cooled in an ice bath, acidified to pH = 1 using 1M HCl. The precipitate was filtered to afford the desired product (540 mg, 63% yield). ^{1}H NMR (400 MHz, dmso) δ 12.67 (s, 1H), 8.14 – 7.15 (m, 5H), 4.04 (s, 1H).

***N*-(3-(*N*-(3-chlorophenyl)sulfamoyl)-4-methylphenyl)-3-oxo-3-phenylpropanamide (KH-2). KH-1** (30 mg, 0.183 mmol) and 5-amino-*N*-(3-chlorophenyl)-2-methylbenzenesulfonamide (56.94 mg, 0.192 mmol) was dissolved in anhydrous DCM (3 mL) at 0 °C. EDC·HCl (36.78 mg, 0.192 mmol), and 4-Dimethylaminopyridine (2.23 mg, 0.0183 mmol) were then added. The solution was stirred at room temperature for 16 h. The reaction mixture was washed with 1% HCl (3x5 mL), 1M $NaHCO_3$ (3x5 mL) and brine (1x5 mL), dried with Na_2SO_4, and concentrated. Column chromatography (20% to 60% EtOAc/hexanes) afforded the desired product (43 mg, 53% yield). ^{1}H NMR (400 MHz, $CDCl_3$) δ 9.57 (s, 1H), 8.09 (d, *J* = 2.4 Hz, 1H), 8.03 (d, *J* = 7.4 Hz, 2H), 7.87 (dd, *J* = 8.3, 2.4 Hz, 1H), 7.67 (t, *J* = 7.5 Hz,

1H), 7.54 (t, *J* = 7.8 Hz, 2H), 7.17 (t, *J* = 8.1 Hz, 1H), 7.09 – 7.05 (m, 2H), 6.98 (t, *J* = 8.2 Hz, 1H), 6.62 (s, 1H), 4.13 (s, 2H), 2.59 (s, 3H). ^{13}C NMR (126 MHz, DMSO) δ 194.92, 166.17, 139.52, 137.94, 137.64, 136.65, 134.13, 133.93, 133.90, 133.69, 131.50, 131.43, 131.40, 129.37, 129.29, 128.85, 125.88, 123.73, 123.61, 120.10, 118.62, 118.59, 117.49, 117.46, 48.51, 19.54, 19.52. HRMS (ESI/Q-TOF) m/z: $[M + Na]^+$ calculated for $C_{22}H_{19}ClN_2O_4S$ 465.07; found 465.0653.

Methyl 2-(2-acetoxyacetamido)-5-chlorobenzoate (KH-3). DCC (0.372 g, 1.80 mmol) was dissolved in DCM (2.5 mL). Methyl 2-amino-5-chlorobenzoate and 2-acetoxyacetic acid were dissolved in DCM (2.5 mL) at 0 °C. DCC solution was added dropwise over 20 mins. The reaction was stirred at room temperature for 16 h. The reaction mixture was filtered, and the filtrate was concentrated. Column chromatography (0% to 20% EtOAc/hexanes) afforded the desired product (0.312 g, 66% yield). ^{1}H NMR (400 MHz, cdcl$_3$) δ 11.65 (s, 1H), 8.73 (d, *J* = 9.0 Hz, 1H), 8.02 (d, *J* = 2.6 Hz, 1H), 7.51 (dd, *J* = 9.1, 2.6 Hz, 1H), 4.73 (s, 2H), 3.94 (s, 3H), 2.32 (s, 3H).

Methyl 5-chloro-2-(2-hydroxyacetamido)benzoate (KH-4). KH-3 (0.312 g, 1.09 mmol) and K_2CO_3 (0.152 g, 1.10 mmol) was dissolved in MeOH (5 mL), stirred at room temperature for 1 h. The reaction mixture was quenched with saturated NH_4Cl. The precipitate was filtered and rinsed with saturated NH_4Cl and water (0.243 g, 91% yield). ^{1}H NMR (400 MHz, cdcl$_3$) δ 11.65 (s, 1H), 8.73 (d, *J* = 9.0 Hz, 1H), 8.02 (d, *J* = 2.6 Hz, 1H), 7.51 (dd, *J* = 9.1, 2.6 Hz, 1H), 4.73 (s, 2H), 3.94 (s, 3H), 2.32 (s, 3H).

Methyl (*E*)-5-chloro-2-(2-((3-(2-methoxyphenyl)acryloyl)oxy)acetamido)benzoate (KH-5). 2-methoxycinnamic acid (0.213 g, 1.197 mmol), EDC·HCl (0.229 g, 1.197 mmol) and 4-Dimethylaminopyridine (24.37 mg, 0.199 mmol) were dissolved in DMF (6 mL), stirred at room temperature for 10 mins. KH-4 (0.243 g, 0.997 mmol) was added. The mixture was stirred at room temperature for 20 h. The precipitate was filtered, rinsed with minimum amount of DMF to afford the desired product (0.319 g, 77% yield). ^{1}H NMR (400 MHz, cdcl$_3$) δ 11.74 (s, 1H), 8.77 (d, *J* = 9.1 Hz, 1H), 8.20 (d, *J* = 16.2 Hz, 1H), 8.01 (d, *J* = 2.6 Hz, 1H), 7.61 (dd, *J* = 7.6, 1.7 Hz, 1H), 7.52 (dd, *J* = 9.1, 2.6 Hz, 1H), 7.41 – 7.37 (m, 1H), 7.03 – 6.91 (m, 2H), 6.80 (d, *J* = 16.2 Hz, 1H), 4.86 (s, 2H), 3.90 (d, *J* = 7.9 Hz, 7H).

(*R*)-2-((4-chloro-2-((1-(naphthalen-1-yl)ethyl)carbamoyl)phenyl)amino)-2-oxoethyl (*E*)-3-(2-methoxyphenyl)acrylate (KH-6). KH-5 (30 mg, 0.074 mmol) was dissolved in pyridine (2 mL). LiI (9.94 mg, 0.074 mmol) was added. The mixture was microwaved at 160 °C for 10 mins. The solvent was removed *in vacuo*. EDC·HCl (17.09 mg, 0.089 mmol) and 4-Dimethylaminopyridine (1.82 mg, 0.015 mmol) were dissolved in DCM (1.5 mL). The reaction mixture was added and stirred at room temperature for 24 h. The reaction mixture was diluted with water, extracted with DCM (3x5 mL). The organic layer was washed with brine, dried with Na_2SO_4, and concentrated. Column chromatography (20% to 60% EtOAc/hexanes) afforded the desired product (3 mg, KH-6a: 7% yield; KH-6b: 7% yield.) ^{1}H NMR (500 MHz, $CDCl_3$) δ 11.72 (s, 1H), 8.65 (d, *J* = 9.0 Hz, 1H), 8.29 (d, *J* = 16.2 Hz, 1H), 8.07 – 7.99 (m, 1H), 7.95 – 7.81 (m, 2H), 7.63 (dd, *J* = 7.7, 1.7 Hz, 1H), 7.59 – 7.55 (m, 1H), 7.54 – 7.46 (m, 3H), 7.43 (dd, *J* = 9.0, 2.4 Hz, 1H), 7.36 – 7.30 (m, 2H), 6.99 – 6.82 (m, 3H), 6.33 (d, *J* = 8.0 Hz, 1H), 6.02 (p, *J* = 7.0 Hz, 1H), 4.94 – 4.79 (m, 2H), 3.83 (s, 3H), 1.72 (d, *J* = 6.7 Hz, 3H). ^{13}C NMR (126 MHz, $CDCl_3$) δ 166.54, 166.42, 166.21, 158.71, 142.46, 137.15, 137.10, 133.99, 132.40, 131.77, 131.01, 129.75, 128.97, 128.89, 128.35, 126.87, 126.23, 126.08, 125.23, 123.33, 122.99, 122.86, 122.80, 122.49, 120.68, 117.54, 111.14, 77.28, 77.03, 76.77, 63.00, 55.40, 45.38, 20.32. HRMS (ESI/Q-TOF) m/z: $[M + Na]^+$ calculated for $C_{31}H_{27}ClN_2O_5$ 565.15; found 565.1493.

Methyl (*E*)-(3-(4-(trifluoromethyl)phenyl)acryloyl)glycinate (KH-7). 4-(trifluoromethyl)cinnamic acid (258.25 mg, 1.19 mmol), EDC·HCl (458.06 mg, 2.39 mmol) and 4-Dimethylaminopyridine (58.38

mg, 0.48 mmol) were dissolved in anhydrous DCM (10 mL). The mixture was stirred at room temperature for 10 mins. Glycine methyl ester hydrochloride salt (150 mg, 1.19 mmol) was added, stirred at room temperature for 20 h. The precipitate was filtered and afforded the desired product (0.194 g, 56% yield). ^{1}H NMR (400 MHz, cdcl$_3$) δ 7.76 – 7.53 (m, 5H), 6.53 (d, *J* = 15.6 Hz, 1H), 6.17 (s, 1H), 4.20 (d, *J* = 5.1 Hz, 2H), 3.80 (s, 3H).

(*E*)-(3-(4-(trifluoromethyl)phenyl)acryloyl)glycine (KH-8). KH-7 was dissolved in 1M NaOH (2 mL) and stirred at room temperature for 16 h. The reaction mixture was acidified by 1M HCl until pH = 1. The precipitate was filtered to afford to desired product (77 mg, 81 % yield). ^{1}H NMR (400 MHz, DMSO) δ 8.49 (t, *J* = 5.8 Hz, 1H), 7.82 – 7.72 (m, 4H), 7.50 (d, *J* = 15.8 Hz, 1H), 6.84 (d, *J* = 15.9 Hz, 1H), 3.88 (d, *J* = 5.9 Hz, 2H).

2-amino-5-chlorobenzoic acid (KH-9). methyl 2-amino-5-chlorobenzoate (100 mg, 0.539 mmol) was dissolved in 1M NaOH (2.6 mL), stirred at room temperature for 16 h. The reaction mixture was acidified with 1M HCl until pH = 1. The precipitate was filtered to afford the desired product (52.43 mg, 57%). ^{1}H NMR (500 MHz, DMSO) δ 7.62 (d, *J* = 2.6 Hz, 1H), 7.25 (dd, *J* = 8.9, 2.7 Hz, 1H), 6.78 (d, *J* = 8.9 Hz, 1H).

2-amino-5-chloro-*N*-(2-(naphthalen-1-yl)propan-2-yl)benzamide (KH-10). KH-9 (52.43 mg, 0.306 mmol), EDC·HCl (70.29 mg, 0.367 mmol) and 4-Dimethylaminopyridine (7.47 mg, 0.061 mmol) were dissolved in DMF (2 mL). (R)-(+)-1-(1-Naphthyl)ethylamine (0.059 mL, 0.367 mmol) was added and stirred at room temperature for 20 h. The reaction mixture was diluted with water, extracted with EtOAc. The organic layer was washed with water (2x5 mL), brine, dried with Na_2SO_4, and concentrated. Column chromatography (20% to 60% EtOAc/hexanes) afforded the desired product (0.073 g, 74%). ^{1}H NMR (400 MHz, CDCl$_3$) δ 8.19 – 8.08 (m, 1H), 7.89 (dd, *J* = 7.8, 1.7 Hz, 1H), 7.82 (d, *J* = 8.3 Hz, 1H), 7.62 – 7.41 (m, 4H), 7.19 (d, *J* = 2.4 Hz, 1H), 7.11 (dd, *J* = 8.7, 2.4 Hz, 1H), 6.59 (d, *J* = 8.7 Hz, 1H), 6.25 (d, *J* = 7.8 Hz, 1H), 6.05 (p, *J* = 7.0 Hz, 1H), 5.52 (s, 2H), 1.75 (d, *J* = 6.7 Hz, 3H).

(*R*,*E*)-5-chloro-*N*-(1-(naphthalen-1-yl)ethyl)-2-(2-(3-(4-(trifluoromethyl)phenyl)acrylamido)acetamido)benzamide (KH-11). KH-10 (0.328g, 1.2 mmol) was dissolved in DCM (15 mL) at 0 °C. Methylsulfonylchloride (0.186 mL, 2.40 mmol) and N-methylimidazole (0.197 g, 2.40 mmol) were added. The mixture was warmed to room temperature, stirred for 20 mins. The mixture was cooled to 0 °C. KH-8 (0.429 g, 1.32 mmol) was added to the mixture, warmed to room temperature, stirred for 16 h. The reaction mixture was diluted with water, extracted with DCM. The organic layer was washed with brine, dried with Na_2SO_4, and concentrated. Column chromatography (0% to 30% EtOAc/hexanes) afforded the desired product (15.32 mg, 2%). ^{1}H NMR (500 MHz, DMSO) δ 11.52 (s, 1H), 9.36 (d, *J* = 7.6 Hz, 1H), 8.98 (t, *J* = 5.9 Hz, 1H), 8.50 (d, *J* = 8.9 Hz, 1H), 7.93 – 7.84 (m, 2H), 7.80 (qd, *J* = 8.4, 5.3 Hz, 6H), 7.63 – 7.57 (m, 3H), 7.52 – 7.42 (m, 2H), 7.31 (ddd, *J* = 8.3, 6.8, 1.4 Hz, 1H), 6.93 (d, *J* = 15.9 Hz, 1H), 5.76 (p, *J* = 7.0 Hz, 1H), 3.96 (d, *J* = 5.8 Hz, 2H), 1.49 (d, *J* = 6.9 Hz, 3H). ^{13}C NMR (126 MHz, $CDCl_3$) δ 167.30, 166.58, 165.47, 140.19, 137.22, 134.02, 132.62, 130.91, 129.08, 128.88, 128.01, 126.92, 126.30, 126.12, 125.84, 125.28, 122.89, 122.76, 122.66, 122.37, 77.28, 77.02, 76.77, 60.41, 45.69, 44.21, 31.60, 22.67, 21.07, 20.61, 14.21, 14.13. HRMS (ESI/Q-TOF) m/z: $[M + Na]^+$ calculated for $C_{31}H_{25}ClF_3N_3O_3$ 602.14; found 602.1418.

***In vitro* assays.**

Protein production. The DNA sequence encoding PL^{pro} SARS-CoV-2 protease was synthetized (optimized for expression in *Escherichia coli*) and cloned into a pD431-SR vector between XbaI and SmaI restriction sites, by Atum (Newwark, CA, USA). The protein sequence was preceded by an *N*-terminal TEV protease site (ENLYFQ ↓ G/S) followed by a 6-His purification tag.

E. coli BL21 (DE3) cells were transformed using the plasmid described above and the $CaCl_2$ method[52] and colonies were selected on LB-agar-Kanamycin plates. A single colony was picked and grew over night in LB media and then used to inoculate a 400 mL LB culture. This was grown at 37 ºC, 250 rpm, until an optical density at 600 nm of 0.7 (O.D.600) was reached and then induced for 18h at 16 ºC (250 rpm) by adding 0.20 mM IPTG. The bacterial pellet was collected after 9,000 rpm centrifugation and resuspended in 30 mL of 50 mM Tris-HCl pH 8.0, 150 mM NaCl, 20 mM imidazole (resuspension buffer). An Ultrasonic Cell Disruption Sonifier 450 (Branson) was used to sonicate the cells (on ice) with 8 pulses of 2 mins (Output Control 7 and 50 % Duty Cycle).

Buffer A (50 mM Tris-HCl pH 8.0, 150 mM NaCl, 20 mM imidazole) and Buffer B (50 mM Tris-HCl, 150 mM NaCl, 500 mM imidazole) were used for purifying PL^{pro} after the clarified supernatant (14,000 rpm centrifugation) was loaded into a 5 mL HisTrap FF (GE Healthcare, IL, USA). 1 ml fractions were collected by three steps linear gradient of buffer B: 0% to 20% in 5 mins, 20% to 30% in 10 mins and 30 to 100% in 5 mins.

After running SDS-PAGE for confirmation (Mini-PROTEAN® TGX™ Precast Gels, Bio-Rad), the fractions from the second linear gradient that show a band of 38 kD were pooled independently and dialyzed overnight against Buffer C (50 mM Tris-HCl, 150 mM NaCl, 1.5 mM DTT). The pool was concentrated using 10K cut-off Amicon® Ultra-15 Centrifugal Filter Units (Millipore Sigma, Burlington, MA, USA). Absorbance at 280 nm was recorded for estimated the protein concentration. These samples were aliquoted and stored with 20% of glycerol at -80 Celsius degrees.

Detection of inhibitors by fluorescence spectrophotometry. For all inhibition experiments, reactions were performed in 100 µL assay with 0.1 or 10 µM of the fluorescence substrates ubiquitin or Z- RLRGG-AMC, respectively from BPS Biosciences (San Diego, CA, USA), which has been previously used for assaying PL^{pro} proteases.[53]

10 µL of 0.8 µM enzyme were mixed with 10 µL of the inhibitor and 70 µL of assay buffer (50 mM Tris-HCl, 150 mM NaCl, 1.5 mM DTT, 0.1 mg/ml BSA) for 30 mins at room temperature. In both screening (duplicates) and IC_{50} experiments (duplicates or triplicates), 10 µL of 1 or 30 µM of the fluorescence substrates ubiquitin or Z-RLRGG-AMC, respectively diluted in assay buffer with were added and the reactions were monitored by following the fluorescence as a function of time (excitation at 360 nm, emission at 460 nm) using a Synergy™ H4 Hybrid Multi-Mode Microplate Reader (Winooski, VT, USA). Controls were (i) positive control, 2 µL of DMSO, (ii) inhibitor control, 2 µL of 500 µM GRL0617 (synthetized by us) (iii) blank, the PL^{pro} without inhibitor. For screening, the compounds were added as DMSO solutions and their final concentration in the reactions was 50 µM. For IC_{50} measurement, serial dilutions were performed to reach a final concentration ranging from 200 µM to 0.2 µM. The reactions ran for at least one hour, and the linear initial slopes of the progress curves were used to calculate the reaction initial velocity in Relative Fluorescent Units in time (RFU per min). GraphPad software was used to determine IC_{50} values.

Liquid chromatography-mass spectrometry (LC-MS). Stored-frozen protein samples were buffer exchanged with 5 mM Tris-HCl pH 8.0, 15 mM NaCl buffer using 4K cut-off Amicon® small Centrifugal Filter Units (Millipore Sigma, Burlington, MA, USA) and prepared at 0.1-0.2 mg/mL. 96 µL of this solution was mixed with 4 µL of 2.5 mM inhibitor. Pure DMSO was used as a negative control. Protein samples were analyzed by LC-MS using a Dionex Ultimate 3000 UHPLC coupled to a Bruker Maxis Impact Q-TOF in positive ESI mode. Samples were separated on an Agilent PLRP-S column (1000Å, 5 µM, 2.1 x 50 mm) heated to 80 ºC at a flow rate of 0.5 ml/min using a gradient of 80% mobile phase A (0.1% formic acid in H2O) and 20% mobile phase B (0.1% formic acid in ACN) for 2 mins, ramped to

60% mobile phase A and 40% mobile phase B in 5 mins, and 10% mobile phase A and 90% mobile phase B in 5 mins. The data was processed and spectra deconvoluted using the Bruker DataAnalysis software version 4.2.

Supporting Information

Addition information on attempted synthesis, LC-MS data, ITC measurement, dose-response curves, LC/MS data and ^{1}H and ^{13}C NMR spectra.

Acknowledgment

We thank the Canadian Institutes of Health Research (CIHR, OV3-170644), the McGill Interdisciplinary Initiative in Infection and Immunity (MI4) and the Faculty of Science for funding. We thank Compute Canada for their very generous CPU time allocations.

References

(1) Wertheim, J. O.; Chu, D. K. W.; Peiris, J. S. M.; Pond, S. L. K.; Poon, L. L. M. A Case for the Ancient Origin of Coronaviruses. *J. Virol.* **2013**, *87* (12), 7039-7045. DOI: doi:10.1128/jvi.03273-12.

(2) Fehr, A. R.; Perlman, S. Coronaviruses: an overview of their replication and pathogenesis. *Methods Mol. Biol.* **2015**, *1282*, 1-23. DOI: 10.1007/978-1-4939-2438-7_1

(3) King, A. An uncommon cold. *New Sci* **2020**, *246* (3280), 32-35. DOI: 10.1016/s0262-4079(20)30862-9

(4) Organization, W. H. WHO Coronavirus Disease (COVID-19) Dashboard. **2013**.

(5) Chu, D. K.; Akl, E. A.; Duda, S.; Solo, K.; Yaacoub, S.; Schünemann, H. J. Physical distancing, face masks, and eye protection to prevent person-to-person transmission of SARS-CoV-2 and COVID-19: a systematic review and meta-analysis. *Lancet* **2020**, *395* (10242), 1973-1987. DOI: 10.1016/s0140-6736(20)31142-9.

(6) Siemieniuk, R. A.; Bartoszko, J. J.; Zeraatkar, D.; Kum, E.; Qasim, A.; Martinez, J. P. D.; Izcovich, A.; Lamontagne, F.; Han, M. A.; Agarwal, A.; et al. Drug treatments for covid-19: living systematic review and network meta-analysis. *Bmj* **2020**, *370*, m2980. DOI: 10.1136/bmj.m2980.

(7) FDA. *FDA Approves First Treatment for COVID-19*. 2020. https://www.fda.gov/news-events/press-announcements/fda-approves-first-treatment-covid-19 (accessed 2023 2023-07-27).

(8) McCreary, E. K.; Angus, D. C. Efficacy of Remdesivir in COVID-19. *JAMA* **2020**, *324* (11), 1041-1042. DOI: 10.1001/jama.2020.16337 (acccessed 7/24/2023).

(9) Pan, H.; Peto, R.; Henao-Restrepo, A. M.; Preziosi, M. P.; Sathiyamoorthy, V.; Abdool Karim, Q.; Alejandria, M. M.; Hernández García, C.; Kieny, M. P.; Malekzadeh, R.; et al. Repurposed Antiviral Drugs for Covid-19 - Interim WHO Solidarity Trial Results. *New Engl. J. Med.* **2021**, *384* (6), 497-511. DOI: 10.1056/NEJMoa2023184.

(10) Kabinger, F.; Stiller, C.; Schmitzová, J.; Dienemann, C.; Kokic, G.; Hillen, H. S.; Höbartner, C.; Cramer, P. Mechanism of molnupiravir-induced SARS-CoV-2 mutagenesis. *Nat. Struct. Mol. Biol.* **2021**, *28* (9), 740-746. DOI: 10.1038/s41594-021-00651-0.

(11) Merck & Co., I. Merck and Ridgeback's Molnupiravir, an Oral COVID-19 Antiviral Medicine, Receives First Authorization in the World. **2021**.

(12) FDA. *Coronavirus (COVID-19) Update: FDA Authorizes Additional Oral Antiviral for Treatment of COVID-19 in Certain Adults*. 2021. https://www.fda.gov/news-events/press-announcements/coronavirus-covid-19-update-fda-authorizes-additional-oral-antiviral-treatment-covid-19-certain (accessed 2023 2023-07-25).

(13) Boras, B.; Jones, R. M.; Anson, B. J.; Arenson, D.; Aschenbrenner, L.; Bakowski, M. A.; Beutler, N.; Binder, J.; Chen, E.; Eng, H.; et al. Discovery of a Novel Inhibitor of Coronavirus 3CL Protease for the Potential Treatment of COVID-19. *bioRxiv* **2021**. DOI: 10.1101/2020.09.12.293498.

(14) Pfizer. Study of PF-07321332 in healthy participants **2021**, *NCT04756531*.

(15) Owen, D. R.; Allerton, C. M. N.; Anderson, A. S.; Aschenbrenner, L.; Avery, M.; Berritt, S.; Boras, B.; Cardin, R. D.; Carlo, A.; Coffman, K. J.; et al. An oral SARS-CoV-2 Mpro inhibitor clinical candidate for the treatment of COVID-19. *Science* **2021**, *374* (6575), 1586-1593. DOI: doi:10.1126/science.abl4784.

(16) Shionogi. *Shionogi Receives U.S. FDA Fast Track Designation for Ensitrelvir Fumaric Acid, an Investigational Oral Antiviral for COVID-19*. 2023. https://www.shionogi.com/global/en/news/2023/04/20230404.html (accessed 2023 2023-07-26).
(17) Lan, S.; Neilsen, G.; Slack, R. L.; Cantara, W. A.; Castaner, A. E.; Lorson, Z. C.; Lulkin, N.; Zhang, H.; Lee, J.; Cilento, M. E.; et al. Nirmatrelvir Resistance in SARS-CoV-2 Omicron_BA.1 and WA1 Replicons and Escape Strategies. *bioRxiv* **2023**, 2022.2012.2031.522389. DOI: 10.1101/2022.12.31.522389.
(18) Dömling, A.; Gao, L. Chemistry and Biology of SARS-CoV-2. *Chem* **2020**, *6* (6), 1283-1295. DOI: 10.1016/j.chempr.2020.04.023.
(19) Jackson, C. B.; Farzan, M.; Chen, B.; Choe, H. Mechanisms of SARS-CoV-2 entry into cells. *Nature Reviews Molecular Cell Biology* **2022**, *23* (1), 3-20. DOI: 10.1038/s41580-021-00418-x.
(20) Lamers, M. M.; Haagmans, B. L. SARS-CoV-2 pathogenesis. *Nat. Rev. Microbiol.* **2022**, *20* (5), 270-284. DOI: 10.1038/s41579-022-00713-0.
(21) Zumla, A.; Chan, J. F. W.; Azhar, E. I.; Hui, D. S. C.; Yuen, K.-Y. Coronaviruses — drug discovery and therapeutic options. *Nat. Rev. Drug Discov.* **2016**, *15* (5), 327-347. DOI: 10.1038/nrd.2015.37.
(22) Maiti, B. K. Can Papain-like Protease Inhibitors Halt SARS-CoV-2 Replication? *ACS Pharmacol. Translat. Sci.* **2020**, *3* (5), 1017-1019. DOI: 10.1021/acsptsci.0c00093.
(23) Shin, D.; Mukherjee, R.; Grewe, D.; Bojkova, D.; Baek, K.; Bhattacharya, A.; Schulz, L.; Widera, M.; Mehdipour, A. R.; Tascher, G.; et al. Papain-like protease regulates SARS-CoV-2 viral spread and innate immunity. *Nature* **2020**, *587* (7835), 657-662. DOI: 10.1038/s41586-020-2601-5.
(24) Frieman, M.; Ratia, K.; Johnston, R. E.; Mesecar, A. D.; Baric, R. S. Severe acute respiratory syndrome coronavirus papain-like protease ubiquitin-like domain and catalytic domain regulate antagonism of IRF3 and NF-kappaB signaling. *J. Virol.* **2009**, *83* (13), 6689-6705. DOI: 10.1128/jvi.02220-08.
(25) Unoh, Y.; Uehara, S.; Nakahara, K.; Nobori, H.; Yamatsu, Y.; Yamamoto, S.; Maruyama, Y.; Taoda, Y.; Kasamatsu, K.; Suto, T.; et al. Discovery of S-217622, a Noncovalent Oral SARS-CoV-2 3CL Protease Inhibitor Clinical Candidate for Treating COVID-19. *J. Med. Chem.* **2022**, *65* (9), 6499-6512. DOI: 10.1021/acs.jmedchem.2c00117.
(26) Tan, H.; Hu, Y.; Jadhav, P.; Tan, B.; Wang, J. Progress and Challenges in Targeting the SARS-CoV-2 Papain-like Protease. *J. Med. Chem.* **2022**, *65* (11), 7561-7580. DOI: 10.1021/acs.jmedchem.2c00303.
(27) Rut, W.; Lv, Z.; Zmudzinski, M.; Patchett, S.; Nayak, D.; Snipas, S. J.; El Oualid, F.; Huang, T. T.; Bekes, M.; Drag, M.; Olsen, S. K. Activity profiling and crystal structures of inhibitor-bound SARS-CoV-2 papain-like protease: A framework for anti–COVID-19 drug design. *Sci. Adv.* **2020**, *6* (42), eabd4596. DOI: doi:10.1126/sciadv.abd4596.
(28) Weglarz-Tomczak, E.; Tomczak, J. M.; Talma, M.; Burda-Grabowska, M.; Giurg, M.; Brul, S. Identification of ebselen and its analogues as potent covalent inhibitors of papain-like protease from SARS-CoV-2. *Sci. Rep.* **2021**, *11* (1), 3640. DOI: 10.1038/s41598-021-83229-6.
(29) Fu, Z.; Huang, B.; Tang, J.; Liu, S.; Liu, M.; Ye, Y.; Liu, Z.; Xiong, Y.; Cao, D.; Li, J.; et al. Structural basis for the inhibition of the papain-like protease of SARS-CoV-2 by small molecules. *bioRxiv* **2020**, 2020.2007.2017.208959. DOI: 10.1101/2020.07.17.208959.
(30) Calleja, D. J.; Lessene, G.; Komander, D. Inhibitors of SARS-CoV-2 PLpro. *Front. Chem.* **2022**, *10*, Review. DOI: 10.3389/fchem.2022.876212.
(31) Ton, A. T.; Pandey, M.; Smith, J. R.; Ban, F.; Fernandez, M.; Cherkasov, A. Targeting SARS-CoV-2 papain-like protease in the postvaccine era. *Trends Pharmacol. Sci.* **2022**, *43* (11), 906-919. DOI: 10.1016/j.tips.2022.08.008.
(32) Kouznetsova, V. L.; Zhang, A.; Tatineni, M.; Miller, M. A.; Tsigelny, I. F. Potential COVID-19 papain-like protease PL(pro) inhibitors: repurposing FDA-approved drugs. *PeerJ* **2020**, *8*, e9965. DOI: 10.7717/peerj.9965.
(33) Lee, H.; Ren, J.; Pesavento, R. P.; Ojeda, I.; Rice, A. J.; Lv, H.; Kwon, Y.; Johnson, M. E. Identification and design of novel small molecule inhibitors against MERS-CoV papain-like protease via high-throughput screening and molecular modeling. *Bioorg. Med. Chem.* **2019**, *27* (10), 1981-1989. DOI: 10.1016/j.bmc.2019.03.050.

(34) Freitas, B. T.; Durie, I. A.; Murray, J.; Longo, J. E.; Miller, H. C.; Crich, D.; Hogan, R. J.; Tripp, R. A.; Pegan, S. D. Characterization and Noncovalent Inhibition of the Deubiquitinase and deISGylase Activity of SARS-CoV-2 Papain-Like Protease. *ACS Infect. Dis.* **2020**, *6* (8), 2099-2109. DOI: 10.1021/acsinfecdis.0c00168.
(35) Ratia, K.; Pegan, S.; Takayama, J.; Sleeman, K.; Coughlin, M.; Baliji, S.; Chaudhuri, R.; Fu, W.; Prabhakar, B. S.; Johnson, M. E.; et al. A noncovalent class of papain-like protease/deubiquitinase inhibitors blocks SARS virus replication. *Proc. Natl. Acad. Sci.* **2008**, *105* (42), 16119-16124. DOI: doi:10.1073/pnas.0805240105.
(36) Swaim, C. D.; Dwivedi, V.; Perng, Y. C.; Zhao, X.; Canadeo, L. A.; Harastani, H. H.; Darling, T. L.; Boon, A. C. M.; Lenschow, D. J.; Kulkarni, V.; Huibregtse, J. M. 6-Thioguanine blocks SARS-CoV-2 replication by inhibition of PLpro. *iScience* **2021**, *24* (10), 103213. DOI: 10.1016/j.isci.2021.103213.
(37) Shen, Z.; Ratia, K.; Cooper, L.; Kong, D.; Lee, H.; Kwon, Y.; Li, Y.; Alqarni, S.; Huang, F.; Dubrovskyi, O.; et al. Design of SARS-CoV-2 PLpro Inhibitors for COVID-19 Antiviral Therapy Leveraging Binding Cooperativity. *J. Med. Chem.* **2022**, *65* (4), 2940-2955. DOI: 10.1021/acs.jmedchem.1c01307.
(38) Sanders, B. C.; Pokhrel, S.; Labbe, A. D.; Mathews, II; Cooper, C. J.; Davidson, R. B.; Phillips, G.; Weiss, K. L.; Zhang, Q.; O'Neill, H.; et al. Potent and selective covalent inhibition of the papain-like protease from SARS-CoV-2. *Nat. Commun.* **2023**, *14* (1), 1733. DOI: 10.1038/s41467-023-37254-w.
(39) Gao, X.; Qin, B.; Chen, P.; Zhu, K.; Hou, P.; Wojdyla, J. A.; Wang, M.; Cui, S. Crystal structure of SARS-CoV-2 papain-like protease. *Acta Pharm Sin B* **2021**, *11* (1), 237-245. DOI: 10.1016/j.apsb.2020.08.014.
(40) Stille, J. K.; Lau, K. S. Y. Mechanisms of oxidative addition of organic halides to Group 8 transition-metal complexes. *Acc. Chem. Res.* **1977**, *10* (12), 434-442. DOI: 10.1021/ar50120a002.
(41) Irwin, J. J.; Shoichet, B. K. Docking Screens for Novel Ligands Conferring New Biology. *J. Med. Chem.* **2016**, *59* (9), 4103-4120. DOI: 10.1021/acs.jmedchem.5b02008.
(42) Lyu, J.; Wang, S.; Balius, T. E.; Singh, I.; Levit, A.; Moroz, Y. S.; O'Meara, M. J.; Che, T.; Algaa, E.; Tolmachova, K.; et al. Ultra-large library docking for discovering new chemotypes. *Nature* **2019**, *566* (7743), 224-229. DOI: 10.1038/s41586-019-0917-9.
(43) Gentile, F.; Fernandez, M.; Ban, F.; Ton, A.-T.; Mslati, H.; Perez, C. F.; Leblanc, E.; Yaacoub, J. C.; Gleave, J.; Stern, A.; et al. Automated discovery of noncovalent inhibitors of SARS-CoV-2 main protease by consensus Deep Docking of 40 billion small molecules. *Chem. Sci.* **2021**, *12* (48), 15960-15974, 10.1039/D1SC05579H. DOI: 10.1039/D1SC05579H.
(44) Fischer, A.; Smieško, M.; Sellner, M.; Lill, M. A. Decision Making in Structure-Based Drug Discovery: Visual Inspection of Docking Results. *J. Med. Chem.* **2021**, *64* (5), 2489-2500. DOI: 10.1021/acs.jmedchem.0c02227.
(45) Moitessier, N.; Englebienne, P.; Lee, D.; Lawandi, J.; Corbeil, C. R. Towards the development of universal, fast and highly accurate docking/scoring methods: a long way to go. *Br. J. Pharmacol.* **2008**, *153 Suppl 1* (Suppl 1), S7-26. DOI: 10.1038/sj.bjp.0707515.
(46) Sterling, T.; Irwin, J. J. ZINC 15 – Ligand Discovery for Everyone. *J. Chem. Inf. Model.* **2015**, *55* (11), 2324-2337. DOI: 10.1021/acs.jcim.5b00559.
(47) Moitessier, N.; Pottel, J.; Therrien, E.; Englebienne, P.; Liu, Z.; Tomberg, A.; Corbeil, C. R. Medicinal Chemistry Projects Requiring Imaginative Structure-Based Drug Design Methods. *Acc. Chem. Res.* **2016**, *49* (9), 1646-1657. DOI: 10.1021/acs.accounts.6b00185.
(48) Labarre, A.; Stille, J. K.; Patrascu, M. B.; Martins, A.; Pottel, J.; Moitessier, N. Docking Ligands into Flexible and Solvated Macromolecules. 8. Forming New Bonds─Challenges and Opportunities. *J. Chem. Inf. Model.* **2022**, *62* (4), 1061-1077. DOI: 10.1021/acs.jcim.1c00701.
(49) Therrien, E.; Englebienne, P.; Arrowsmith, A. G.; Mendoza-Sanchez, R.; Corbeil, C. R.; Weill, N.; Campagna-Slater, V.; Moitessier, N. Integrating medicinal chemistry, organic/combinatorial chemistry, and computational chemistry for the discovery of selective estrogen receptor modulators with Forecaster, a novel platform for drug discovery. *J. Chem. Inf. Model.* **2012**, *52* (1), 210-224. DOI: 10.1021/ci2004779.
(50) BIOVIA, D. S. BIOVIA Discovery Studio Visualizer, v20.1.0.1929. *San Diego: Dassault Systèmes* **2020**.
(51) System, T. P. M. G. *Version 2.0 Schrödinger, LLC* **2020**.

(52) Hanahan, D. Studies on transformation of Escherichia coli with plasmids. *J. Mol. Biol.* **1983**, *166* (4), 557-580. DOI: 10.1016/s0022-2836(83)80284-8.
(53) Chen, S.; Chen, L. L.; Luo, H. B.; Sun, T.; Chen, J.; Ye, F.; Cai, J. H.; Shen, J. K.; Shen, X.; Jiang, H. L. Enzymatic activity characterization of SARS coronavirus 3C-like protease by fluorescence resonance energy transfer technique. *Acta Pharmacol. Sin.* **2005**, *26* (1), 99-106. DOI: 10.1111/j.1745-7254.2005.00010.